CORAL RECORDS OF CENTRAL TROPICAL PACIFIC SEA-SURFACE TEMPERATURE AND SALINITY VARIABILITY OVER THE 20th CENTURY

A Dissertation
Presented to
The Academic Faculty

By

Intan Suci Nurhati

In Partial Fulfillment
of the Requirements for the Degree
Doctor of Philosophy in the
School of Earth and Atmospheric Sciences

Georgia Institute of Technology
August 2010

CORAL RECORDS OF CENTRAL TROPICAL PACIFIC SEA-SURFACE TEMPERATURE AND SALINITY VARIABILITY OVER THE 20th CENTURY

Approved by:

Dr. Kim Cobb (Advisor)
School of Earth and Atmospheric Sciences
Georgia Institute of Technology

Dr. Jean Lynch-Stieglitz
School of Earth and Atmospheric Sciences
Georgia Institute of Technology

Dr. Emanuele Di Lorenzo
School of Earth and Atmospheric Sciences
Georgia Institute of Technology

Dr. Peter Webster
School of Civil and Environmental Engineering
Georgia Institute of Technology

Dr. Annalisa Bracco
School of Earth and Atmospheric Sciences
Georgia Institute of Technology

Date Approved: June 28, 2010

For my parents, Anis & Rahmat.

ACKNOWLEDGEMENTS

Firstly, I would like to thank my academic advisor, Dr. Kim Cobb, for her relentless guidance and supports over the past five years. Through numerous examples, Kim has taught me objective and collaborative conducts of science, excellence in the quality of works, and the dissemination of scientific knowledge for the greater public needs. I admire her brilliance, drive and perseverance; and am grateful for her empathetic mentoring throughout the years. How she balances her shining career with a family of two children and three dogs is inspiring. I am privileged to have worked with and learned from her, all of which will resonate with me as I thread my career as a climate scientist.

I would like to thank my dissertation committee members: Drs. Jean Lynch-Stieglitz, Emanuele Di Lorenzo, Annalisa Bracco and Peter Webster for their insightful comments throughout the process. Many of whom have been sitting in my committee since my comprehensive exam, and supporting my grants seeking to postdoc applications with their letters of recommendations. Thanks to Cobb Lab technicians for all the logistical helps, especially to Nitya Sharma with whom I overlapped the longest with during my labwork intensive period. Hussein Sayani and Heather Crespo lent their assistances in generating the beautiful and interesting SEM images presented in this dissertation. My former senior graduate student, Dr. Jud Partin, passed down numerous tips to master the ICP-OES. I am indebted to Dr. Branwen Williams and Jordan Watson for their company and enormous supports during my southern Line Islands cruise. And to Dr. Katie Matthews for training me a series of trace metal analyses at the University of Maryland. The friendly and curious radiology crews at the GT Health Center always

made my coral x-raying trips enjoyable ones. My graduate school experience would not be complete without fellow EAS graduate students. I cherish many fond memories of my first year officemates of assorted personalities and interests. I counted on Dana Ionita for numerous favors. Jason Furtado lent his expert helps to buy my first car, which made long ICP runs much easier to go through. Dana, Jason, Sara Vieira, Lina Ceballos, Yuley Cardona and Vincent Combes are always awesome companies to spend times with.

I am grateful for supports and companies from many people outside the ES&T building, whom I will always remember much of my Atlanta years by. My Indonesian Students Association (ISA) family at Georgia Tech with whom I spent many eat-outs, road trips - planned or not, and shared laughs with. Kiki Tan has been there from A to Z; listening to and witnessing stages of my grad school years, helping with organizing ISA events to cooking us meals. Jessica Kamal always amazes me with the beautiful world of human innocence. It only takes seconds before Sisca Wijaya and I can argue on anything, which I admittedly will dearly miss. Vera Halim endured my driving to help me get my license. Sherlin Tan is the little sister to bug, in between writing this dissertation. Also to Johny Franslay, Ajiv Parnata, Edwin Tandiono, Denny Lie, Yanto Huang and all ISAers. I am forever grateful to my “love for all, hatred for none” Ahmadiyya Muslim Community family in the US and abroad for all the supports and comforts, *jazakAllah*.

Terima kasih to my family who always trusts and supports me from afar. I recalled my mother wishing her child to earn a doctoral degree abroad, which sounded nothing but an empty wish back then. When opportunities present themselves, one leads to another, I am repeatedly reminded on the endless possibilities that life offers. I am forever indebted to Mr. Buck Freeman for giving me the free ride and life-long privilege

to be part of Wesleyan University. Dr. Suzanne O'Connell was instrumental in sparking my scientific interests in paleoclimatology during my college years. And throughout the past decade, my family always sent their encouragements and wise words from literally the other side of the planet. My mother may never taste the experience of higher education, but her supports and encouragements for me to achieve the highest degree in academia and learn from the journey are something to be thankful and celebrated for!

I must thank corals that brought me to study what I believe is one of the most relevant scientific endeavors to our society today – climate science. The road that led to my doctoral work in coral Sr/Ca was unexpected in my academic life that I started as an economics major. Corals caught my interests during my freshman year's environmental science course, and the fascination grew as I learned the utility of coral Sr/Ca as a proxy for sea-surface temperature in geochemistry class. The reliability of coral as a tropical climate archive to decipher ENSO variability was an icing on the cake, having witnessed the extraordinary 1997-98 ENSO ran amok in my own backyard, but most importantly, how significant it could impact our society. I was fortunate to have my first hands-on experience on corals right in the Great Barrier Reefs, where I learned to utilize coral tissues and skeletons as environmental indicators during my intern at the Australian Institute of Marine Sciences. While spending days blasting tissues off *Pocillopora damicormis* corals at AIMS, I found out that coral tissues actually give me an awful allergic reaction. Coral skeletons on the other hand, have been helping me to understand how tropical Pacific climate might evolve under global warming – a line of scientific research that I hope to contribute to our scientific understandings for the benefits of societies.

TABLE OF CONTENTS

ACKNOWLEDGEMENTS……...…… iv

LIST OF TABLES…..……..…… x

LIST OF FIGURES……...…… xi

LIST OF SYMBOLS AND ABBREVIATIONS……..…..…….... xiii

SUMMARY……...…..….. xv

CHAPTER 1: INTRODUCTION…….……..……...……...…..…... 1

1.1. Tropical Pacific Climate……..……...……..... 1

1.1.1. Interannual El Niño-Southern Oscillation (ENSO) Variability…...…..……..…… 1

1.1.2. Pacific Decadal Climate Variability: Characteristic and Mechanisms……....…....…..…... 6

1.1.3. Anthropogenic Signatures of Tropical Pacific Climate... 9

1.2. Central Tropical Pacific Coral Proxy Climate Records…..…..… 11

1.2.1. Overview of Coral Paleoclimate Reconstruction…....… 12

1.2.2. Description of Line Islands Study Sites……... 14

1.2.2.1. Climatology……..... 14

1.2.2.2. Interannual Variability…...……..... 16

1.2.2.3. Decadal Variability…….……... 17

1.2.3. Overview of Central Tropical Pacific Coral Records..... 19

1.3. References……...… 23

CHAPTER 2: LATE 20th CENTURY WARMING AND FRESHENING TRENDS IN THE CENTRAL TROPICAL PACIFIC……... 34

2.1. Abstract……..……....… 34

2.2. Introduction……..……...… 35

2.3. Methods.……..…….... 38

2.4. Results and Discussion……..……...……..…. 39

2.5. Auxiliary Material..…..……...……..... 44
2.5.1. Coral Sampling & Analytical Analyses……..……..… 44
2.5.2. Assessment of Coral Reproducibility…….....…… 45
2.5.3. Assessment of Coral Diagenesis……...…… 47
2.5.4. Deriving δ^{18}Osw……...…… 49
2.5.5. Propagated Error Estimates...……..……...…… 49
2.5.5.1. Coral δ^{18}O Trend…….….. 49
2.5.5.2. Sr/Ca-derived SST……..… 50
2.5.5.3. δ^{18}Osw……..... 51
2.5.6. Comparison of SST Trends from Instrumental SST and Coral……...…….….. 53
2.6. Acknowledgements.……..... 54
2.7. Electronic Data Access……..... 54
2.8. Revised Error Propagation Analyses for Late 20th Century Trends in Coral δ^{18}O, Sr/Ca-derived SST and δ^{18}Osw…… 55
2.8.1. Coral δ^{18}O Trend…….. 55
2.8.2. Sr/Ca-derived SST Trend……. 57
2.8.3. δ^{18}Osw Trend…… 59
2.9. References……..... 63

CHAPTER 3: DECADAL-SCALE SST AND SALINITY VARIABILITY IN THE CENTRAL TROPICAL PACIFIC: SIGNATURES OF NATURAL AND ANTHROPOGENIC CLIMATE CHANGE...…. 67

3.1. Abstract……...……...……..... 67
3.2. Introduction..……...……...……..... 68
3.3. Methods……....……...…….……...…… 71
3.3.1. Study Site…….…..…… 71
3.3.2. Coral Sr/Ca Measurements…….……...… 73
3.3.3. Reconstructing SST and Salinity Records....……...… 73
3.3.4. Assessment of Diagenesis…….……...… 75

3.4. Results and Discussion..... 77
3.4.1. Interannual to Decadal-scale Tropical Pacific Climate Variability... 78
3.4.1.1. Sr/Ca-derived SST Variability..... 78
3.4.1.2. δ^{18}Osw-based Salinity Variability..... 82
3.4.2. Anthropogenic Signatures on Tropical Pacific Climate Variability 85
3.4.2.1. Sr/Ca-derived SST Trend..... 86
3.4.2.2. δ^{18}Osw-based Salinity Trend..... 86
3.5. Conclusion..... 88
3.6. Acknowledgements..... 89
3.7. Appendix..... 89
3.7.1. Data Availability..... 89
3.7.2. Error Propagation Analysis for Sr/Ca-derived SST Record..... 89
3.7.3. Error Propagation Analysis for $\delta^{18}O_{SW}$-based Salinity Record..... 90
3.8. References..... 93

VITA..... 99

LIST OF TABLES

Table 2.1. 1σ error estimates for coral $\delta^{18}O$ (‰) …….. 50

Table 2.2. 1σ error estimates for Sr/Ca-derived SST (ºC)……. 51

Table 2.3. 1σ error estimates for $\delta^{18}Osw$ (‰)……... 53

Table 2.4. Comparison of SST trends from instrumental SST datasets with our coral-derived SST record (in ºC) for each island for period 1972-1998... 54

Table 2.5. SST trends at the islands for different end-member years…… 54

Table 2.6. Late 20th century coral $\delta^{18}O$ trends and their associated errors at Palmyra, Fanning and Christmas…….. 56

Table 2.7. Late 20th century coral Sr/Ca-derived SST trends and their associated errors at Palmyra, Fanning and Christmas……..…….. 59

Table 2.8. Late 20th century coral-based $\delta^{18}Osw$ trends and their associated errors at Palmyra, Fanning and Christmas…….. 62

LIST OF FIGURES

Figure 1.1. Tropical Pacific climatology SST, salinity and precipitation…..……. 15

Figure 1.2. SST and precipitation during moderate and strong ENSO…….…. 16

Figure 1.3. The regression of SST anomalies with decadal-scale Pacific climate variability…….……..….. 18

Figure 1.4. Central tropical Pacific coral $\delta^{18}O$ records…...……... 21

Figure 2.1. Map of the study islands in the central tropical Pacific ……...….... 37

Figure 2.2. Comparison of coral Sr/Ca records with instrumental SST…...……. 40

Figure 2.3. Central tropical Pacific coral climate proxy records…..…… 42

Figure 2.4. Coral $\delta^{18}O$ reproducibility……...…… 46

Figure 2.5. Coral Sr/Ca reproducibility.....… 47

Figure 2.6. Comparison of coral surfaces with and without diagenesis……...…….. 48

Figure 2.7. Comparison of satellite-derived and *in situ* instrumental SST data from Palmyra…… 53

Figure 2.8. Uncertainty in coral $\delta^{18}O$ trend at Palmyra associated with analytical error……. 56

Figure 2.9. Uncertainty in coral Sr/Ca-derived SST trend at Palmyra associated with analytical error..... 57

Figure 2.10. Uncertainty in coral Sr/Ca-derived SST trend at Palmyra associated with slope error of the coral Sr/Ca-SST calibration……...……. 58

Figure 2.11. Uncertainty in coral-based δ^{18}Osw trend at Palmyra associated with analytical error in coral δ^{18}O……... 60

Figure 2.12. Uncertainty in coral-based δ^{18}Osw trend at Palmyra associated with analytical error in Sr/Ca……... 61

Figure 3.1. SST anomalies, precipitation anomalies and mean wind stress associated with eastern Pacific and central Pacific ENSO variability…. 72

Figure 3.2. Scanning electron microscope (SEM) images of the Palmyra modern coral……. 76

Figure 3.3. Palmyra coral monthly-resolved δ^{18}O, Sr/Ca-derived SST, and δ^{18}Osw records from 1886-1998…….. 77

Figure 3.4. Interannual and decadal-scale coral Sr/Ca-derived SST variability at Palmyra plotted with tropical Pacific instrumental climate indices…… 79

Figure 3.5. Regressions of Pacific SST anomalies with two indices of Pacific decadal-scale climate variability……. 81

Figure 3.6. Interannual and decadal-scale variability of the Palmyra coral δ^{18}Osw record plotted with instrumental climate indices……. 84

LIST OF SYMBOLS AND ABBREVIATIONS

$\delta^{18}O$	Oxygen isotopic composition
$\delta^{18}Osw$	Oxygen isotopic composition of seawater
CO_2	Carbon dioxide
Sr/Ca	The ratio of strontium to calcium
‰	Per mil or per thousand
CI	Confidence Interval
CTP	Central Tropical Pacific
CPW	Central Pacific Warming
DJF	December-January-February
EMI	ENSO Modoki Index
ENSO	El Niño-Southern Oscillation
EOF	Empirical Orthogonal Function
ERSST	Extended Reconstructed Sea-Surface Temperature
GCM	Global Climate Models or General Circulation Models
ICP-OES	Inductively Coupled Plasma Optical Emission Spectrometer
IGOSS	Integrated Global Ocean Services System
IPCC	Inter-governmental Panel on Climate Change
IPO	Interdecadal Pacific Oscillation
ITCZ	Inter-Tropical Convergence Zone
N_{eff}	Effective degrees of freedom
NECC	North Equatorial Countercurrent

NINO1.2	Boxed region of 90°W-80°W and 0°-10°S
NINO3	Boxed region of 150°W-90°W and 5°N-5°S
NINO3.4	Boxed region of 170°W-120°W and 5°S-5°N
NINO4	Boxed region of 160°E-150°W and 5°N-5°S
NPGO	North Pacific Gyre Oscillation
PDO	Pacific Decadal Oscillation
SEC	South Equatorial Counter Current
SEM	Scanning Electron Microscope
SOI	Southern Oscillation Index
SPCZ	South Pacific Convergence Zone
SST	Sea-Surface Temperature
SSTa	Sea-Surface Temperature Anomaly
SSS	Sea-Surface Salinity
TNI	Trans-Niño Index

SUMMARY

Accurate forecasts of future regional temperature and rainfall patterns in many regions largely depend on characterizing anthropogenic trends in tropical Pacific climate. However, strong interannual to decadal-scale tropical Pacific climate variability, combined with sparse spatial and temporal coverage of instrumental climate datasets in this region, have obscured potential anthropogenic climate signals in the tropical Pacific. In this dissertation, I present sea-surface temperature (SST) and salinity proxy records that span over the 20th century using living corals from several islands in the central tropical Pacific. I reconstruct the SST proxy records via coral Sr/Ca, that are combined with coral oxygen isotopic ($\delta^{18}O$) records to quantify changes in seawater $\delta^{18}O$ (hereafter $\delta^{18}Osw$) as a proxy for salinity.

Chapter 2 investigates the spatial and temporal character of SST and $\delta^{18}Osw$-based salinity trends in the central tropical Pacific from 1972-1998, as revealed by corals from Palmyra (6ºN, 162ºW), Fanning (4ºN, 159ºW) and Christmas (2ºN, 157ºW) Islands. The late 20th century SST proxy records exhibit warming trends that are larger towards the equator, in line with a weakening of equatorial Pacific upwelling over this period. Freshening trends revealed by the salinity proxy records are larger at those sites most affected by the Inter-Tropical Convergence Zone (ITCZ), suggesting a strengthening and/or an equatorward shift of the ITCZ. Taken together, the late 20th century SST and salinity proxy records document warming and freshening trends that are consistent with a trend towards a weakened tropical Pacific zonal SST gradient under continued anthropogenic forcing.

Chapter 3 characterizes the signatures of natural and anthropogenic variability in central tropical Pacific SST and δ^{18}Osw-based salinity over the course of 20th century using century-long coral proxy records from Palmyra. On interannual timescales, the SST proxy record from Palmyra tracks El Niño-Southern Oscillation (ENSO) variability. The salinity proxy record tracks eastern Pacific-centered ENSO events but is poorly correlated to central Pacific-centered ENSO events – the result of profound differences in precipitation and ocean advection that occur during the two types of ENSO. On decadal timescales, the coral SST proxy record is significantly correlated to the North Pacific Gyre Oscillation (NPGO), suggesting that strong dynamical links exist between the central tropical Pacific and the North Pacific. The salinity proxy record is significantly correlated to the Pacific Decadal Oscillation (PDO), but poorly correlated to the NPGO, suggesting that, as was the case with ENSO, these two modes of Pacific decadal climate variability have unique impacts on equatorial precipitation and ocean advection. However, the most striking feature of the salinity proxy record is a prominent late 20th century freshening trend that is likely related to anthropogenic climate change. Taken together, the coral data provide key constraints on tropical Pacific climate trends, and when used in combination with model simulations of 21st century climate, can be used to improve projections of regional climate in areas affected by tropical Pacific climate variability.

CHAPTER 1

INTRODUCTION

1.1. Tropical Pacific Climate

The tropical Pacific's significant role in the global climate system highlights the need to constrain its natural and anthropogenic variability in order to improve regional climate projections. Analyses of instrumental and historical climate records over the last decades have identified strong internal climate variability in the Pacific basin that has widespread repercussions for climate patterns and ecosystems on interannual to decadal timescales [*McPhaden et al*., 2006; *Chavez et al*., 2003]. Such strong internal climate variability makes it challenging to characterize tropical Pacific climate changes under anthropogenic greenhouse gas forcing that is projected to accelerate in the coming decades [*IPCC*, 2007]. The signatures of anthropogenic forcing in the tropical Pacific climate may manifest as changes in the characters of natural tropical Pacific climate variability as well as in the mean state of tropical Pacific climate [c.f. *Latif and Keenlyside*, 2009; *Collins et al*., 2010]. The following sub-sections review the characteristics of interannual to decadal-scale natural tropical Pacific climate variability and potential anthropogenic signatures in tropical Pacific climate, as revealed by analyses of instrumental and proxy climate datasets as well as numerical climate model outputs.

1.1.1. Interannual El Niño-Southern Oscillation (ENSO) Variability

The tropical Pacific is the center of action for the El Niño-Southern Oscillation (ENSO) phenomenon, which is the largest source of natural global-scale temperature

[*Deser et al*., 2010] and precipitation variability on interannual timescales [*Dai et al*., 1997]. The tropical Pacific climate is characterized by a strong zonal sea-surface temperature (SST) gradient (the eastern equatorial Pacific is roughly 10ºC cooler than the western equatorial Pacific), that is maintained by trade winds associated with the atmospheric Walker Circulation. In this tightly coupled ocean-atmosphere system, strong easterly winds along the equator drive the upwelling of cooler waters from depth in the central and eastern equatorial Pacific, leading to atmospheric subsidence associated with the descending branch of the Walker Cell. Conversely, warmer waters in the Western Pacific Warm Pool region drive deep convection associated with the ascending branch of the Walker Circulation.

Every 2-7 years, the warm phase of ENSO, referred to as El Niño, brings warm SST and positive rainfall anomalies to the eastern and central tropical Pacific while precipitation deficits occur in the Western Pacific Warm Pool [*Rasmusson and Carpenter*, 1982]. In a feedback first identified by *Bjerknes* [1969], weakened trade winds, perhaps initially associated with a westerly wind burst [*Luther et al*., 1983], lead to a reduction in upwelling and associated warm SST anomalies in the central and eastern equatorial Pacific. The resulting reduction in the tropical Pacific zonal SST gradient weakens the Walker circulation and its associated trade winds [*Lindzen and Nigam*, 1987], which in turn further warms the central and eastern equatorial Pacific. Conversely, the strengthening of the Walker Circulation during the cold phase of ENSO or La Niña enhances the zonal SST gradient across the tropical Pacific, thereby leading to anomalously cool and dry conditions in the central and eastern tropical Pacific, with wetter conditions in the western tropical Pacific. On average, ENSO anomalies persist for

roughly six months, although ENSO is skewed such that El Niño events tend to be stronger and more frequent than La Niña events [*Burgers and Stephenson*, 1999]. The propagation of ENSO-driven temperature and precipitation anomalies to extratropics and adjoining ocean basins via atmospheric teleconnections [*Diaz et al.*, 2001; *Alexander et al*., 2002] accounts for the pervasive impact of ENSO on the global climate system. Indeed, El Niño increases the global temperature in the order of +0.1ºC [*Jones*, 1989].

Theoretical works suggest that ENSO may be a self-sustained oscillatory mode or a damped stable mode of the coupled tropical ocean-atmosphere system. *Wyrtki* [1975] identified an important role of equatorial easterly winds in maintaining a zonal sea-level gradient across the equatorial Pacific. With a collapse of the trade winds during El Niño, warm waters begin to spread into the central and eastern Pacific. The delayed oscillator theory [*Suarez and Schopf*, 1988; *Battisti and Hirst,* 1989] hypothesizes that wind perturbation in the equatorial Pacific excites an eastward-moving equatorial downwelling Kelvin wave that deepens the thermocline in the eastern equatorial Pacific during El Niño. At the same time, the off-equatorial wave response to the wind perturbation propagates westward as Rossby waves that are reflected by the western boundary as an eastward upwelling Kelvin wave – thereby leading to the recovery of the eastern equatorial Pacific thermocline. Others have proposed variations in the oscillatory mechanisms, such as the recharge oscillator that involves the discharge of heat from the tropics to higher latitudes [*Jin*, 1997]. Alternatively, other theoretical studies conceive of ENSO as a damped stable mode that requires stochastic atmospheric forcing to maintain the oscillation [*Penland and Sardeshmukh*, 1995; *Moore and Kleeman*, 1999]. Observational data lend supports for the propagation of Kelvin waves during El Niño

[*McPhaden*, 1999], and the reflection of the Rossby waves at the western boundary [*Boulanger et al*., 2003]. Synoptic events of westerly wind bursts that may be associated with the Madden-and-Julian Oscillation have also been shown to initiate ENSO occurrences [*Zhang and Gottschalck*, 2002].

The evolution of ENSO extremes as revealed by a network of ocean-atmosphere observation systems in the equatorial Pacific exhibits strong event-to-event variations [*McPhaden et al*., 1998]. Variations in the amplitude of SST anomalies in the eastern Pacific associated with El Niño extremes can range from 0-2ºC for a "very weak" event to >3ºC for a "strong" event [*Quinn et al.*, 1978]. However, considerable differences also exist in the spatial and temporal evolution of ENSO extremes. For example, satellite observations during the strong 1982/83 El Niño event identify an eastward phase propagation of anomalous warm SSTs, which is distinct from the westward propagating of many other El Niño events [*Gill and Rasmusson*, 1983; *Philander*, 1990]. And among ENSO events of similar intensity, their durations may also vary. For example, the 1972/73 El Niño was 4 months longer than the 1976/77 El Niño event [*Trenberth*, 1997], although both events shared similar westward phase propagation. The observed heterogeneity in ENSO event magnitudes and evolutions highlights the complexity of the physical mechanisms that can give rise to ENSO occurrences, and challenges existing theories of ENSO mechanisms [c.f. *Neelin et al*., 1998; *Wang and Picaut*, 2004].

While canonical ENSO is characterized by anomalous warming in the central and eastern equatorial Pacific, recent studies have identified an expression of ENSO that is characterized by maximum anomalies in the central tropical Pacific [*Latif et al*., 1997*; Trenberth and Stepahaniak,* 2001*; Larkin and Harrison,* 2005*; Ashok et al.,* 2007*; Kao*

and Yu, 2009; *Kug et al.,* 2009]. Indeed, central Pacific ENSO represents the second leading mode of tropical Pacific SST variability after the canonical eastern Pacific ENSO pattern [*Trenberth and Stephaniak*, 2001; *Ashok et al.*, 2007; *Kao and Yu*, 2009]. This mode of ENSO gained much attention following a series of "persistent" El Niño events from 1990-1994, when the warmest SST anomalies occurred in the central tropical Pacific [*Kleeman et al.,* 1996*; Trenberth and Hoar,* 1996*; Goddard and Graham,* 1997]. More recently, this pattern has been studied under different names, including the "dateline ENSO" [*Larkin and Harrison,* 2005], the "ENSO Modoki" [*Ashok et al.,* 2007], the "central Pacific ENSO" [*Kao and Yu,* 2009], and the "warm pool ENSO" [*Kug et al.,* 2009]. The concentrated warming in the central tropical Pacific drives teleconnection patterns that differ appreciably from those associated with canonical El Niño [*Weng et al*., 2009]. For example, the central Pacific warming pattern has been linked to changes in ENSO teleconnections to the western Pacific [*Wang and Hendon*, 2007] and the Asian monsoon [*Kumar et al*., 2006], as well as an increase in the frequency of tropical cyclones in the Pacific and Atlantic basins [*Kim et al*., 2009; *Chen and Tam*, 2010].

In order to study the time history of ENSO variability, researchers have developed a wide variety of instrumental climate indices. The atmospheric component of ENSO variability is well-captured by the Southern Oscillation Index (SOI), defined as the sea level pressure difference between Tahiti and Darwin, which captures large-scale changes in the Walker Circulation. SST anomalies averaged across the central and eastern tropical Pacific – defined as the NINO3.4 region (170°W-120°W and 5°S-5°N) – has been widely used as an index for ENSO, because this region reflects the locus of maximum atmospheric sensitivity to ENSO SST anomalies [*Trenberth*, 1997]. However, these two

popular ENSO indices are not sufficient to isolate ENSO variability associated with the central Pacific ENSO mode. *Trenberth and Stephaniak* [2001] proposed an additional ENSO index orthogonal to the NINO3.4 SST index called the Trans-Niño Index (TNI) that better captures the evolution of central Pacific ENSO. The TNI is derived by taking the difference of SST anomalies between the eastern (NINO1.2 region of 90°W-80°W, 0°-10°S) and the west-central (NINO4 region of 160°E-150°W, 5°N-5°S) equatorial Pacific. *Ashok et al*. [2007] developed an index for ENSO Modoki, characterized by warm SST anomalies in the central Pacific flanked by cooler SST anomalies to the west and east. The ENSO Modoki Index is defined as the mean warm SST anomalies in the central tropical Pacific (165°E-140°W, 10°N-10°S) that is subtracted by half of the mean cold SST anomalies in the eastern (110°W-70°W, 5°N-15°S) and western (125°E-145°E, 20°N-10°S) tropical Pacific. The central Pacific ENSO indices are generally only weakly correlated to the SOI and/or NINO3.4 SST anomaly, perhaps indicative of different physical mechanisms underlying the two ENSO modes [*Trenberth and Stephaniak*, 2001; *Ashok et al*., 2007; *Kug et al*., 2009].

1.1.2. Pacific Decadal Climate Variability: Characteristics and Mechanisms

The Pacific Ocean exhibits significant natural decadal-scale climate variability. To date, two different modes of Pacific decadal variability have been isolated: the Pacific Decadal Oscillation and the North Pacific Gyre Oscillation.

The Pacific Decadal Oscillation (PDO), defined as the leading mode of SST variability in the North Pacific, has spatial patterns of anomalous SST that resemble those of the eastern Pacific ENSO [*Mantua et al.*, 1997]. Compared to the eastern Pacific

ENSO, the PDO has weaker warm anomalies in the tropical Pacific but stronger cold anomalies in the northwest Pacific associated with a strengthening the atmospheric Aleutian Low pressure system. A proposed "regime shift" of the PDO in the mid-1970s was associated with strong impacts to marine ecosystems in the Pacific basin [*Chavez et al*., 2003], and was well-documented in instrumental data [*Nitta and Yamada*, 1989; *Graham*, 1994; *Trenberth and Hurrell*, 1994; *Mantua et al*., 1997; *Zhang et al*., 1997]. Over the length of the instrumental record, the PDO exhibits an approximately ~20-30-year periodicity, with a cool phase persisting from the mid-1940's to the mid 1970's. *Power et al.* [1999] identified the Interdecadal Pacific Oscillation (IPO) as the Pacific basin-wide manifestation of the PDO that includes a southern hemisphere component. Reconstructions of the PDO based on a network of centuries-long tree-rings and coral-based climate proxy records have provided valuable insights on the long term evolution of the PDO over the last several centuries [*Evans et al*., 2000a; *Biondi et al*., 2001; *Gedalof et al*., 2002].

Climate model simulations have proposed several mechanisms for Pacific decadal climate variability, all involving ocean-atmosphere feedbacks in both the tropics and the extratropics. On one hand, climate dynamics in the tropics may give rise to decadal-scale variability without involving feedbacks in the extratropics [*Timmermann and Jin*, 2002]. Climate anomalies in the tropical Pacific can propagate efficiently to the extratropics via the atmospheric bridge teleconnections [*Alexander et al*., 2002]. Decadal-scale SST variability in the North Pacific may also result from the low-passed integration of ENSO-related atmospheric variability in the extratropical ocean [*Newman et al*., 2003]. Alternatively, climate models suggest that the PDO could originate from stochastically

driven atmospheric variability and the oscillatory mode of the coupled ocean-atmosphere system in the North Pacific [*Latif and Barnett*, 1994; *Barnett et al*., 1999]. Schneider and Cornuelle [2005] proposed that the PDO may represent the integration of atmospheric variability associated with the Aleutian Low by the North Pacific Ocean. The propagation of climate anomalies in the North Pacific into the tropics can be conveyed via the Subtropical Cell [*Gu and Philander*, 1997; *Kleeman et al*., 1999], the source of almost half of the thermocline waters in the eastern equatorial Pacific [*McCreary and Lu*, 1994]. Changes in the strength of the Subtropical Cell may also play a role in regulating decadal-scale tropical Pacific SST variability, as shown in observational [*McPhaden and Zhang*, 2002] and modeling studies [*Kleeman et al*., 1999].

The North Pacific Gyre Oscillation (NPGO) is the second leading SST mode in the North Pacific, characterized by cool anomalies in the northwest Pacific, warm anomalies in the Gulf of Alaska, and warming in the central tropical Pacific [*Di Lorenzo et al*., 2008]. Whereas the PDO is the oceanic expression of variations in the Aleutian Low linked to ENSO [*Newman et al*., 2003], the NPGO has been linked to variations in the atmospheric North Pacific Oscillation [*Chhak et al*., 2009], which may be driven by central Pacific ENSO [*Di Lorenzo et al*., submitted]. Previous studies have identified a range of dynamical feedbacks between the North Pacific and the central tropical Pacific. North Pacific Oscillation variability in the boreal spring drives SST anomalies in the central tropical Pacific that precondition the mature phase of ENSO in the ensuing winter via the seasonal footprinting mechanism [*Anderson*, 2003; *Vimont et al*., 2003]. Some studies suggest that the equatorial Pacific may also influence the North Pacific Oscillation [*Anderson*, 2004]. Taken together, the dynamical feedbacks between climate

variability in the tropical Pacific and the North Pacific may support sustained decadal-scale oscillations in the Pacific Ocean [*Di Lorenzo et al*., submitted].

1.1.3. Anthropogenic Signatures of Tropical Pacific Climate

The signatures of anthropogenic forcing in tropical Pacific climate may manifest as (i) changes in the frequency and/or amplitudes of natural tropical Pacific climate variability, and/or (ii) a shift in the mean state of tropical Pacific climate.

Analyses of instrumental climate data and numerical climate model outputs present a broad range of scenarios for anthropogenic climate trends in the tropical Pacific. The observation that El Niño events have become stronger and more frequent since the 1970s has been attributed to anthropogenic forcing by some researchers [*Trenberth and Hoar*, 1997]. Indeed, a high resolution climate model of the tropical Pacific projected an increase in ENSO frequency under continued greenhouse forcing [*Timmermann et al*., 1999]. Although global climate models are skilled in simulating ENSO with several months' lead time, currently there is no consensus on the response of ENSO to global warming [c.f. *Meehl et al*., 2007; *Latif and Keenlyside*, 2009; *Collins et al*., 2010]. Recent work has identified a shift towards central Pacific ENSO events at the expense of canonical ENSO events in observations [*Ashok et al*., 2007] and the Intergovernmental Panel on Climate Change (IPCC) model projections [*Yeh et al*., 2009], but uncertainties in the instrumental data and model physics are significant.

Trends in the mean climate of the tropical Pacific under anthropogenic forcing have largely been discussed in terms of "ENSO-like" shifts. There is a long standing debate between research that suggests a weakening [*Knutson and Manabe*, 1995; *Meehl*

and Washington, 1996] and a strengthening [*Clement et al*., 1996; *Cane et al*., 1997] of the tropical Pacific zonal SST gradient. These studies identify various physical mechanisms that may be critical to future climate projections. One of the mechanisms underlying a weakened zonal SST gradient in climate models is the cloud-albedo feedback, which limits SST warming in the western tropical Pacific [*Meehl and Washington*, 1996]. Increased water vapor in the atmosphere under global warming is predicted from the Clausius-Clapeyron relationship, and implies a weakening of the tropical Walker Circulation, which would reduce the zonal SST gradient along the equatorial Pacific [*Vecchi at al*., 2006]. On the other hand, according to the dynamical "ocean thermostat" hypothesis [*Clement* et al., 1996; *Cane et al.*, 1997], uniform warming over the tropical Pacific would result in immediate warming of the Western Pacific Warm Pool region and inefficient warming of the eastern Pacific cold tongue region, thereby increasing trade winds and the zonal SST gradient. Conflicting climate model simulations and large uncertainties in gridded instrumental datasets [*Vecchi et al*., 2008] have perpetuated the debate.

Recent work has suggested that the signatures of anthropogenic forcing in the tropical Pacific may manifest as warming trends along the equator [*DiNezio et al*., 2009] that are more pronounced in the central Pacific [*Xie et al.*, 2010]. Indeed, the two leading empirical orthogonal functions (EOFs) in tropical Pacific SST trends show warming trends across the basin as well as a cooling trend in the equatorial eastern Pacific [*Lau and Weng*, 1999]. A central tropically-weighted warming trend echoes the proposed increased frequency of ENSO Modoki events under global warming [*Ashok et al*., 2007; *Yeh et al.,* 2009], yet is difficult to confirm in instrumental climate records.

While anthropogenic SST trends in the tropical Pacific likely depend on ocean-atmosphere dynamics in the basin, hydrologic trends in the basin may be shaped by the global atmospheric response to a warming climate. Under the Clausius-Clapeyron relationship, the water vapor concentration in the lower troposphere would increase by ~7% per 1ºC warming, but the rate of precipitation increases more slowly at about ~2% per 1ºC warming. The differential rates of responses of water vapor and precipitation to surface warming increases the residence of water vapors in the atmosphere, implying a weakening of the large-scale atmospheric circulation. This implies an enhancement of the global hydrological patterns that would bring more precipitation to convective regions in the tropical Pacific [*Held and Soden*, 2006]. Indeed, increased precipitation in the tropical Pacific has been observed in rain gauge measurements [*Morrissey and Graham*, 1996], as well as seawater freshening trends inferred from instrumental salinity data [*Delcroix et al.*, 2007].

1.2. Central Tropical Pacific Coral Proxy Climate Records

The reconstruction of paleoclimate proxy records has played a vital role in complementing the coverage of instrumental datasets to enable the detection of anthropogenic climate trends against a long-term natural climate baseline [*IPCC*, 2007]. The need for paleoclimate proxy records is great in the tropical Pacific, where instrumental climate data are particularly sparse [*Deser et al.*, 2010]. Indeed, the calculation of tropical Pacific climate trends from gridded instrumental datasets has provided conflicting results, due to different interpolation techniques used to fill the missing data points in both space and time [*Hurrell and Trenberth*, 1999*; Rayner et al.*,

2009]. The following sub-sections review the principles of coral paleoclimate reconstruction (section 1.2.1), describe the research sites (section 1.2.2), and provide an overview of existing coral climate proxy records in the tropical Pacific (section 1.2.3).

1.2.1. Overview of Coral Paleoclimate Reconstruction

High-resolved, decades- to centuries-long coral-based climate proxy records provide valuable insights for the study of low-frequency tropical Pacific climate variability. Typically sub-monthly resolved coral-based climate proxy records rival the resolution of instrumental datasets for studying climate variability of the last century. Bathed in the tropical ocean waters, coral skeletal geochemistry provides direct records of tropical SST and hydrological variability that, unlike instrumental climate data from this region, are continuous and unbiased through time.

Coral reconstructions of past tropical climates most commonly utilize the oxygen isotopes composition ($\delta^{18}O$) of the coral skeleton, which are sensitive to changes in SST and hydrology. Coral $\delta^{18}O$ is measured in coral powders on a mass spectrometer, and is reported in units of per mil or per thousand, according the following definition:

$$\delta^{18}O\ (‰) = \left[\left[\frac{(^{18}O/^{16}O)_{sample}}{(^{18}O/^{16}O)_{standard}}\right] - 1\right] \times 1000 \qquad \text{(Eq. 1.1)}$$

The temperature-dependent fractionation of $\delta^{18}O$ in carbonates exhibits a change of roughly -0.22‰ per 1ºC increase in temperature [*Eipstein et al*., 1953]. However, as the $\delta^{18}O$ of seawater changes in response to evaporation-precipitation cycles (more positive under net evaporation and more negative under net precipitation [*Dansgaard*, 1964]), corals also record changes in seawater $\delta^{18}O$ (hereafter $\delta^{18}Osw$) through time. Therefore,

potentially large changes in δ^{18}Osw arising from hydrological variability in the tropics generally make it impossible to determine a simple coral δ^{18}O-SST relationship at any given site. However, as warm waters (lower coral δ^{18}O) tend to drive deep convection in the tropical Pacific (lower coral δ^{18}O), it is often assumed that lower coral δ^{18}O reflects warmer and/or wetter conditions, and vice versa for higher coral δ^{18}O [c.f. *Corrège*, 2006; *Grottoli and Eakin*, 2007].

Coral Sr/Ca has been extensively developed as a proxy for SST [*Beck et al*., 1992; *Alibert and McCulloch*, 1997)], and can be measured in tandem with coral δ^{18}O to isolate changes in SST and δ^{18}Osw though time [*Corrège*, 2006 and references therein]. Paired measurements of coral δ^{18}O and Sr/Ca allow us to derive the residual seawater δ^{18}O by removing the Sr/Ca-derived SST contribution from coral δ^{18}O. *Fairbanks et al*. [1997] resolved a linear relationship between δ^{18}Osw and sea-surface salinity in the central tropical Pacific, such that the δ^{18}Osw-based salinity proxy can be used to reconstruct tropical Pacific hydrology in this region.

Reconstructions of coral climate proxy records must control for the potential impacts of diagenesis on the coral skeletal geochemistry that may compromise the fidelity of the records. Although living corals are less likely to experience diagenesis than fossil corals, studies have documented evidence of diagenesis in living corals [*Enmar et al*., 2000; *Quinn and Taylor*, 2006; *Hendy et al*., 2007]. Diagenesis may take the forms of secondary aragonite precipitation, dissolution, and calcite precipitation. Secondary aragonite increases coral δ^{18}O and Sr/Ca ratios, yielding a cool SST bias in the resulting coral paleoclimate record that can go unnoticed without careful screening. Dissolution

also yields a cool bias [*Hendy et al*., 2007], whereas calcite yields a warm bias in coral Sr/Ca ratios [*McGregor and Gagan*, 2003].

1.2.2. Description of Line Islands Study Sites

This dissertation presents 20th century coral $\delta^{18}O$, Sr/Ca and $\delta^{18}Osw$ records from Palmyra (6ºN, 162ºW), Fanning (4ºN, 159ºW) and Christmas (2ºN, 157ºW) Islands of the Line Islands chain in the central tropical Pacific.

1.2.2.1. Climatology

Mean climate conditions in the central tropical Pacific are characterized by strong meridional SST gradients associated with the influence of zonal ocean currents in the equatorial Pacific (Figure 1.1a). Palmyra at the northern end, is bathed by the eastward-flowing North Equatorial Counter Current (NECC) that advects warm waters from the Western Pacific Warm Pool at a speed of about 20 cm/second [*Philander*, 1990]. At 2ºN, SST variability at Christmas is influenced by the westward-flowing South Equatorial Current (SEC) that advects cold upwelled waters at a speed of about 100 cm/second. Thus, average SSTs decrease from Palmyra to Fanning to Christmas, with average values of ~28.5ºC, ~28.0ºC and ~27.5ºC, respectively [*Reynolds et al*., 2002].

Central tropical Pacific precipitation is influenced by the presence of the Inter-Tropical Convergence Zone (ITCZ) that drives a strong salinity gradient across the Line Islands (Figure 1.1b). Residing just north of Palmyra at 10°N, the ITCZ brings high precipitation to Palmyra (~10 mm/day), while the mean annual precipitation decreases towards Christmas (~5 mm/day at Fanning and ~2 mm/day at Christmas) [*Xie and Arkin*,

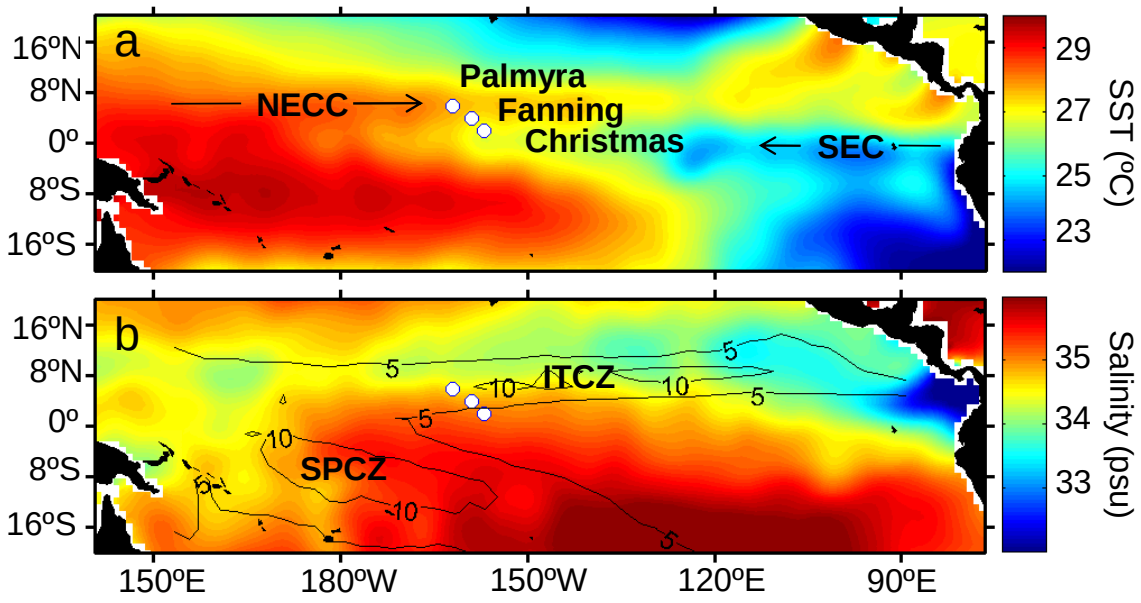

Figure 1.1. Tropical Pacific climatology SST, salinity and precipitation. (a) Climatology Dec-Jan-Feb (DJF) SST (color, in ºC) in the tropical Pacific showing the eastward flowing North Equatorial Counter Current (NECC) warm waters and the westward flowing South Equatorial Current (SEC) cold waters that drive strong SST gradient across the study islands. **(b)** Climatology DJF salinity (color, in psu) and rainfall (contour, in mm/day) showing high convection in the Inter-Tropical Convergence Zone (ITCZ) along northern tropical Pacific, and the South Pacific Convergence Zone (SPCZ) in the southwestern tropical Pacific. The strong precipitation associated with the ITCZ drives a strong sea-surface salinity gradient across the study islands. SST and salinity data from *Levitus et al*. [1994], and precipitation data from *Xie and Arkin* [1997].

1997]. Given the strong influence of precipitation minus evaporation balance on salinity in the tropics, the strong precipitation gradient is well-reflected in sea-surface salinity across the Line Islands (~34.8 psu at Palmyra, ~34.9 psu at Fanning, and ~35.1 psu at Christmas) [*Levitus et al*., 1994].

Seasonally, changes in the inter-hemispheric heating gradient weaken (strengthen) trade winds during boreal summer (winter) in the central tropical Pacific, affecting the strength of zonal ocean currents in the equatorial Pacific. Northeasterly winds during boreal winter drive cool and saline upwelled equatorial waters into the islands, whereas southeasterly winds that occur during boreal summer weaken the Ekman-driven

upwelling and the strength of the SEC. The seasonal SST variability is ~1.3-1.5°C at these islands, while the salinity variability is ~0.2-0.3 psu [*Levitus et al.*, 1994].

1.2.2.2. Interannual Variability

The central tropical Pacific islands experience warming and freshening anomalies during El Niño events, and vice versa during La Niña (Figure 1.2a, b). The anomalous warming is largest in the eastern to central equatorial Pacific, such that El Niño warm

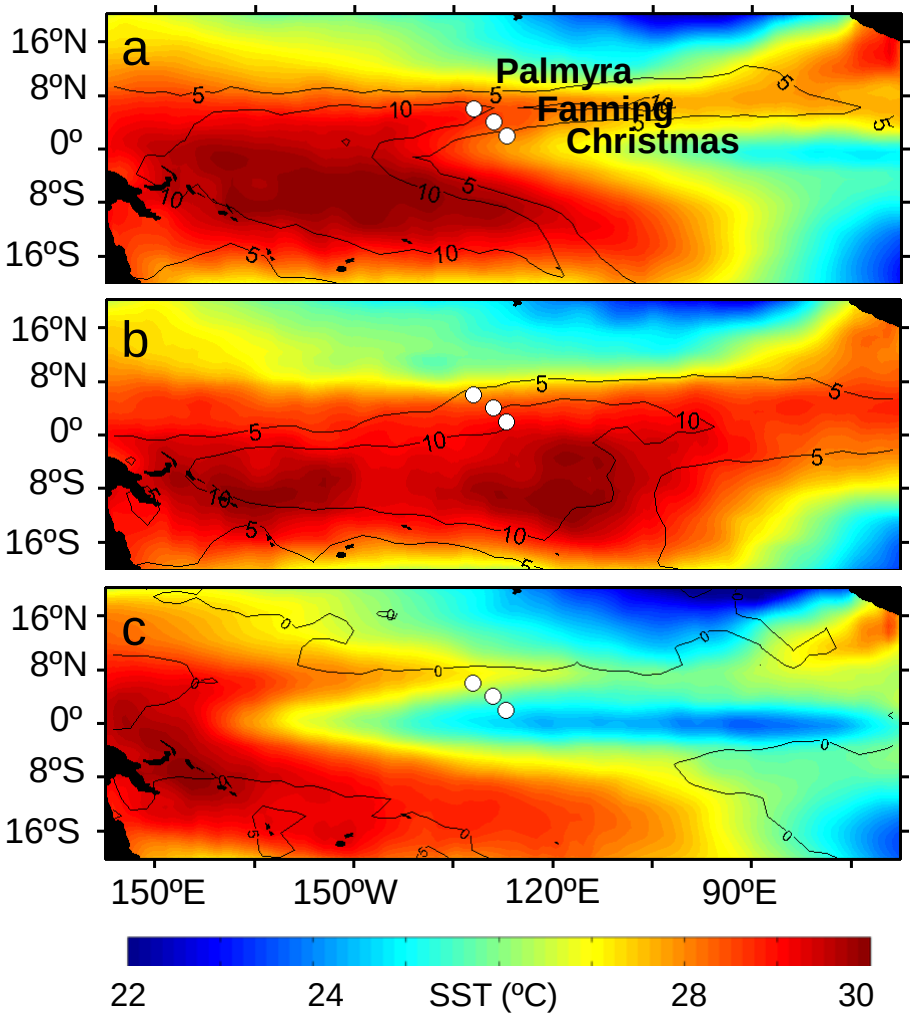

Figure 1.2. SST and precipitation during moderate and strong ENSO. Dec-Jan-Feb (DJF) SST during: **(a)** moderate (NINO3.4 SST anomalies between 1-2ºC) 1986/87 and 1994/95 El Niño events. **(b)** Strong (NINO3.4 SST anomalies >2ºC) 1982/83 and 1997/98 El Niño events. **(c)** Strong (NINO3.4 SST anomalies reached -2ºC) 1988/89 and 1998/99 La Niña events. SST dataset of *Reynolds et al.* [2002].

anomalies are stronger at Christmas. El Niño SST anomalies drive an equatorward movement of the ITCZ that causes enhanced precipitation across all the Line Islands. The largest events bring the greatest precipitation increase on the equator, while moderate events are characterized by large precipitation increases off the equator, along the ITCZ. During moderate El Niño events (NINO3.4 SST anomalies between 1-2ºC), the precipitation anomaly at Christmas is ~+0.5 mm/day but can reach ~+3 mm/day at Palmyra, whereas the strongest precipitation anomaly at Christmas that occur during strong El Niño events (NINO3.4 SST > 2ºC) can be as high as ~+6 mm/day. Anomalous SST patterns are fairly similar for a range of magnitudes of La Niña events, characterized by cold (up to ~2ºC) anomalies and reduced precipitation that are associated with a strengthening of wind-driven upwelling along the equator (Figure 1.2c).

1.2.2.3. Decadal Variability

The PDO warm regime and the NPGO cold regime bring anomalous warming to the central tropical Pacific that are weaker in magnitude than those associated with ENSO (Figure 1.3). Similar to the eastern tropical Pacific ENSO, warming anomalies associated with the PDO extend from the eastern tropical Pacific to the northeast Pacific, but with distinctively strong cool anomalies in the northwest Pacific. The central tropical Pacific warming associated with the NPGO on the other hand, does not extend to the eastern tropical Pacific. In the North Pacific, the NPGO also shows distinct imprints of strong anomalous warming that is concentrated in the Gulf of Alaska, and cool SST anomalies in the northwest Pacific that are smaller and shifted southward compared to those associated with the PDO.

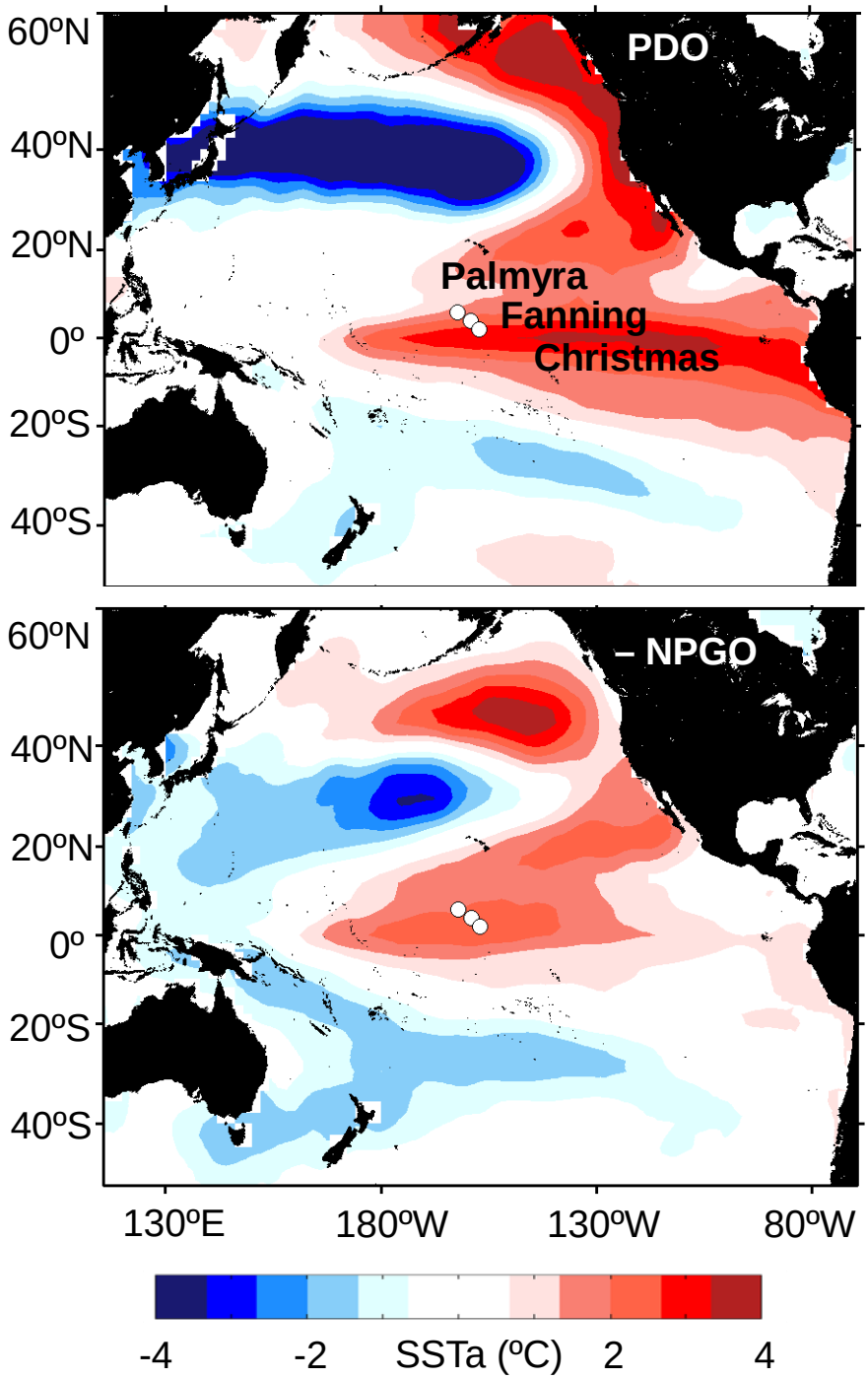

Figure 1.3. The regression of SST anomalies with decadal-scale Pacific climate variability. (a) The Pacific Decadal Oscillation index [*Mantua et al*., 1997], and **(b)** the North Pacific Gyre Oscillation index [*Di Lorenzo et al*., 2008]. SST dataset of *Reynolds et al.* [2002].

The impacts of decadal-scale Pacific climate variability on precipitation patterns in the tropical Pacific are difficult to quantify given the sparse availability of instrumental rainfall data in the tropical Pacific Ocean. Continuous satellite-based rainfall record has only been available since the late 1970s [*Xie and Arkin*, 1997], making it difficult to characterize any decadal-scale variations. Analysis of compiled ship-based salinity datasets from the tropical Pacific hints at PDO-like variability in salinity [*Delcroix et al*., 2007], which is likely integrated in the ocean on decadal timescales. The influence of the NPGO on tropical Pacific hydrology is still unknown, although a strong relationship between the NPGO and salinity has been revealed in the North Pacific, the result of changes in wind-driven ocean advection [*Di Lorenzo et al.*, 2008].

1.2.3. Overview of Central Tropical Pacific Coral Records

Coral $\delta^{18}O$ records from the central tropical Pacific have provided key information on ENSO and decadal-scale Pacific climate variability that complement short instrumental climate timeseries in the region [*Cole et al*., 1993; *Evans et al*., 1999; *Guilderson and Schrag*, 1999; *Urban et al*., 2000; *Cobb et al*., 2001]. The correlation between central tropical Pacific coral $\delta^{18}O$ records and ENSO indices are uniformly high (R=-0.84 at Palmyra [*Cobb et al*., 2001] and Christmas [*Evans et al*., 1999] for their interannual 2-7-year components), which enables the reconstruction of global large-scale ENSO variability through the last several centuries [e.g. *Evans et al*., 2000b]. Central tropical Pacific coral $\delta^{18}O$ records have revealed significant ENSO variability throughout the past centuries, including a strong 3-year periodicity in the early 20^{th} century that gave way to a 5-year periodicity in the 1940-1950s [*Cole et al*., 1993; *Urban et al*., 2000].

Such observations lend observational support to theoretical studies on changes in ENSO frequency under different mean ocean-atmospheric states [*Fedorov et al*., 2000]. Central tropical Pacific coral $\delta^{18}O$ records also capture decadal-scale variability associated with the PDO [*Linsley et al*., 2000], as well as a significant spectral density peak at 10-16-year periodicities [*Cobb et al*., 2001; *Holland et al*., 2007]. As with interannual variability, decadal-scale tropical climate variability exhibits strong temporal variations, most notably a trend towards weaker decadal-scale variability since the early 20th century [*Ault et al*., 2009].

The most striking features of coral $\delta^{18}O$ records from the central tropical Pacific is their late 20th century trends toward depleted coral $\delta^{18}O$ values, implying warming and/or freshening (Figure 1.4) [*Cole et al*., 1993; *Guilderson and Schrag*, 1999; *Urban et al*., 2000; *Cobb et al*., 2001]. The onset and magnitude of these coral $\delta^{18}O$ trends vary from site to site, and it is important to remember that undetected diagenesis - secondary aragonite precipitation at the base of the record - may contribute to 20th century trends towards depleted coral $\delta^{18}O$. Nevertheless, the coral $\delta^{18}O$ trends are a robust feature of coral records from the central tropical Pacific. Coral $\delta^{18}O$ records reconstructed using fossil corals from Palmyra suggest that the 20th century warming and/or freshening trend are likely unprecedented in the last millennium (Figure 1.4a), therefore hinting at the signature of anthropogenic forcing on tropical Pacific climate [*Cobb et al*., 2003].

However, the attributions of SST and hydrology on late 20th century coral $\delta^{18}O$ trends have been difficult to resolve without accompanying records of coral Sr/Ca-based SST. To date, only a very short (5 year-long) Sr/Ca record is available from the central tropical Pacific [*Evans et al*., 1999]. Most long paired coral $\delta^{18}O$ and Sr/Ca records are

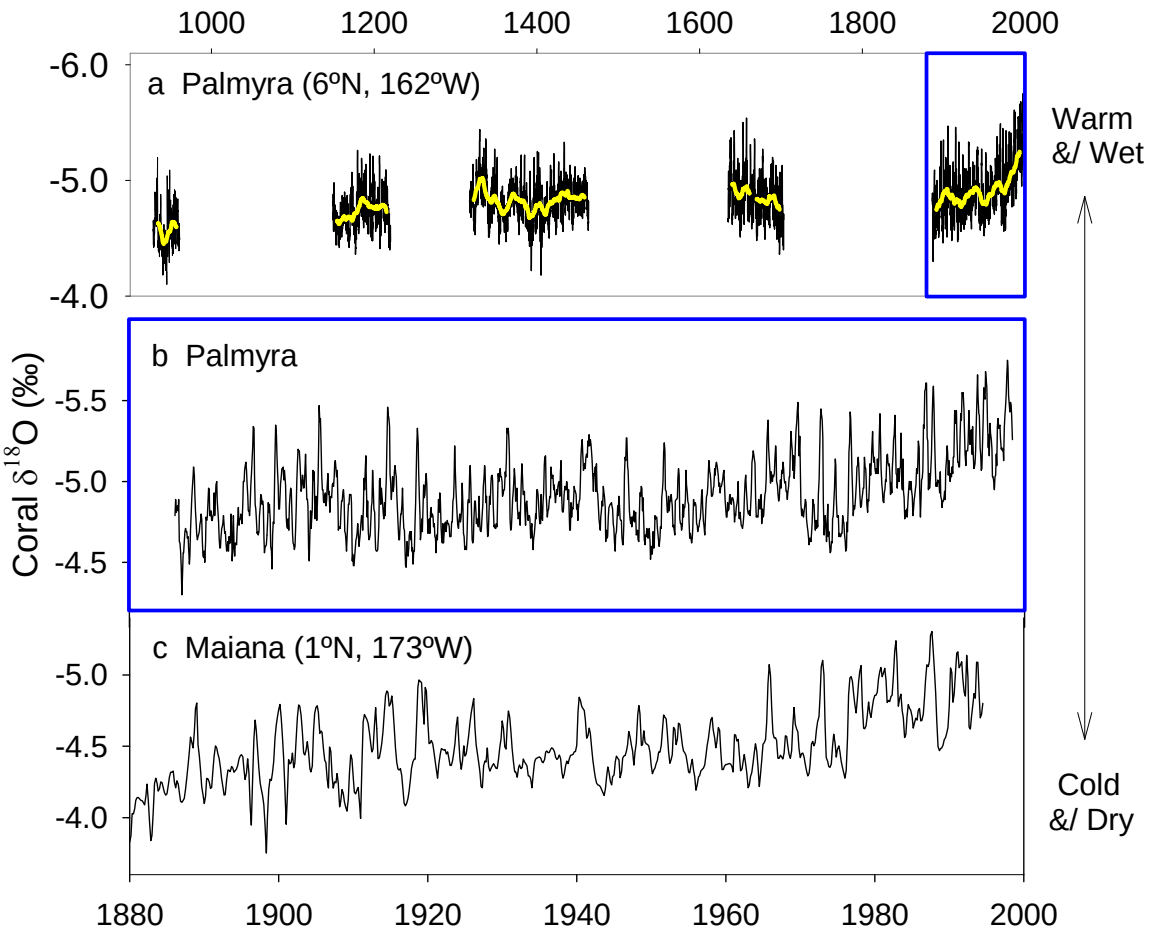

Figure 1.4. Central tropical Pacific coral $\delta^{18}O$ records from (a) Palmyra that spans over the last millennium [*Cobb et al*., 2001, 2003]. **(b)** The 20th century section of the Palmyra record. **(c)** Maiana [*Urban et al*., 2000]. The records exhibit late 20th century trends towards depleted values.

available from the southwest Pacific, which resolve strong trends towards depleted δ^{18}Osw (freshening) associated with a 20th century expansion of the SPCZ [*Kilbourne et al*., 2004] that may be unprecedented since ~1800AD [*Linsley et al*., 2006]. *Wu et al*. [in review] reconstructed Sr/Ca-based SST and δ^{18}Osw records from the Clipperton Atoll in the eastern tropical Pacific, and uncovered a weak trend towards more saline conditions. Given the motley and incomplete picture of 20th century coral δ^{18}Osw trends from different sites in the tropical Pacific, new coral-based Sr/Ca and δ^{18}Osw records from the

Line Islands are required to refine our understanding of anthropogenic impacts on tropical Pacific climate. This dissertation addresses the characters of tropical Pacific climate changes over the 20th century using coral $\delta^{18}O$, coral Sr/Ca and $\delta^{18}Osw$ records from the Line Islands of the central tropical Pacific.

1.3. References

Alexander, M. A., I. Blade, M. Newman, J. R. Lanzante, N. C. Lau, and J. D. Scott, 2002: The atmospheric bridge: The influence of ENSO teleconnections on air-sea interaction over the global oceans. *Journal of Climate*, 15, 2205-2231.

Alibert, C., and M. T. McCulloch, 1997: Strontium/calcium ratios in modern *Porites* corals from the Great Barrier Reef as a proxy for sea surface temperature: Calibration of the thermometer and monitoring of ENSO. *Paleoceanography*, 12, 345-363.

Anderson, B. T., 2003: Tropical Pacific sea-surface temperatures and preceding sea level pressure anomalies in the subtropical North Pacific. *Journal of Geophysical Research-Atmospheres*, 108, D23, 4732.

Anderson, B. T., 2004: Investigation of a large-scale mode of ocean-atmosphere variability and its relation to tropical Pacific sea surface temperature anomalies. *Journal of Climate*, 17, 4089-4098.

Ashok, K., S. K. Behera, S. A. Rao, H. Y. Weng, and T. Yamagata, 2007: El Niño Modoki and its possible teleconnection. *Journal of Geophysical Research-Oceans*, 112, C11007.

Ault, T. R., J. E. Cole, M. N. Evans, H. Barnett, N. J. Abram, A. W. Tudhope, and B. K. Linsley, 2009: Intensified decadal variability in tropical climate during the late 19th century. *Geophysical Research Letters*, 36, L08602.

Barnett, T. P., D. W. Pierce, M. Latif, D. Dommenget, and R. Saravanan, 1999: Interdecadal interactions between the tropics and midlatitudes in the Pacific basin. *Geophysical Research Letters*, 26, 615-618.

Battisti, D. S., and A. C. Hirst, 1989: Interannual variability in the tropical atmosphere-ocean system: Influence of the basic state and ocean geometry. *Journal of Atmospheric Sciences*, 46, 1687-1712.

Beck, J. W., R. L. Edwards, E. Ito, F. W. Taylor, J. Recy, F. Rougerie, P. Joannot, and C. Henin, 1992: Sea-surface temperature from coral skeletal strontium/calcium ratios. *Science*, 257, 644-647.

Biondi, F., A. Gershunov, and D. R. Cayan, 2001: North Pacific decadal climate variability since 1661. *Journal of Climate*, 14, 5-10.

Bjerknes, J., 1969: Atmospheric teleconnections from equatorial Pacific. *Monthly Weather Review*, 97, 163-172.

Boulanger, J-P., S. Cravatte, and C. Menkes, 2003: Reflected and locally wind-forced interannual equatorial Kelvin waves in the western Pacific Ocean. *Journal of Geophysical Research*, 108, C10, 3311.

Burgers, G., and D. B. Stephenson, 1999: The "normality" of El Niño. *Geophysical Research Letters*, 26, 1027-1030.

Cane, M. A., and Coauthors, 1997: Twentieth-century sea surface temperature trends. *Science*, 275, 957-960.

Chavez, F. P., J. Ryan, S. E. Lluch-Cota, and M. Niquen, 2003: From anchovies to sardines and back: Multidecadal change in the Pacific Ocean. *Science*, 299, 217-221.

Chen, G. H., and C. Y. Tam, 2010: Different impacts of two kinds of Pacific Ocean warming on tropical cyclone frequency over the western North Pacific. *Geophysical Research Letters*, 37, L01803.

Chhak, K. C., E. Di Lorenzo, N. Schneider, and P. F. Cummins, 2009: Forcing of Low-Frequency Ocean Variability in the Northeast Pacific. *Journal of Climate*, 22, 1255-1276.

Clement, A. C., R. Seager, M. A. Cane, and S. E. Zebiak, 1996: An ocean dynamical thermostat. *Journal of Climate*, 9, 2190-2196.

Cobb, K. M., C. D. Charles, and D. E. Hunter, 2001: A central tropical Pacific coral demonstrates Pacific, Indian, and Atlantic decadal climate connections. *Geophysical Research Letters*, 28, 2209-2212.

Cobb, K. M., C. D. Charles, H. Cheng, and R. L. Edwards, 2003: El Niño/Southern Oscillation and tropical Pacific climate during the last millennium. *Nature*, 424, 271-276.

Cole, J. E., R. G. Fairbanks, and G. T. Shen, 1993: Recent variability in the Southern Oscillation: Isotopic results from a Tarawa Atoll coral. *Science*, 260, 5115, 1790-1793.

Collins, M., and Coauthors, 2010: The impact of global warming on the tropical Pacific ocean and El Niño. *Nature Geoscience*, 3, 391-397.

Corrège, T., 2006: Sea surface temperature and salinity reconstruction from coral geochemical tracers. *Palaeogeography Palaeoclimatology Palaeoecology*, 232, 408-428.

Dai, A., I. Y. Fung, and A. D. DelGenio, 1997: Surface observed global land precipitation variations during 1900-88. *Journal of Climate*, 10, 2943-2962.

Dansgaard, W., 1964: Stable isotopes in precipitation. *Tellus*, 16, 436-468.

Delcroix, T., S. Cravatte, and M. J. McPhaden, 2007: Decadal variations and trends in tropical Pacific sea surface salinity since 1970. *Journal of Geophysical Research-Oceans*, 112, C03012.

Deser, C., M. A. Alexander, S. P. Xie, and A. S. Phillips, 2010: Sea Surface Temperature Variability: Patterns and Mechanisms. *Annual Review of Marine Science*, 2, 115-143.

Di Lorenzo, E., and Coauthors, 2008: North Pacific Gyre Oscillation links ocean climate and ecosystem change. *Geophysical Research Letters*, 35, L08607.

Di Lorenzo, K. M. Cobb, J. C. Furtado, N. Schneider, B. Anderson, A. Bracco, M. A. Alexander, and D. Vimont. Central Pacific El Niño and decadal climate change in the North Pacific (submitted).

Diaz, H. F., M. P. Hoerling, and J. K. Eischeid, 2001: ENSO variability, teleconnections and climate change. *International Journal of Climatology*, 21, 1845-1862.

DiNezio, P. N., A. C. Clement, G. A. Vecchi, B. J. Soden, and B. P. Kirtman, 2009: Climate Response of the Equatorial Pacific to Global Warming. *Journal of Climate*, 22, 4873-4892.

Eipstein, S., R. Buchsbaum, H. A. Lowenstam, and H. C. Urey, 1953: Revised carbonate-water isotopic temperature scale. *Geological Society of America Bulletin*, 64, 1315-1325.

Enmar, R., M. Stein, M. Bar-Matthews, E. Sass, A. Katz, and B. Lazar, 2000: Diagenesis in live corals from the Gulf of Aqaba. I. The effect on paleo-oceanography tracers. *Geochimica et Cosmochimica Acta*, 64, 18, 3123-3132.

Evans, M. N., R. G. Fairbanks, and J. L. Rubenstone, 1999: The thermal oceanographic signal of El Niño reconstructed from a Kiritimati Island coral. *Journal of Geophysical Research-Oceans*, 104, 13409-13421.

Evans, M. N., A. Kaplan, R. Villalba, and M. A. Cane, 2000a: *Globality and Optimality in Climate Field Reconstructions from Proxy Data, Interhemispheric Climate Linkages* (ed. V. Markgraf). San Diego, Academic: 53-72.

Evans, M.N., A. Kaplan and M. A. Cane, 2000b: Intercomparison of coral oxygen isotope data and historical sea surface temperature (SST): Potential for coral-based SST field reconstructions. *Paleoceanography*, 15, 5. 551-563.

Fairbanks, R. G., M. N. Evans, J. L. Rubenstone, R. A. Mortlock, K. Broad, M. D. Moore, and C. D. Charles, 1997: Evaluating climate indices and their geochemical proxies measured in corals. *Coral Reefs*, 16, S93-S100.

Fedorov, A. V., and S. G. Philander, 2000: Is El Niño changing? *Science*, 288, 1997-2002.

Gedalof, Z., N. J. Mantua, and D. L. Peterson, 2002: A multi-century perspective of variability in the Pacific Decadal Oscillation: New insights from tree rings and coral. *Geophysical Research Letters*, 29, 24, 2204.

Gill, A. E., and E. M. Rasmusson, 1983: The 1982-83 climate anomaly in the equatorial Pacific. *Nature*, 306, 229-234.

Goddard, L., and N. E. Graham, 1997: El Niño in the 1990s. *Journal of Geophysical Research-Oceans*, 102, 10423-10436.

Graham, N. E., 1994: Decadal-scale climate variability in the tropical and North Pacific during the 1970s and 1980s – observations and model results. *Climate Dynamics*, 10, 135-162.

Grottoli, A. G., and C. M. Eakin, 2007: A review of modern coral $\delta^{18}O$ and $\Delta^{14}C$ proxy records. *Earth-Science Reviews*, 81, 67-91.

Gu, D. F., and S. G. H. Philander, 1997: Interdecadal climate fluctuations that depend on exchanges between the tropics and extratropics. *Science*, 275, 805-807.

Guilderson, T. P., and D. P. Schrag, 1999: Reliability of coral isotope records from the western Pacific warm pool: A comparison using age-optimized records. *Paleoceanography*, 14, 457-464.

Held, I. M., and B. J. Soden, 2006: Robust responses of the hydrological cycle to global warming. *Journal of Climate*, 19, 5686-5699.

Hendy, E. J., M. K. Gagan, J. M. Lough, M. McCulloch, and P. B. deMenocal, 2007: Impact of skeletal dissolution and secondary aragonite on trace element and isotopic climate proxies in *Porites* corals. *Paleoceanography*, 22.

Holland, C. L., R. B. Scott, S. I. An, and F. W. Taylor, 2007: Propagating decadal sea surface temperature signal identified in modern proxy records of the tropical Pacific. *Climate Dynamics*, 28, 163-179.

Hurrell, J. W., and K. E. Trenberth, 1999: Global sea surface temperature and analyses: Multiple problems and their implications for climate analysis, modeling, and reanalysis. *Bulletin of the American Meteorological Society*, 80, 2661-2678.

Intergovernmental Panel on Climate Change (IPCC), 2007: *Climate Change 2007: The Physical Science Basis. Contribution of Working Group I to the Fourth Assessment Report of the Intergovernmental Panel on Climate Change*, edited by S. Solomon et al., Cambridge Univ. Press, Cambridge, U. K.

Jin, F.-F., 1997: An equatorial ocean recharge paradigm for ENSO. Part I: Conceptual model. *Journal of Atmospheric Sciences*, 54, 811-829.

Jones, P. D., 1989: The influence of ENSO on global temperatures. *Climate Monitor*, 17, 80-89.

Kao, H. Y., and J. Y. Yu, 2009: Contrasting Eastern-Pacific and Central-Pacific types of ENSO. *Journal of Climate*, 22, 615-632.

Kilbourne K. H., T. M. Quinn, F. W. Taylor, T. Delcroix, and Y. Gouriou Y, 2004: El Niño-Southern Oscillation-related salinity variations recorded in the skeletal geochemistry of a *Porites* coral from Espiritu Santo, Vanuatu. *Paleoceanography*, 19, PA4002.

Kim, H. M., P. J. Webster, and J. A. Curry, 2009: Impact of shifting patterns of Pacific Ocean warming on North Atlantic tropical cyclones. *Science*, 325, 77-80.

Kleeman, R., R. A. Colman, N. R. Smith, and S. B. Power, 1996: A recent change in the mean state of the Pacific basin climate: Observational evidence and atmospheric and oceanic responses. *Journal of Geophysical Research-Oceans*, 101, 20483-20499.

Kleeman, R., J. P. McCreary, and B. A. Klinger, 1999: A mechanism for generating ENSO decadal variability. *Geophysical Research Letters*, 26, 1743-1746.

Knutson, T. R., and S. Manabe, 1995: Time-mean response over the tropical Pacific to increased CO_2 in a coupled ocean-atmosphere model. *Journal of Climate*, 8, 2181-2199.

Kug, J. S., F. F. Jin, and S. I. An, 2009: Two Types of El Niño Events: Cold Tongue El Niño and Warm Pool El Niño. *Journal of Climate*, 22, 1499-1515.

Kumar, K. K., B. Rajagopalan, M. Hoerling, G. Bates, and M. Cane, 2006: Unraveling the mystery of Indian monsoon failure during El Niño. *Science*, 314, 115-119.

Larkin, N. K., and D. E. Harrison, 2005: Global seasonal temperature and precipitation anomalies during El Niño autumn and winter. *Geophysical Research Letters*, 32, L13705.

Latif, M., and T. P. Barnett, 1994: Causes of decadal climate variability over the North Pacific and North-America. *Science*, 266, 634-637.

Latif, M., R. Kleeman, and C. Eckert, 1997: Greenhouse warming, decadal variability, or El Niño? An attempt to understand the anomalous 1990s. *Journal of Climate*, 10, 2221-2239.

Latif, M., and N. S. Keenlyside, 2009: El Niño/Southern Oscillation response to global warming. *Proceedings of the National Academy of Sciences of the United States of America*, 106, 20578-20583.

Lau, K. M., and H. Y. Weng, 1999: Interannual, decadal-interdecadal, and global warming signals in sea surface temperature during 1955-97. *Journal of Climate*, 12, 1257-1267.

Levitus, S., R. Burgett, and T. P. Boyer, 1994: *World Ocean Atlas 1994*, vol. 3, Salinity, NOAA Atlas NESDIS, vol. 3, 111 pp., NOAA, Silver Spring, Md.

Lindzen, R. S., and S. Nigam, 1987: On the role of sea surface temperature gradients in forcing low-level winds and convergence in the tropics. *Journal of Atmospheric Sciences*, 44, 17, 2418-2436.

Linsley, B. K., G. M. Wellington, and D. P. Schrag, 2000: Decadal sea surface temperature variability in the subtropical South Pacific from 1726 to 1997 AD. *Science*, 290, 1145-1148.

Linsley, B. K., A. Kaplan, Y. Gouriou, J. Salinger, P. B. deMenocal, G. M. Wellington, and S. S. Howe, 2006: Tracking the extent of the South Pacific Convergence Zone since the early 1600s. *Geochemistry, Geophysics and Geosystems*, 7, Q05003.

Luther, D. S., D. E. Harrison, and R. A. Knox, 1983: Zonal winds in the central equatorial Pacific and El Niño. *Science*. 222, 4621, 327-330.

Mantua, N. J., S. R. Hare, Y. Zhang, J. M. Wallace, and R. C. Francis, 1997: A Pacific interdecadal climate oscillation with impacts on salmon production. *Bulletin of the American Meteorological Society*, 78, 1069-1079.

McCreary, J. P., and P. Lu, 1994: Interaction between the subtropical and equatorial ocean circulations – the subtropical cell. *Journal of Physical Oceanography*, 24, 466-497.

McGregor, H. V., and M. K. Gagan, 2003: Diagenesis and geochemistry of *Porites* corals from Papua New Guinea: Implications for paleoclimate reconstruction. *Geochimica et Cosmochimica Acta*, 67, 12, 2147-2156.

McPhaden, M. J., 1999: Genesis and evolution of the 1997-98 El Niño. *Science*, 283, 950-954.

McPhaden, M. J., and Coauthors., 1998: The tropical ocean global atmosphere observing system: A decade of progress. *Journal of Geophysical Research-Oceans*, 103, 14169-14240.

McPhaden, M. J., S. E. Zebiak, and M. H. Glantz, 2006: ENSO as an integrating concept in Earth science. *Science*, 314, 1740-1745.

McPhaden, M. J., and D. X. Zhang, 2002: Slowdown of the meridional overturning circulation in the upper Pacific Ocean. *Nature*, 415, 603-608.

Meehl, G. A., and W. M. Washington, 1996: El Niño-like climate change in a model with increased atmospheric CO_2 concentrations. *Nature*, 382, 56-60.

Meehl, G.A., and Coauthors, 2007: Global Climate Projections. In: *Climate Change 2007: The Physical Science Basis. Contribution of Working Group I to the Fourth Assessment Report of the Intergovernmental Panel on Climate Change* [eds. Solomon, S., D. Qin, M. Manning, Z. Chen, M. Marquis, K. B. Averyt, M. Tignor and H. L. Miller]. Cambridge University Press, Cambridge, UK and New York, NY, USA.

Moore, A., and R. Kleeman, 1999: Stochastic forcing of ENSO by the intraseasonal oscillations. *Journal of Climate*, 12, 1199-1220.

Morrissey, M. L., and N. E. Graham, 1996: Recent trends in rain gauge precipitation measurements from the tropical Pacific: Evidence for an enhanced hydrologic cycle. *Bulletin of the American Meteorological Society*, 77, 1207-1219.

Neelin, J. D., D. S. Battisti, A. C. Hirst, F. F. Jin, Y. Wakata, T. Yamagata, and S. E. Zebiak, 1998: ENSO theory. *Journal of Geophysical Research-Oceans*, 103, 14261-14290.

Newman, M., G. P. Compo, and M. A. Alexander, 2003: ENSO-forced variability of the Pacific decadal oscillation. *Journal of Climate*, 16, 3853-3857.

Nitta, T., and S. Yamada, 1989: Recent warming of tropical sea-surface temperature and its relationship to the northern hemisphere circulation. *Journal of the Meteorological Society of Japan,* 67, 375-383.

Penland, C., and P. D. Sardeshmukh, 1995: The optimal growth of tropical sea surface temperature anomalies. *Journal of Climate*, 8, 1999-2024.

Philander, S. G. H., 1990: *El Niño, La Niña and the Southern Oscillation*. Academic Press.

Power, S., T. Casey, C. Folland, A. Colman, and V. Mehta, 1999: Inter-decadal modulation of the impact of ENSO on Australia. *Climate Dynamics*, 15, 319-324.

Quinn, W. H., D. O. Zopf, K. S. Short, and R. Yang, 1978: Historical trends and statistics of Southern Oscillation, El Niño, and Indonesian droughts. *Fishery Bulletin*, 76, 663-678.

Quinn, T. M., and F. W. Taylor, 2006: SST artifacts in coral proxy records produced by early marine diagenesis in a modern coral from Rabaul, Papua New Guinea. *Geophysical Research Letters*, 33, 4.

Rasmusson, E. M., and T. H. Carpenter, 1982: Variations in tropical sea-surface and surface wind fields associated with the Southern Oscillation El Niño. *Monthly Weather Review*, 110, 354-384.

Rayner, N. A., and Coauthors, 2009: Evaluating climate variability and change from modern and historical SST observations, in *Proceedings of Ocean Observation 2009: Sustained Ocean Observations and Information for Society,* vol. 2, edited by J. Hall, D. E. Harrison, and D. Stammer, Eur. Space Agency Spec. Publ., WPP-306.

Reynolds, R. W., N. A. Rayner, T. M. Smith, D. C. Stokes, and W. Q. Wang, 2002: An improved in situ and satellite SST analysis for climate. *Journal of Climate*, 15, 1609-1625.

Schneider, N., and B. D. Cornuelle, 2005: The forcing of the Pacific Decadal Oscillation. *Journal of Climate*, 18, 4355-4373.

Suarez, M. J., and P. S. Schopf, 1988: A delayed action oscillator for ENSO. *Journal of Atmospheric Sciences,* 45, 3283-3287.

Timmermann, A., M. Latif, A. Bacher, J. Oberhuber, and E. Roeckner, 1999: Increased El Niño frequency in a climate model forced by future greenhouse warming. *Nature*, 398, 694-696.

Timmermann, A., and F. F. Jin, 2002: A nonlinear mechanism for decadal El Niño amplitude changes. *Geophysical Research Letters*, 29, 1, 1003.

Trenberth, K. E. 1997: The definition of El Niño. *Bulletin of American Meteorological Society,* 78, 2771-2777.

Trenberth, K. E., and T. J. Hoar, 1996: The 1990-1995 El Niño Southern Oscillation event: Longest on record. *Geophysical Research Letters*, 23, 57-60.

Trenberth, K. E., and T. J. Hoar, 1997: El Niño and climate change. *Geophysical Research Letters*, 24, 3057-3060.

Trenberth, K. E., and J. W. Hurrell, 1994: Decadal atmosphere-ocean variations in the Pacific. *Climate Dynamics*, 9, 303-319.

Trenberth, K. E., and D. P. Stepaniak, 2001: Indices of El Niño evolution. *Journal of Climate*, 14, 1697-1701.

Urban, F. E., J. E. Cole, and J. T. Overpeck, 2000: Influence of mean climate change on climate variability from a 155-year tropical Pacific coral record. *Nature*, 407, 989-993.

Vecchi, G. A., B. J. Soden, A. T. Wittenberg, I. M. Held, A. Leetmaa, and M. J. Harrison, 2006: Weakening of tropical Pacific atmospheric circulation due to anthropogenic forcing. *Nature*, 441, 73-76.

Vecchi, G. A., A. Clement, and B. J. Soden, 2008: Examining the tropical Pacific's response to global warming, *Eos Trans. AGU*, 89, 81-83.

Vimont, D. J., J. M. Wallace, and D. S. Battisti, 2003: The seasonal footprinting mechanism in the Pacific: Implications for ENSO. *Journal of Climate*, 16, 2668-2675.

Wang, G., and H. H. Hendon, 2007: Sensitivity of Australian rainfall to inter-El Niño variations. *Journal of Climate*, 20, 4211-4226.

Wang, C., and J. Picaut, 2004: Understanding ENSO physics - A review. In: *Earth's Climate: The Ocean-Atmosphere Interaction.* C. Wang, S.-P. Xie, and J. A. Carton, Eds., AGU Geophysical Monograph Series, 147:21-48.

Weng, H. Y., S. K. Behera, and T. Yamagata, 2009: Anomalous winter climate conditions in the Pacific rim during recent El Niño Modoki and El Niño events. *Climate Dynamics*, 32, 663-674.

Wu, H. C., B.K. Linsley, and D. P. Schrag, Evaluating replicated *Porites lobata* coral Sr/Ca records from Clipperton Atoll (1894-1994) as proxy for sea surface temperature (*in review*).

Wyrtki, K., 1975: El Niño – The dynamic response of the equatorial Pacific Ocean to atmospheric forcing, *Journal of Physical Oceanography*, 5, 572-584.

Xie, P. P., and P. A. Arkin, 1997: Global precipitation: A 17-year monthly analysis based on gauge observations, satellite estimates, and numerical model outputs. *Bulletin of the American Meteorological Society*, 78, 2539-2558.

Xie, S. P., C. Deser, G. A. Vecchi, J. Ma, H. Y. Teng, and A. T. Wittenberg, 2010: Global Warming Pattern Formation: Sea Surface Temperature and Rainfall. J*ournal of Climate*, 23, 966-986.

Yeh, S. W., J. S. Kug, B. Dewitte, M. H. Kwon, B. P. Kirtman, and F. F. Jin, 2009: El Niño in a changing climate. *Nature*, 461, 511-U570.

Zhang, C., and J. Gottschalck, 2002: SST anomalies of ENSO and the Madden-Julian Oscillation in the equatorial Pacific. *Journal of Climate*, 15, 2429-2445.

Zhang, Y., J. M. Wallace, and D. S. Battisti, 1997: ENSO-like interdecadal variability: 1900-93. *Journal of Climate*, 10, 1004-1020.

CHAPTER 2

LATE 20th CENTURY WARMING AND FRESHENING TRENDS IN THE CENTRAL TROPICAL PACIFIC

This chapter is published in:

Nurhati, I. S., Cobb, K. M., Charles, C. D. and Dunbar, R. B. (2009). Late 20th century warming and freshening in the central tropical Pacific. *Geophysical Research Letters*, 36, L21606, doi:10.1029/2009GL040270.

2.1. Abstract

Global climate models and analyses of instrumental datasets provide a wide range of scenarios for future tropical Pacific climate change, limiting the accuracy of regional climate projections. Coral records provide continuous reconstructions of tropical Pacific climate trends that are difficult to quantify using the short, sparse instrumental datasets available from the tropical Pacific. Here, we present coral-based reconstructions of late 20th century sea-surface temperature and salinity trends from several islands in the central tropical Pacific. The coral data reveal warming trends that increase towards the equator, implying a decrease in equatorial upwelling in the last decades. Seawater freshening trends on the southern edge of the Inter-Tropical Convergence Zone suggest a strengthening and/or an equatorward shift of the convergence zone. Together, the new coral records support a late 20th century trend towards "El Niño-like" conditions in the tropical Pacific, in line with the majority of coupled global climate model projections.

2.2. Introduction

A comprehensive understanding of how tropical Pacific climate might evolve under global warming is critical in formulating adaptation strategies for future climate change. Tropical Pacific climate variability is responsible for a significant fraction of global temperature and precipitation variability via atmospheric teleconnections. However, climate models provide opposing views on the evolution of tropical Pacific climate under global warming [*Knutson and Manabe*, 1995; *Meehl and Washington*, 1996; *Vecchi et al*., 2006; *Clement et al*., 1996; *Cane et al*., 1997]. A majority of atmosphere-ocean coupled general circulation models (GCMs) project a weakening of the tropical Pacific zonal sea-surface temperature (SST) gradient (often referred to as "El Niño-like" conditions) under increasing atmospheric CO_2 concentrations [*Intergovernmental Panel on Climate Change* (*IPCC*), 2007]. On the other hand, some models suggest that the zonal SST gradient may increase (akin to "La Niña-like" conditions) in response to anthropogenic warming [*Clement et al*., 1996; *Cane et al*., 1997].

Large uncertainties associated with instrumental climate datasets obscure tropical Pacific trends over the 20th century. For example, it has been shown that instrumental SST datasets contain tropical Pacific trends of different signs over the late 20th century [*Vecchi et al*., 2008]. Further, biases in satellite-derived SST products that are larger early in these datasets and non-uniform in space and time are now widely recognized [*Reynolds et al*., 2007]. Precipitation trends derived from satellites, which require extensive calibrations, are prone to even larger uncertainties [e.g., *New et al*., 2001].

Coral skeletal geochemistry provides continuous, monthly-resolved tropical climate proxy records to reconstruct climate trends over the last decades to centuries. While the coral-based timeseries are derived from discrete locations, the fact that the recording process within coral skeletons does not change through time allows for the estimation of climate trends that complement those derived from the instrumental climate record. Furthermore, the regional-scale significance of coral-based climate trends can be assessed through replication of the coral geochemical records among multiple sites [*Hendy et al*., 2002]. Most coral reconstructions are based on the oxygen isotopic ratio ($\delta^{18}O$) of the coral skeleton that reflects changes in SST and the $\delta^{18}O$ of seawater ($\delta^{18}Osw$), with the latter linearly correlated to sea-surface salinity (SSS) changes [*Fairbanks et al*., 1997]. In the case of the central tropical Pacific (CTP), warm SSTs and positive precipitation anomalies that occur during El Niño events (Figure 2.1b) both contribute to negative coral $\delta^{18}O$ anomalies, making CTP corals valuable archives for the reconstruction of the El Niño/Southern Oscillation (ENSO) [*Evans et al*., 1999; *Cobb et al*., 2001]. Several CTP corals exhibit prominent trends towards depleted coral $\delta^{18}O$ values over the late 20th century [*Evans et al*., 1999; *Urban et al*., 2000; *Cobb et al*., 2001], suggesting that some combination of warming and freshening has occurred in this region. That such trends are very likely unprecedented in the last millennium [*Cobb et al*., 2003] strongly suggests that they are related to anthropogenic forcing.

It is important to quantify both the SST and SSS contributions to the unprecedented CTP coral $\delta^{18}O$ trends in order to resolve the character of late 20th century tropical Pacific climate change. Coral Sr/Ca ratio can be used to quantify SST changes [*Beck et al*., 1992; *Alibert and McCulloch*, 1997] that can in turn be removed from the

coral $\delta^{18}O$ records to yield reconstructions of $\delta^{18}Osw$ [*McCulloch et al*., 1994; *Gagan et al*., 1998]. In the context of the debate surrounding late 20th century tropical Pacific climate trends, an "El Niño-like" trend would imply positive SST and freshening trends in the CTP, and vice versa for a "La Niña-like" trend. In reconstructing both SST and hydrology in multiple long coral records from the CTP, we provide data that can be used to directly address the nature of CTP climate trends.

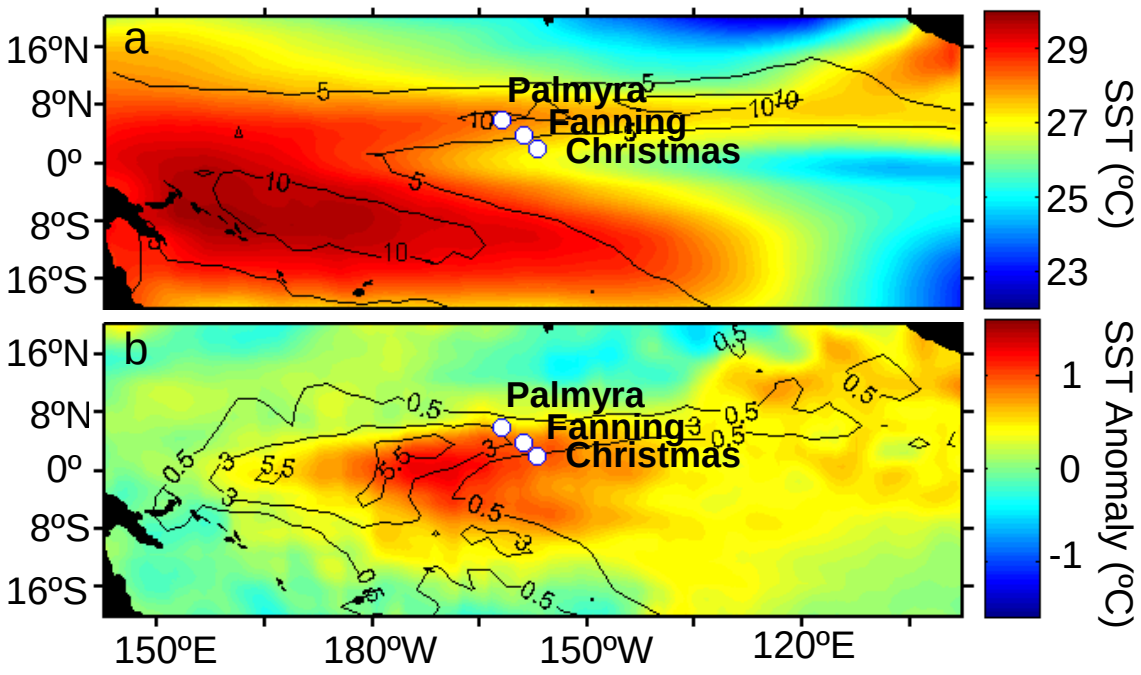

Figure 2.1. Map of the study islands in the central tropical Pacific. (a) Climatological Dec-Jan-Feb (DJF) SST shown in color [*Reynolds et al*., 2002] and precipitation shown by the solid lines [*Xie and Arkin*, 1997] (in units of mm/day) averaged over 1982-1998. (b) DJF SST and precipitation anomalies for composite 1987 and 1994 moderate El Niño events (NIÑO3.4 SST anomalies between 1-2ºC).

Here, we generate coral $\delta^{18}O$, Sr/Ca and $\delta^{18}Osw$ records from multiple coral cores from Palmyra, Fanning, and Christmas Islands (2ºN-6ºN, 157ºW-162ºW) during the late 20th century (1972-1998). The three islands span large gradients in annually-averaged SST and SSS (Figure 2.1a). Palmyra, as the northernmost island at 6ºN, lies in the path of

the eastward flowing North Equatorial Counter Current that delivers warm (~28.5ºC) waters from the West Pacific Warm Pool to the CTP [*Reynolds et al*., 2002]. Palmyra receives substantial rainfall associated with the Inter-Tropical Convergence Zone (ITCZ), as reflected by average SSS values of ~34.8 psu [*Levitus et al*., 1994]. At 2ºN, Christmas is bathed by cooler (~27.5ºC) waters that highlight the influence of equatorial upwelling on climate in this region. During non-El Niño years, Christmas receives less than 2 mm/year of rainfall [*Xie and Arkin*, 1997], leading to relatively high average SSS values of ~35.1 psu. Fanning lies between Palmyra and Christmas Islands, and as such is characterized by intermediate climatological SST (~28ºC) and SSS (~34.9 psu). During moderate El Niño events, Christmas exhibits the strongest warming due to the reduction in upwelling, while Palmyra experiences high rainfall associated with an equatorward movement of the ITCZ (Figure 2.1b). The north–south alignment of these CTP islands allows us to isolate the relative importance of ocean circulation versus ITCZ-related trends in this region by quantifying the relative differences in SST (via coral Sr/Ca) and SSS (via δ^{18}Osw) trends across these three islands.

2.3. Methods

Coral δ^{18}O and Sr/Ca analyses were conducted on *Porites sp.* coral cores from Palmyra, Fanning, and Christmas with sub-monthly resolution, following standard procedures (see auxiliary material). The Palmyra coral δ^{18}O record is previously published [*Cobb et al*., 2001], while the coral δ^{18}O records from both Fanning and Christmas are presented here for the first time, as are all the coral Sr/Ca records. Coral δ^{18}O and Sr/Ca reproducibility studies were carried out with multiple cores from the three

islands (see auxiliary material). It is important to note that the final Fanning coral $\delta^{18}O$ and Sr/Ca timeseries were constructed by splicing together records from two separate Fanning cores in order to avoid sampling secondary aragonite in one of the cores (see auxiliary material). We reconstruct changes in $\delta^{18}O$ of seawater ($\delta^{18}Osw$) as a proxy for SSS by subtracting the Sr/Ca-derived SST contribution to the coral $\delta^{18}O$ records following *Ren et al*. [2003] (see auxiliary material). We limit our analysis to the 1972-1998 period, when we have coral records from all three islands, noting that the unprecedented coral $\delta^{18}O$ trend occurs in this interval.

2.4. Results and Discussion

Over the 1972-1998 period, all three coral $\delta^{18}O$ records exhibit significant trends towards depleted coral $\delta^{18}O$ values, confirming that warming and/or freshening has occurred in the region (Figure 2.3b). Coral $\delta^{18}O$ trends over the 26-year period are -0.52 ± 0.09% (1σ) at Palmyra, -0.40 ± 0.09% (1σ) at Fanning, and -0.32 ± 0.10% (1σ) at Christmas. The errors indicated for these coral $\delta^{18}O$ trends account for uncertainties in both analytical precision and the coral $\delta^{18}O$ trend estimation (see auxiliary material). Strong correlations between the coral Sr/Ca and instrumental SST records confirm the fidelity of the Sr/Ca-derived SST proxy at these CTP sites (Figure 2.2). The coral-based SST reconstructions are generated by calibrating the coral Sr/Ca timeseries against SST using 1º x 1º Blended ship and satellite IGOSS SST data from each island [*Reynolds et al*., 2002], as the IGOSS SST data are most consistent with in situ SST data available from Palmyra (see auxiliary material). We apply reduced major axis regression analysis to calculate the Sr/Ca-SST relationship, a technique which minimizes residuals in two

variables that have nonzero uncertainties [*Solow and Huppert*, 2004]. The coral Sr/Ca (reported in mmol/mol) is highly correlated to instrumental SST at all three islands:

$$SST_{PALMYRA} = 130.43 - 11.39 \times Sr/Ca_{PALM}$$

(Nov 1981-Mar 1998, R=-0.71, CI>99%) (Eq. 2.1)

$$SST_{FANNING} = 166.81 - 15.47 \times Sr/Ca_{FANN}$$

(Nov 1981-Jun 2005, R=-0.79, CI>99%) (Eq.2.2)

$$SST_{CHRISTMAS} = 141.57 - 12.66 \times Sr/Ca_{CHRS}$$

(Nov 1981-Mar 1998, R=-0.80, CI>99%) (Eq.2.3)

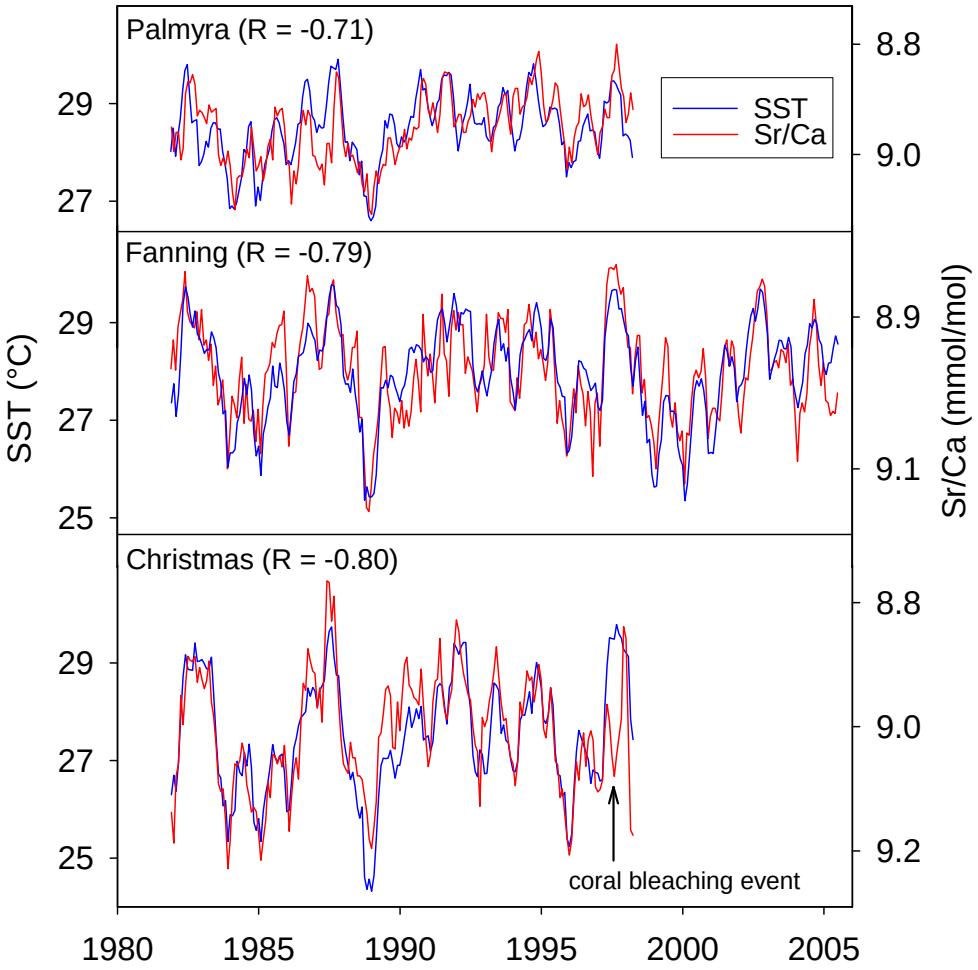

Figure 2.2. Comparison of coral Sr/Ca records with instrumental SST. Coral Sr/Ca is calibrated with monthly 1°x1° grid IGOSS SST dataset at each island [*Reynolds et al.*, 2002]. Coral bleaching witnessed by K. M. Cobb at Christmas Island during the 1997/98 El Niño.

The Sr/Ca-SST slopes shown here are not sensitive to the choice of calibration period, and fall within the range of existing Sr/Ca-SST calibration slopes calculated for *Porites sp.* corals [*Corrège*, 2006]. High reproducibility of intra and inter-coral colony Sr/Ca records from our corals further illustrates the fidelity of coral Sr/Ca-based SST reconstructions from these sites (see auxiliary material).

Over the 1972-1998 period, the coral Sr/Ca-derived SST reconstructions reveal warming trends at all three islands, ranging from 0.94 ± 5.81ºC (1σ) at Palmyra, to 1.37 ± 6.57ºC (1σ) at Fanning, to 1.65 ± 5.73ºC (1σ) at Christmas (Figure 2.3c). The coral-based warming trends are in relatively good agreement with gridded instrumental SST data from each island (see auxiliary material). The error estimates for the coral-based SST trends, while relatively large, are conservative estimates that combine uncertainties in analytical measurement, trend estimation, and the slope of the Sr/Ca-SST calibration from each island (see auxiliary material). Choosing slightly different intervals for trend estimation does not change the result that all three islands have warmed since 1972, with Christmas Island warming the most (see auxiliary material).

The relatively large late 20th century CTP warming trends, and specifically the evidence for enhanced equatorial warming, are consistent with a recent shift towards "El Niño-like" conditions in the tropical Pacific [*Vecchi et al.*, 2006]. Stronger equatorial warming is in line with instrumental observations of reduced equatorial upwelling over the late 20th century [*McPhaden and Zhang*, 2002], and is a robust feature of CO_2-doubling GCM simulations [*DiNezio et al.*, 2009].

We investigate the impact of the late 20th century enhanced equatorial warming on hydrology in the central tropical Pacific. Over the period 1972-1998, the δ^{18}Osw

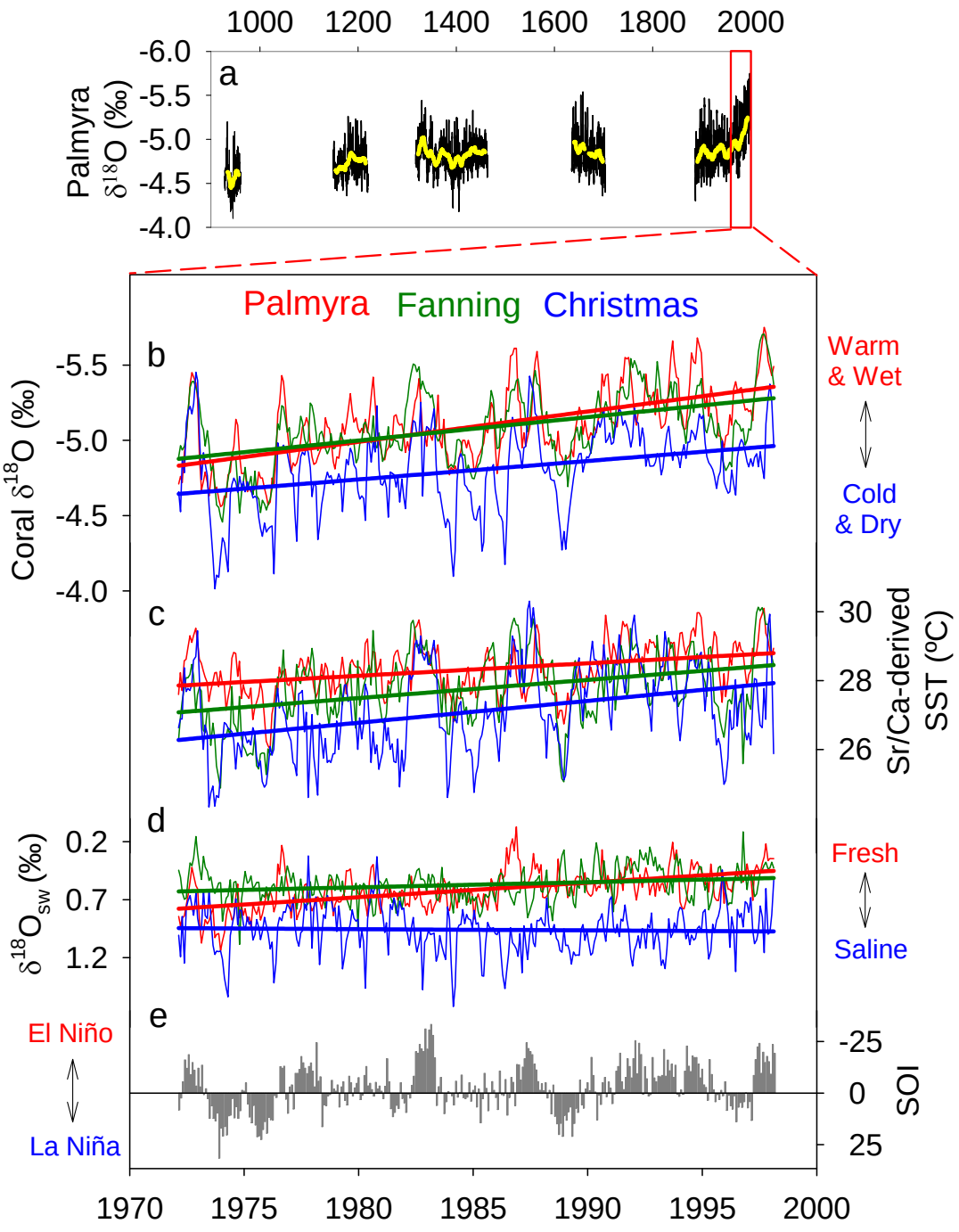

Figure 2.3. Central tropical Pacific coral climate proxy records. (a) A millennium-long coral $\delta^{18}O$ reconstruction from Palmyra Island [*Cobb et al.*, 2003] showing the unprecedented late 20th century trend towards lower coral $\delta^{18}O$ values (warmer, wetter conditions; note inverted y-axis). (b) Coral $\delta^{18}O$ records from Palmyra [*Cobb et al.*, 2001] (red), Fanning (green), and Christmas (blue) islands (note inverted y-axis). (c) Sr/Ca-derived SST reconstructions from Palmyra, Fanning, and Christmas. (d) $\delta^{18}Osw$ (SSS proxy) reconstructions from Palmyra, Fanning, and Christmas. (e) The Southern Oscillation Index (SOI).

records from Palmyra and Fanning exhibit freshening trends of -0.32 ± 0.08% (1σ) and -0.12 ± 0.08% (1σ) respectively, while the δ^{18}Osw record from Christmas exhibits no statistically significant trend (0.03 ± 0.11% at 1σ; Figure 2.3d). The error bars for these trends include uncertainties in the slopes of the Sr/Ca-SST calibration at each island and the δ^{18}O-SST regression from *Ren et al*. [2003], as well as analytical uncertainty of Sr/Ca, and uncertainty in the δ^{18}Osw trend (see auxiliary material). The largest freshening trend is observed at Palmyra, the island closest to the ITCZ, suggesting that warmer equatorial SSTs may have caused a strengthening and/or an equatorward migration of the ITCZ. Freshening trends at Palmyra and Fanning, as well as a minimal or lack of freshening trend at Christmas, follow a pattern that mimics weak to moderate El Niño conditions (Figure 2.1b).

Freshening trends observed in the CTP corals are in line with analyses of instrumental data documenting enhanced precipitation [*Morrissey and Graham*, 1996] and decreased SSS [*Delcroix et al*., 2007] in the CTP over the late 20th century. The coral-based δ^{18}Osw trends are also in line with projections for an enhancement of the hydrological cycle, based on theoretical and GCM results [*Held and Soden*, 2006].

Taken together, the pattern of warming and freshening evident in the CTP corals is reminiscent of weak El Niño conditions, characterized by enhanced equatorial warming and convection in the central tropical Pacific. Significant late 20th century warming in the central equatorial Pacific emerges from recent efforts to reconstruct instrumental SSTs in this region [*Bunge and Clarke*, 2009]. Likewise, a late 20th century reduction in the Walker circulation has been inferred from analyses of available wind stress [*Clarke and*

Lebedev, 1996] and sea-level pressure data [*Vecchi et al*., 2006; *Bunge and Clarke*, 2009].

The enhanced equatorial Pacific warming and strengthened ITCZ are consistent with an "El Niño-like" shift in tropical Pacific climate, but this analogy likely oversimplifies the complexity of tropical Pacific anthropogenic climate change. Indeed, any of a number of large-scale climate changes that are likely to occur in a greenhouse world might overwhelm or at the very least fundamentally reshape the expected impacts of an "El Niño-like" trend. For example, a projected enhancement of global precipitation minus evaporation patterns may dominate regional hydrological responses to global warming [*Held and Soden*, 2006; *IPCC*, 2007]. In this regard, the prominent warming and freshening trends uncovered in the coral reconstructions undoubtedly represent a combination of dynamics that are fundamentally different than those associated with the ENSO phenomenon. Nonetheless, this study demonstrates the utility of generating well-reproduced 20th century paleoclimate reconstructions to compare with model simulations of greenhouse climate changes – an approach that is particularly important for constraining future hydrological changes.

2.5. Auxiliary Material

2.5.1. Coral Sampling & Analytical Analyses

Coral cores of genus *Porites* were retrieved using an underwater drill from shallow (6-12 m) reefs off the western side of Palmyra (May 1998), Fanning (Sept 1997 and Aug 2005), and Christmas (May 1998); slabbed, x-rayed to determine their maximum growth axes, and sampled at 1 mm increments to generate sub-monthly

resolution timeseries (given annual coral growth of 1-2 cm). Coral $\delta^{18}O$ analyses were conducted using a GV Isoprime-Multiprep mass spectrometer with an analytical precision of ±0.05‰ (1σ), while Sr/Ca ratios were measured using a JY Ultima 2C ICP-OES with analytical precision of ±0.08-0.24% or 0.11-0.27°C (1σ) using the *Schrag* [1999] nearest-neighbor correction method.

2.5.2. Assessment of Coral Reproducibility

We assess the inter-colony reproducibility of coral $\delta^{18}O$ records at our sites by comparing the $\delta^{18}O$ records from different cores collected at each island (Figure 2.4). Two coral cores were retrieved from Palmyra, and show high reproducibility during their overlapping period. The two Fanning coral cores also show good agreement down to where diagenesis occurs in one of the cores. The variability in our Christmas $\delta^{18}O$ record is nearly identical to that of a previously published coral $\delta^{18}O$ record from the island [*Evans et al.*, 1999]. Note that the 1997/98 El Niño event is not well captured in our Christmas core, which was drilled three months prior to peak El Niño anomalies that occurred from December 1997 to February 1998.

We assess the intra- and inter-colony reproducibility of coral Sr/Ca records at our sites by comparing the Sr/Ca records from different cores collected at each island (Figure 2.5). Two coral cores from the same coral head were retrieved from Palmyra, and show excellent agreement in their Sr/Ca values. The two Fanning coral cores come from different coral colonies, and show good Sr/Ca agreement down to the diagenetically altered depth horizon. Comparison of our Christmas Sr/Ca record with a previously published Sr/Ca record from the island [*Evans et al.*, 1999] also shows high

reproducibility between the two records. Note that the large offset in absolute Sr/Ca values can be attributed to poor inter-laboratory calibration of absolute Sr/Ca values, and in no way impacts the interpretation of relative changes in coral Sr/Ca.

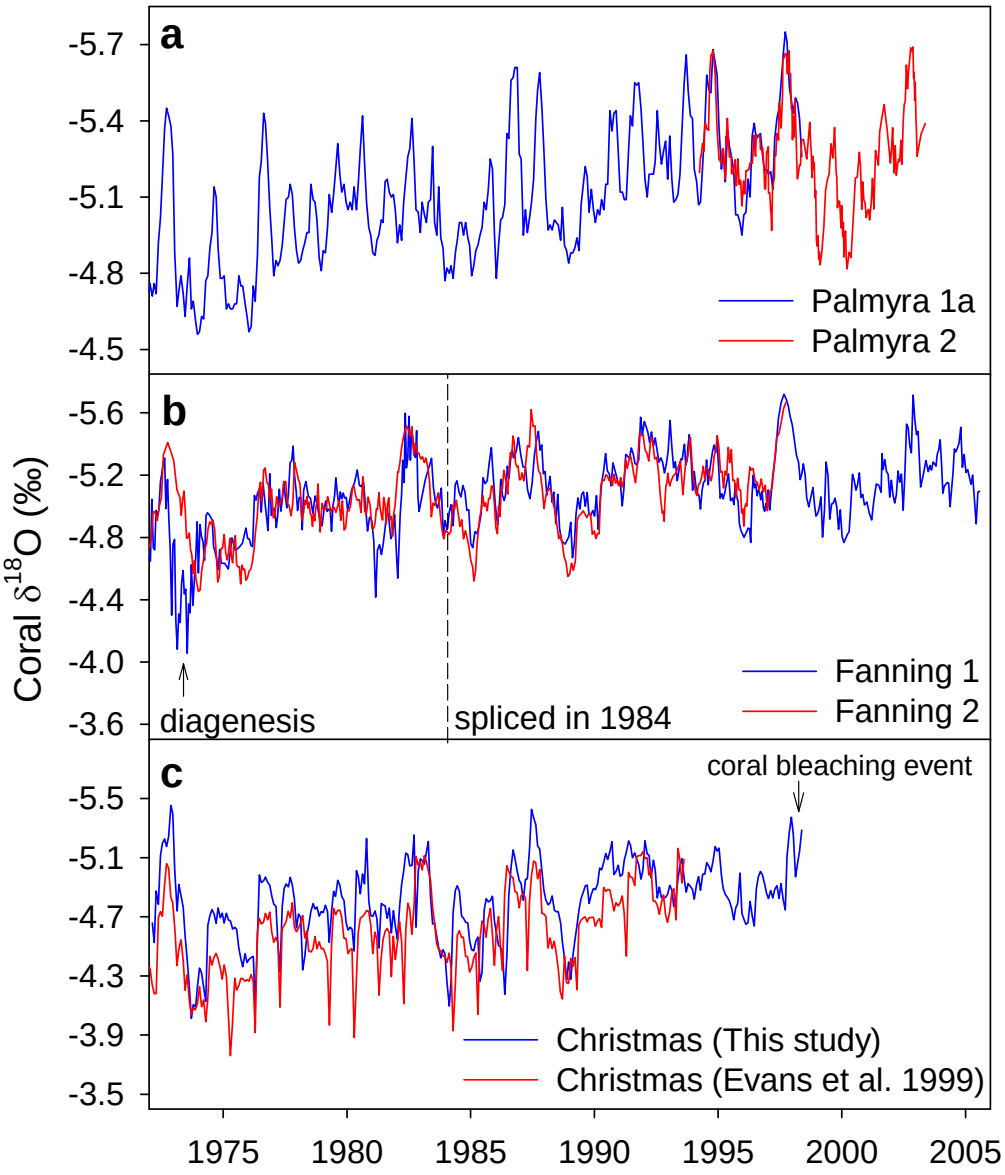

Figure 2. 4. Coral $\delta^{18}O$ reproducibility. Inter-colony coral $\delta^{18}O$ reproducibility between two corals cores drilled from separate colonies at (a) Palmyra, (b) Fanning, showing the diagenesis-related artifacts and the location of the splice (at a depth corresponding to 1984), and (c) Christmas, showing coral bleaching event during the 1997/98 El Niño event.

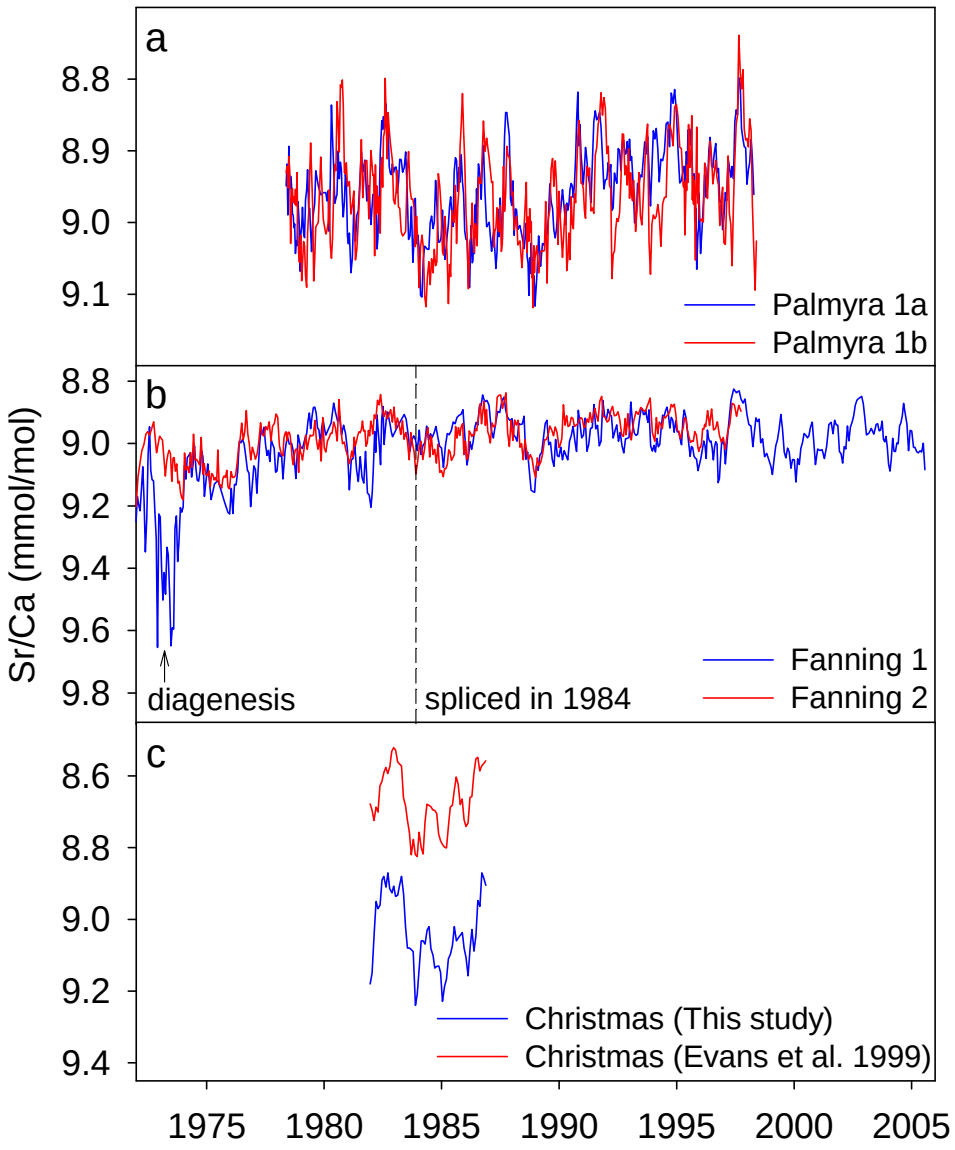

Figure 2.5. Coral Sr/Ca reproducibility. (a) Intra-colony Sr/Ca reproducibility between two corals cores retrieved from the same colony at Palmyra. (b) Inter-colony Sr/Ca reproducibility between two Fanning corals drilled from separate colonies, showing the diagenesis-related artifacts and the location of the splice (at a depth corresponding to 1984). (c) Inter-colony Sr/Ca reproducibility between two Christmas cores drilled from separate colonies. The offset in absolute value is likely due to poor inter-laboratory calibration of coral Sr/Ca measurements. Note for Fanning and Christmas, the same colors used in Figure 2.4 correspond to the same cores in this figure.

2.5.3. Assessment of Coral Diagenesis

One of the Fanning cores contains secondary aragonite precipitation at a depth corresponding to the mid-1970's (Figure 2.6), which introduces artificially heavy coral

$\delta^{18}O$ values (Figure 2.4) and high coral Sr/Ca ratios (Figure 2.5), as previously documented in corals from a variety of settings [*Enmar et al*., 2000; *Hendy et al*., 2007].

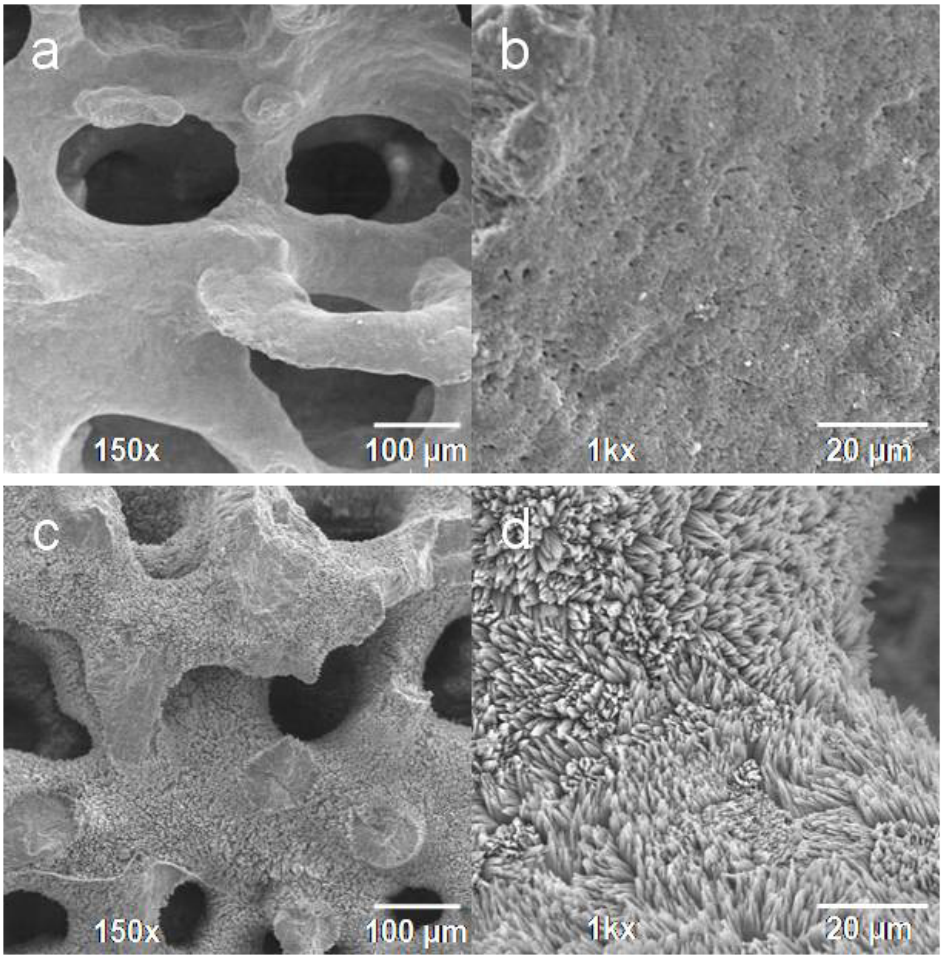

Figure 2.6. Comparison of coral surfaces with and without diagenesis. Scanning Electron Microscope images of (a, b) Non-diagenetically altered Palmyra coral from a depth corresponding to 1950, and (c, d) Diagenetically altered Fanning coral from a depth corresponding to 1973 with visible precipitation of secondary aragonite needles.

Therefore, we rely on measurements from a second Fanning core to generate a continuous Fanning record back to 1972. We splice the two Fanning cores together at a depth corresponding to 1984, to ensure that we avoid all traces of secondary aragonite in the altered core. Our conclusions are not sensitive to the choice of splice depth.

2.5.4. Deriving δ^{18}Osw

We reconstruct changes in δ^{18}O of seawater (δ^{18}Osw) as a proxy for SSS by subtracting the Sr/Ca-derived SST contribution to the coral δ^{18}O records from the measured coral δ^{18}O records following *Ren et al*. [2002], where

$$\Delta\delta^{18}O_{CORAL} = \Delta\delta^{18}O_{SST} + \Delta\delta^{18}O_{SW} \quad \text{(Eq.2.4)}$$

and

$$\Delta\delta^{18}O_{SST} = \Delta Sr/Ca \text{ x } (\partial\delta^{18}O_{CORAL}/\partial SST) \,/\, (\partial Sr/Ca/\partial SST) \quad \text{(Eq.2.5)}$$

We use an empirically-derived $\partial\delta^{18}O_{CORAL}/\partial$SST value of -0.21 ± 0.03‰/°C [*Ren et al*., 2002]. Island-specific ∂Sr/Ca/∂SST slopes were determined by Sr/Ca-SST calibrations performed for each island (Figure 2.2). We derive the δ^{18}Osw timeseries by integrating $\Delta\delta^{18}$Osw values at each time step, beginning with δ^{18}Osw values of 0.38-0.39‰ estimated from climatological SSS and δ^{18}Osw-SSS relationship in the CTP [*Fairbanks et al*., 1997]. The starting δ^{18}Osw value may be inaccurate, but does not affect the relative changes in δ^{18}Osw and therefore does not affect our conclusions.

2.5.5. Propagated Error Estimates

2.5.5.1. Coral δ^{18}O Trend

The total error estimates for the coral δ^{18}O trends consist of errors associated with (i) the analytical precision of coral δ^{18}O measurements via mass spectrometer (±0.05‰, 1σ), and (ii) the slope of coral δ^{18}O trend at each island. The slope of the coral δ^{18}O trends are obtained via a regression of:

$$\delta^{18}O_{CORAL} = a + m \cdot year \quad \text{(Eq.2.6)}$$

The 26-years coral $\delta^{18}O$ trend and its slope error are calculated following:

$$\text{trend} = (m \pm \sigma_m) \cdot 26 \text{ years} \quad \text{(Eq.2.7)}$$

$$\sigma_{trend} = \sigma_m \cdot 26 \text{ years} \quad \text{(Eq.2.8)}$$

And the total error for coral $\delta^{18}O$ trend (σ_{total}) represents the sum of analytical and trend:

$$\sigma_{total} = \sigma_{analytical} + \sigma_{trend} \quad \text{(Eq.2.9)}$$

The error estimates for the other islands' coral $\delta^{18}O$ trends are given here:

Table 2.1. 1σ error estimates for coral $\delta^{18}O$ (‰).

	$\sigma_{analytical}$	σ_{trend}	σ_{total}
Palmyra	0.05	0.04	0.09
Fanning	0.05	0.04	0.09
Christmas	0.05	0.05	0.10

2.5.5.2. Sr/Ca-derived SST

Total error estimates for the Sr/Ca-derived SST trends consist of errors associated with (i) analytical precision of Sr/Ca measurements via ICP-OES, (ii) the slope of Sr/Ca-derived SST trend, and (iii) the slope of Sr/Ca-SST calibration at each island. Analytical precision of Sr/Ca measurements (at 1σ) differ slightly for each record: ± 0.13ºC (or, 0.13% of $\overline{Sr/Ca}$ = 8.97 mmol/mol) for Palmyra, ± 0.11ºC (0.08% of $\overline{Sr/Ca}$ = 8.98 mmol/mol) for Fanning, and ± 0.27ºC (0.24% of $\overline{Sr/Ca}$ = 9.04 mmol/mol) for Christmas. The slope of Sr/Ca-derived SST trends are obtained via a regression of:

$$SST = a + m \cdot year \quad \text{(Eq.2.10)}$$

The 26-years coral $\delta^{18}O$ trend and its slope error are calculated following:

$$\text{trend} = (m \pm \sigma_m) \cdot 26 \text{ years} \quad \text{(Eq.2.11)}$$

$$\sigma_{trend} = \sigma_m \cdot 26 \text{ years} \quad \text{(Eq.2.12)}$$

The error associated with the slope of Sr/Ca-SST calibration contributes to uncertainty in Sr/Ca-derived SST trend whereas error in the intercept does not. Starting with Equation 10, the error associated with Sr/Ca-SST calibration (Equation 11) and the total error (Equation 12) follow:

$$SST = a + [\,(b \pm \sigma_b) \cdot \overline{SrCa}\,] \quad \text{(Eq.2.13)}$$

$$\sigma_{calibration} = \sigma_b \cdot \overline{SrCa} \quad \text{(Eq.2.14)}$$

$$\sigma_{total} = \sigma_{analytical} + \sigma_{trend} + \sigma_{calibration} \quad \text{(Eq.2.15)}$$

As an example, the calculation for the error in Palmyra's coral-based SST trend is shown below.

$$SST = 130.43 + [\,(-11.39 \pm 0.62) \cdot 8.97]$$

$$\sigma_{calibration} = 0.62 \cdot 8.97 = 5.55°C$$

$$\sigma_{total} = 0.13 + 0.13 + 5.55 = 5.81°C$$

The error estimates for the other islands' Sr/Ca-derived SST trends are given here:

Table 2.2. 1σ error estimates for Sr/Ca-derived SST (ºC).

	$\sigma_{analytical}$	σ_{trend}	$\sigma_{calibration}$	σ_{total}
Palmyra	0.13	0.13	5.55	5.81
Fanning	0.11	0.19	6.27	6.57
Christmas	0.27	0.23	5.23	5.73

2.5.5.3. δ^{18}Osw

Total error estimates for the δ^{18}Osw trends consist of errors associated with analytical precisions of (i) coral δ^{18}O and (ii) Sr/Ca, (iii) the slope of coral δ^{18}O-SST

regression, (iv) the slopes of Sr/Ca-SST calibration, and (v) δ^{18}Osw trend line at each island. Compounded error associated with analytical precisions and slopes calibrations ($\sigma_{\text{analytical+calibration}}$) is obtained following the equation from *Ren et al.* [2002]:

$$\Delta\delta^{18}O_{SW} = \Delta\delta^{18}O_{CORAL} - \left[\Delta SrCa \cdot \frac{\partial SST}{\partial SrCa} \cdot \frac{\partial \delta^{18}O_{CORAL}}{\partial SST}\right] \quad \text{(Eq.2.16)}$$

where the compounded error from the last term (σ_{lt}) is a multiplicative error propagation:

$$\sigma_{lt} = \left|\overline{\Delta SrCa} \cdot \frac{\partial SST}{\partial SrCa} \cdot \frac{\partial \delta^{18}O_{CORAL}}{\partial SST}\right| \cdot \sqrt{\left(\frac{\sigma_{\Delta SrCa}}{\Delta SrCa}\right)^2 + \left(\frac{\sigma_{SST-SrCa\ slope}}{SST-SrCa\ slope}\right)^2 + \left(\frac{\sigma_{coral\ \delta^{18}O-SST\_slope}}{coral\ \delta^{18}O-SST\_slope}\right)^2} \quad \text{(Eq.2.17)}$$

and error on $\Delta\delta^{18}O_{SW}$ ($\sigma_{\Delta\delta^{18}O_{SW}}$) is an additive error propagation:

$$\sigma_{\Delta\delta^{18}O_{SW}} = \sqrt{\sigma_{lt}{}^2 + \sigma_{\Delta\delta^{18}O_{CORAL}}{}^2} \quad \text{(Eq.2.18)}$$

We calculate error estimates for δ^{18}Osw due to analytical and calibration error, where:

$$\sigma_{\text{analytical+calibration}} = \sigma_{\Delta\delta^{18}O_{SW}}/\sqrt{2} \quad \text{(Eq.2.19)}$$

Finally, the total error is:

$$\sigma_{total} = \sigma_{\text{analytical+calibration}} + \sigma_{trend} \quad \text{(Eq.2.20)}$$

Taking Palmyra as an example, the required inputs are:

$\Delta SrCa = 4.2 \times 10^{-4}$ mmol/mol

$\sigma_{\Delta SrCa} = \sigma_{SrCa}\sqrt{2} = 0.01$ mmol/mol $\cdot \sqrt{2} = 0.02$ mmol/mol

Coral $\delta^{18}O - SST$ slope $= -0.21 \pm 0.03$‰/°C [*Ren et al.*, 2002]

$SST - Sr/Ca$ slope $= -11.39 \pm 0.62$°C/(mmol/mol)

$\sigma_{\Delta\delta^{18}O_{CORAL}} = \sigma_{\delta^{18}O_{CORAL}}\sqrt{2} = 0.05$‰ $\cdot \sqrt{2} = 0.07$‰

Therefore Equation (14) for Palmyra becomes:

$$\sigma_{lt} = |4.2 \times 10^{-4} \cdot -0.21 \cdot -11.39| \cdot \sqrt{\left(\frac{0.02}{4.2 \times 10^{-4}}\right)^2 + \left(\frac{0.03}{-0.21}\right)^2 + \left(\frac{0.62}{-11.39}\right)^2} = 0.039$$

Subsequently:

$$\sigma_{\Delta\delta^{18}O_{sw}} = \sqrt{0.039^2 + 0.07^2} = 0.081$$

$$\sigma_{\delta^{18}O_{sw}} = 0.081\sqrt{2} = 0.057$$

$$\sigma_{total} = 0.057 + 0.027 = 0.084$$

The error estimates for the other islands' δ^{18}Osw trends are given here:

Table 2.3. 1σ error estimates for δ^{18}O**sw** (‰).

	$\sigma_{analytical+calibration}$	σ_{trend}	σ_{total}
Palmyra	0.06	0.03	0.08
Fanning	0.06	0.03	0.08
Christmas	0.08	0.04	0.11

2.5.6. Comparison of SST Trends from Instrumental SST and Coral

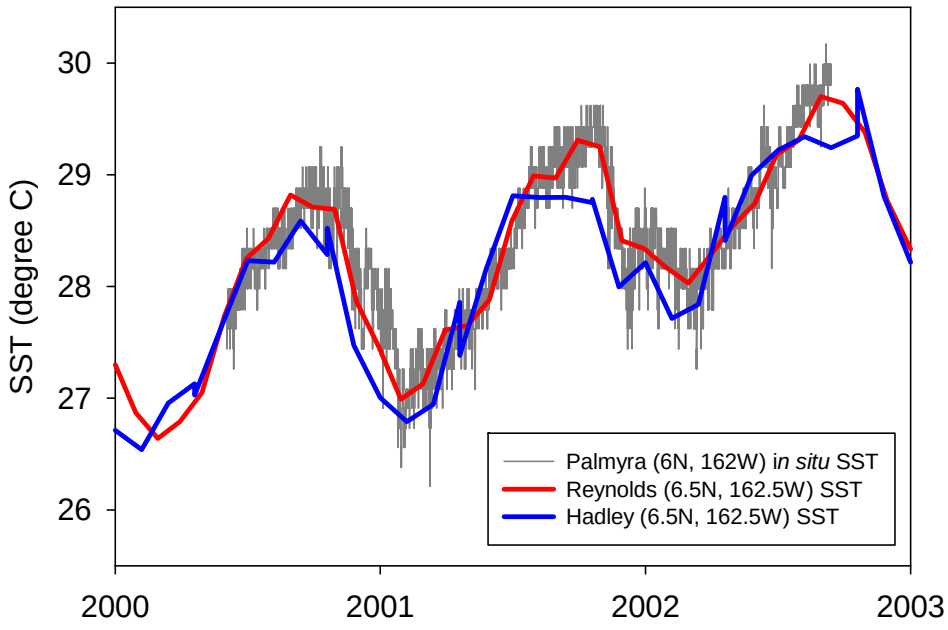

Figure 2.7. Comparison of satellite-derived and *in situ* instrumental SST data from Palmyra. A comparison of instrumental SST datasets from IGOSS SST [*Reynolds et al.*, 2002] and HadSST2 [*Rayner et al.*, 2005] with available in situ data from Palmyra supports the use of the IGOSS SST data in our coral Sr/Ca calibrations due to its accuracy in capturing local SST variations at Palmyra.

Table 2.4. Comparison of SST trends from instrumental SST datasets with our coral-derived SST record (in ºC) for each island for period 1972-1998.

	Palmyra	Fanning	Christmas
Coral	0.94	1.37	1.65
IGOSS/ERSST v2	1.05	1.09	1.11
HadSST	1.11	1.25	1.08

Table 2.5. SST trends at the islands for different end-member years.

	1972-1995	1973-1996	1974-1997	1975-1998
Palmyra	0.81	0.97	1.00	1.16
Fanning	1.47	1.37	0.86	0.97
Christmas	2.13	2.18	1.71	1.65

2.6. Acknowledgements

The Norwegian Cruise Lines provided transportation and support for a 2005 expedition to Fanning Island, which owed its success to Jordan Watson and Roland Klein. The Nature Conservancy and the Palmyra Atoll Research Consortium provided travel and logistical support for a second 2005 cruise to the Line Islands. The research was supported by funds from the ACS-PRF to KMC, and NSF grants ATM-0402562 and OCE-0551792 to RBD.

2.7. Electronic Data Access

Data presented in this chapter is available at NOAA Paleoclimate website via: ftp://ftp.ncdc.noaa.gov/pub/data/paleo/coral/east_pacific/line-islands2009.txt

2.8. Revised Error Propagation Analyses for Late 20th Century Trends in Coral $\delta^{18}O$, Sr/Ca-derived SST and $\delta^{18}Osw$

This revision is made to correct the estimations of uncertainty in late 20th century coral $\delta^{18}O$, Sr/Ca-derived sea-surface temperature (SST) and $\delta^{18}Osw$ trends. The previous version assumed uncertainty of data points in the timeseries, whereas the corrected version calculates uncertainty of the 26-year trends. The revised calculation increases the significance of the Sr/Ca-derived SST trends (from previously insignificant to significant trends). Increased uncertainty of the $\delta^{18}Osw$-based sea-surface salinity (SSS) trends in this revision is expected, given the number of variables used in deriving $\delta^{18}Osw$.

2.8.1. Coral $\delta^{18}O$ Trend

The late 20th century trends in coral $\delta^{18}O$ are -0.52‰ at Palmyra, -0.40‰ at Fanning and -0.32‰ at Christmas.

There are two sources of uncertainty that contribute to uncertainties in these coral $\delta^{18}O$ trends: (i) analytical precision of coral $\delta^{18}O$ via mass spectrometer, and (ii) slope error of the trend; with the following details:

i). The analytical precision of coral $\delta^{18}O$ via mass spectrometer is ±0.06‰ (1σ). We can apply the two most conservative cases where the analytical error can influence coral $\delta^{18}O$ trends, by assuming that half of the timeseries contains an analytical error of one sign (i.e. positive or negative 0.06‰), while the rest contains the opposite sign (Figure 2.8).

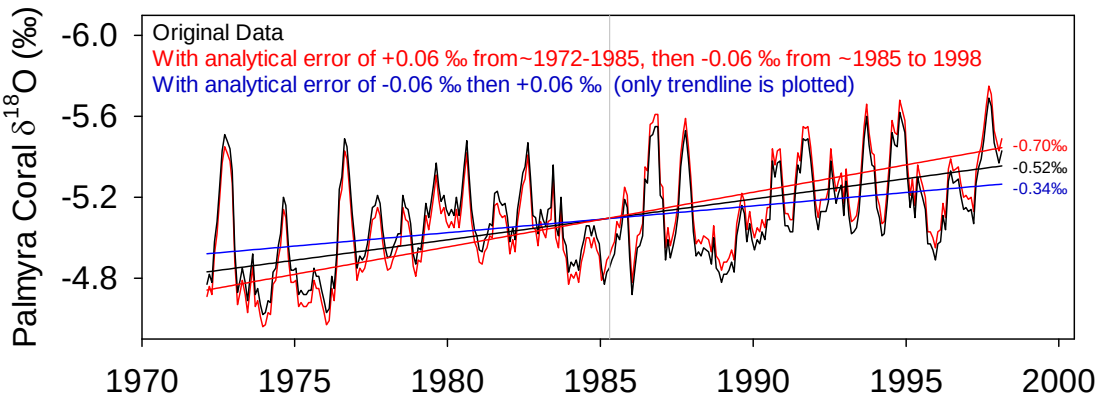

Figure 2.8. Uncertainty in coral $\delta^{18}O$ trend at Palmyra associated with analytical error. The black lines show Palmyra coral $\delta^{18}O$ record and its derived linear trend without analytical error. The red and blue lines show the timeseries with ±0.06‰ (1σ) analytical error that has different signs over the period ~1972-1985 versus ~1985-1998.

Therefore the uncertainty in coral $\delta^{18}O$ trends associated with the analytical error is ±0.18‰, which is the difference between the trends with analytical error (-0.70‰ and -0.34‰) and the original trend of -0.52‰ at Palmyra. Similarly, Fanning and Christmas coral $\delta^{18}O$ records also yield an error range of ±0.18‰.

ii). The fitting of trend line on coral $\delta^{18}O$ records has slope errors of ±0.04‰ at Palmyra and Fanning, and ±0.05‰ at Christmas.

Taken together, the late 20th century coral $\delta^{18}O$ trends and their associated errors at each island are summarized below:

Table 2.6. Late 20th century coral $\delta^{18}O$ trends and their associated errors at Palmyra, Fanning and Christmas.

(in ‰)	Trend	Analytical Error	Trend Slope Error	Total Error
Palmyra	-0.52	± 0.18	± 0.04	± 0.22
Fanning	-0.40	± 0.18	± 0.04	± 0.22
Christmas	-0.32	± 0.18	± 0.05	± 0.23

2.8.2. Sr/Ca-derived SST Trend

The late 20th century trends in coral Sr/Ca-derived SST are +0.94°C at Palmyra, +1.37°C at Fanning, and +1.65°C at Christmas.

There are three sources of uncertainty that contribute to uncertainties in these coral Sr/Ca-derived SST trends: (i) analytical precision of coral Sr/Ca via ICP-OES, (ii) slope error of the trend, and (iii) slope error of the coral Sr/Ca-SST calibration; with the following details:

i). The analytical precision of coral Sr/Ca via ICP-OES is ±0.01mmol/mol (1σ) for Palmyra and Fanning, and ±0.02 mmol/mol (1σ) for Christmas. We can apply the two most conservative cases where the analytical error can influence coral Sr/Ca-derived SST trends, by assuming that half of the timeseries contains an analytical error of one sign, while the rest contains the opposite sign (Figure 2.9).

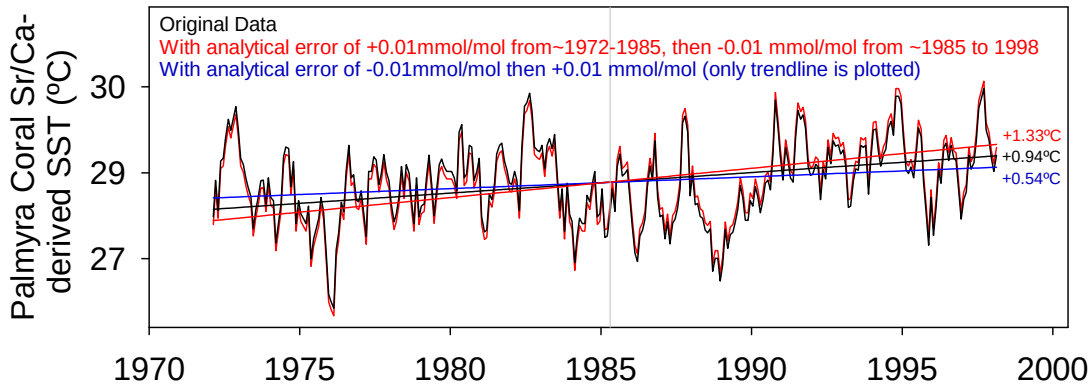

Figure 2.9. Uncertainty in coral Sr/Ca-derived SST trend at Palmyra associated with analytical error. The black lines show Palmyra coral Sr/Ca-derived SST record and its derived linear trend without analytical error. The red and blue lines show the timeseries with ±0.01mmol/mol (1σ) analytical error of Sr/Ca that has different signs over the period ~1972-1985 versus ~1985-1998.

Therefore the uncertainty in coral Sr/Ca-derived SST trends associated with the analytical error is ±0.40°C, which is the difference between the trends that have

analytical error (+1.33°C and +0.54°C) and the original trend of +0.94°C at Palmyra. The error ranges are ±0.33°C at Fanning, and ±0.82°C at Christmas.

ii). The fitting of trend line on coral Sr/Ca-derived SST records has slope errors of ±0.13°C at Palmyra, ±0.19°C at Fanning, and ±0.23°C at Christmas.

iii). The calibration slopes and slope errors of the coral Sr/Ca-SST regression are -11.39 ± 0.62 (1σ) at Palmyra, -15.47 ± 0.70 (1σ) at Fanning, and -12.66 ± 0.58 (1σ) at Christmas. The slope errors yield Sr/Ca-derived SST records that contain different trends over the late 20th century (Figure 2.10).

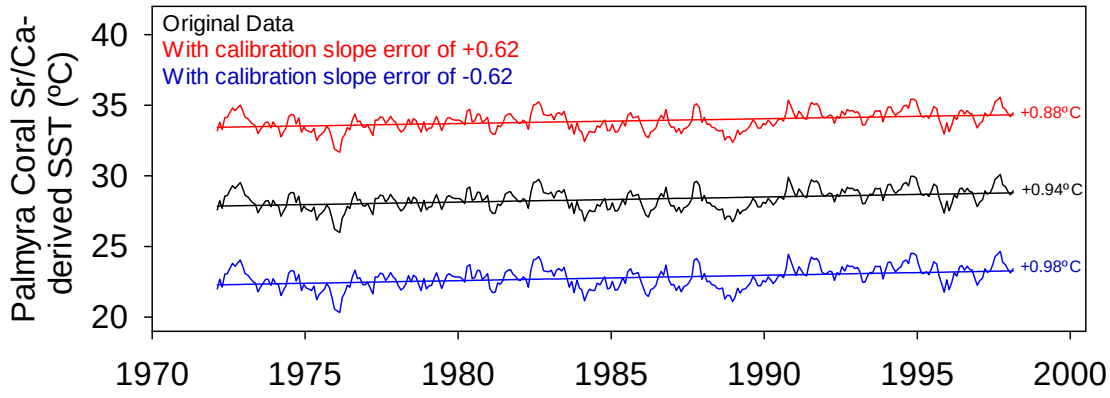

Figure 2.10. Uncertainty in coral Sr/Ca-derived SST trend at Palmyra associated with slope error of the coral Sr/Ca-SST calibration. The black lines show Palmyra coral Sr/Ca-derived SST record and its derived linear trend without analytical error. The red and blue lines show the timeseries with ±0.62(1σ) slope error in the coral Sr/Ca-SST calibration.

The uncertainty in coral Sr/Ca trends associated with calibration slope error is ±0.05°C, which is the difference between the trends with analytical error (+0.88°C and +0.98°C) from the original trend of +0.94°C at Palmyra. And the error ranges are ±0.06°C at Fanning, and ±0.08°C at Christmas.

Taken together, the late 20th century coral Sr/Ca-derived SST trends and their associated errors at each island are summarized below:

Table 2.7. Late 20th century coral Sr/Ca-derived SST trends and their associated errors at Palmyra, Fanning and Christmas.

(in °C)	Trend	Analytical Error	Trend Slope Error	Calibration Slope Error	Total Error
Palmyra	+0.94	± 0.40	± 0.13	± 0.05	± 0.57
Fanning	+1.37	± 0.33	± 0.19	± 0.06	± 0.58
Christmas	+1.65	± 0.82	± 0.23	± 0.08	± 1.13

2.8.3. δ^{18}Osw Trend

The late 20th century trends in coral-based δ^{18}Osw are –0.32‰ at Palmyra, -0.12‰ at Fanning, and +0.03‰ at Christmas.

There are five sources of uncertainty that contribute to uncertainties in these coral δ^{18}Osw trends: (i) analytical precision of coral δ^{18}O via mass spectrometer, (ii) analytical precision of coral Sr/Ca via ICP-OES, (iii) slope error of the trend, (iv) slope error in the coral Sr/Ca-SST calibration, and (v) slope error in the coral δ^{18}O-SST regression; with the following details:

i). The analytical precision of coral δ^{18}O via mass spectrometer is ±0.06‰ (1σ). We can apply the two most conservative cases where the analytical error can influence coral-based δ^{18}Osw trends, by assuming that half of the timeseries contains an analytical error of one sign (i.e. positive or negative 0.06‰), while the rest contains the opposite sign (Figure 2.11). This would yield an uncertainty in δ^{18}Osw trends of ±0.18‰ at Palmyra, Fanning and Christmas.

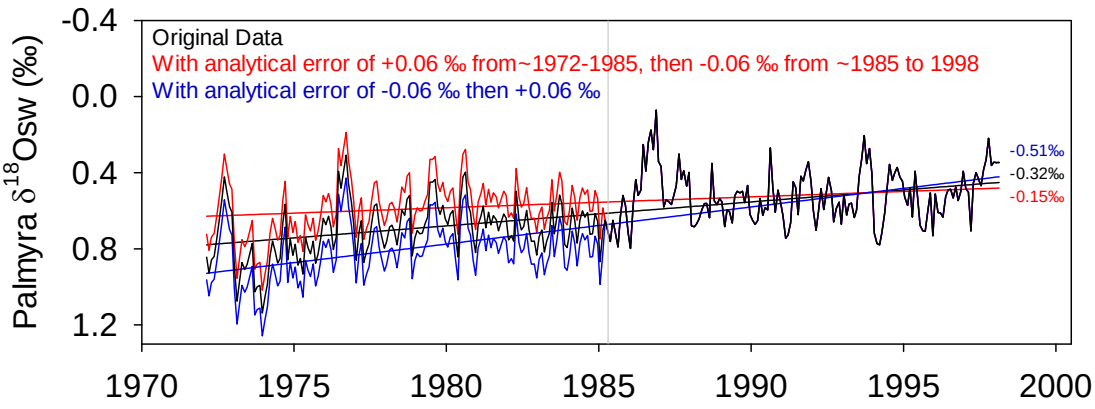

Figure 2.11. Uncertainty in coral-based δ^{18}Osw trend at Palmyra associated with analytical error in coral δ^{18}O. The black lines show Palmyra coral δ^{18}Osw record and its derived linear trend without analytical error. The red and blue lines show the timeseries with ±0.06‰ (1σ) analytical error in coral δ^{18}O that has different signs over the period ~1972-1985 versus ~1985-1998.

Note that that there is no difference between timeseries with and without analytical error during the period 1985-1998 following the method of *Ren et al*. [2002], which calculates δ^{18}Osw values via instantaneous changes in coral δ^{18}O and Sr/Ca between monthly data points.

ii). The analytical precision of coral Sr/Ca via ICP-OES is ±0.01 mmol/mol (1σ) at Palmyra and Fanning, and ±0.02 mmol/mol (1σ) at Christmas. Specifically, these numbers are derived from analytical precisions of Sr/Ca measurements of: ±0.13% of $\overline{Sr/Ca}$ = 8.97 mmol/mol for Palmyra, ±0.08% of $\overline{Sr/Ca}$ = 8.98 mmol/mol for Fanning, and ±0.24% of $\overline{Sr/Ca}$ = 9.04 mmol/mol for Christmas. We can apply the two most conservative cases where the analytical error can influence coral-based δ^{18}Osw trends, by assuming that half of the timeseries contains an analytical error of one sign, while the rest contains the opposite sign (Figure 2.12). This yields

uncertainty in δ^{18}Osw trends of ±0.07‰ at Palmyra, ±0.10‰ at Fanning and ±0.16‰ Christmas.

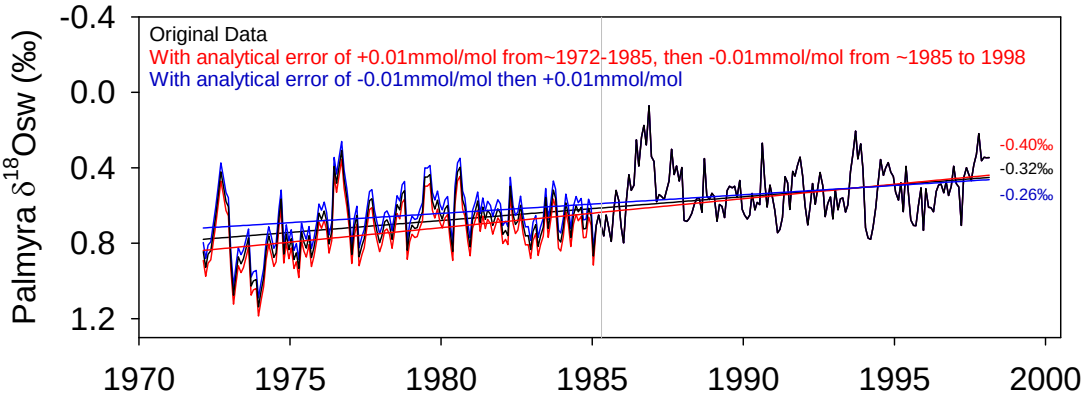

Figure 2.12. Uncertainty in coral-based δ^{18}Osw trend at Palmyra associated with analytical error in Sr/Ca. The black lines show Palmyra coral δ^{18}Osw record and its derived linear trend without analytical error. The red and blue lines show the timeseries with ±0.01 mmol/mol (1σ) analytical error in Sr/Ca that has different signs over the period ~1972-1985 versus ~1985-1998.

Similar with the previous case, there is no difference between timeseries with and without analytical error during the period 1985-1998 following the method of *Ren et al.* [2002], which calculates δ^{18}Osw values via instantaneous changes in coral δ^{18}O and Sr/Ca between monthly data points.

iii). The fitting of trend line on coral-based δ^{18}Osw records has slope errors of ±0.03‰ at Palmyra and Fanning, and ±0.04‰ at Christmas.

iv). The calibration slopes and slope errors of the coral Sr/Ca-SST regression is -11.39 ± 0.62 (1σ) at Palmyra, -15.47 ± 0.70 (1σ) at Fanning, and -12.66 ± 0.58 (1σ) at Christmas. The slope errors yield δ^{18}Osw records that contain different trends over the late 20th century. The uncertainty in coral-based δ^{18}Osw trends associated with

Sr/Ca-SST calibration slope error is ±0.01‰ at Palmyra and Fanning, and ±0.02‰ at Christmas.

v). The empirical slope for coral δ^{18}O-SST regression is -0.21±0.03‰/°C following values compiled by *Ren et al*. [2002]. Therefore, uncertainty in δ^{18}Osw trends associated with the coral δ^{18}O-SST slope error is ±0.03‰ and Palmyra, Fanning and Christmas.

Taken together, the late 20th century coral-based δ^{18}Osw trends and their associated errors at each island are summarized below:

Table 2.8. Late 20th century coral-based δ^{18}Osw trends and their associated errors at Palmyra, Fanning and Christmas.

(in ‰)	Trend	Analytical δ^{18}O Error	Analytical Sr/Ca Error	Trend Slope Error	Sr/Ca-SST Slope Error	δ^{18}O -SST Slope Error	Total Error
Palmyra	-0.32	± 0.18	± 0.07	± 0.03	± 0.01	± 0.03	± 0.32
Fanning	-0.12	± 0.18	± 0.10	± 0.03	± 0.01	± 0.03	± 0.35
Christmas	+0.03	± 0.18	± 0.16	± 0.04	± 0.02	± 0.03	± 0.43

2.9. References

Alibert, C., and M. T. McCulloch (1997), Strontium/calcium ratios in modern *Porites* corals from the Great Barrier Reef as a proxy for sea surface temperature: Calibration of the thermometer and monitoring of ENSO, *Paleoceanogr.*, 12, 345 – 363, doi:10.1029/97PA00318.

Beck, J. W., R. L. Edwards, E. Ito, F. W. Taylor, J. Recy, F. Rougerie, P. Joannot, and C. Henin (1992), Sea-surface temperature from coral skeletal strontium/calcium ratios, *Science*, 257, 644 – 647, doi:10.1126/science.257.5070.644.

Bunge, L., and A. J. Clarke (2009), A verified estimation of the El Niño Index Niño-3.4 since 1877, *J. Clim.*, 22, 3979 – 3992, doi:10.1175/2009JCLI2724.1.

Cane, M. A., A. C. Clement, A. Kaplan, Y. Kushnir, D. Pozdnyakov, R. Seager, S. E. Zebiak, and R. Murtugudde (1997), Twentieth-century sea surface temperature trends, *Science*, 275, 957 – 960, doi:10.1126/science.275.5302.957.

Clarke, A. J., and A. Lebedev (1996), A. Long-term changes in the equatorial Pacific trade winds, *J. Clim.*, 9, 1020 – 1029, doi:10.1175/1520-0442(1996)009<1020:LTCITE>2.0.CO;2.

Clement, A. C., R. S. Seager, M. A. Cane, and S. E. Zebiak (1996), An ocean dynamical thermostat, *J. Clim.*, 9, 2190 – 2196, doi:10.1175/1520-0442(1996)009<2190:AODT>2.0.CO;2.

Cobb, K. M., C. D. Charles, and D. E. A. Hunter (2001), A central tropical Pacific coral demonstrates Pacific, Indian, and Atlantic decadal climate connections, *Geophys. Res. Lett.*, 28, 2209 – 2212, doi:10.1029/2001GL012919.

Cobb, K. M., C. D. Charles, H. Cheng, and R. L. Edwards (2003), El Niño/Southern Oscillation and tropical Pacific climate during the last millennium, *Nature*, 424, 271 – 276, doi:10.1038/nature01779.

Corrège, T. (2006), Sea surface temperature and salinity reconstruction from coral geochemical tracers, *Palaeogeogr., Palaeoclim., Palaeoecol.*, 232, 408 – 428, doi:10.1016/j.palaeo.2005.10.014.

Delcroix, T., S. Cravatte, and M. J. McPhaden (2007), Decadal variations and trends in tropical Pacific sea surface salinity since 1970, *J. Geophys. Res.*, 112, C03012, doi:10.1029/2006JC003801.

DiNezio, P. N., A. C. Clement, G. A. Vecchi, B. J. Soden, B. P. Kirtman, and S. K. Lee (2009), Climate response of the equatorial Pacific to global warming, *J. Clim.*, 22, 4873 – 4892, doi:10.1175/2009JCLI2982.1.

Enmar, R., M. Stein, M, Bar-Matthews, E. Sass, A. Katz, and B. Lazar (2000), Diagenesis in live corals from the Gulf of Aqaba. I. The effect on paleo-oceanography tracers, *Geochim. Cosmochim. Acta.*, 64(18), 3123-3132.

Evans, M. N., R. G. Fairbanks, and J. L. Rubenstone (1999), The thermal oceanographic signal of El Niño reconstructed from a Kiritimati Island coral, *J. Geophys. Res.*, 104, 13,409 – 13,421, doi:10.1029/1999JC900001.

Fairbanks, R. G., M. N. Evans, J. L. Rubenstone, R. A. Mortlock, K. Broad, M. D. Moore, and C. D. Charles (1997), Evaluating climate indices and their geochemical proxies measured in corals, *Coral Reefs*, 16, S93 – S100, doi:10.1007/s003380050245.

Gagan, M. K., L. K. Ayliffe, D. Hopley, J. A. Cali, G. E. Mortimer, J. Chappell, M. T. McCulloch, and M. J. Head (1998), Temperature and surface-ocean water balance of the mid-Holocene tropical western Pacific, *Science*, 279, 1014 – 1018, doi:10.1126/science.279.5353.1014.

Held, I. M., and B. J. Soden (2006), Robust responses of the hydrological cycle to global warming, *J. Clim.*, 19, 5686 – 5699, doi:10.1175/JCLI3990.1.

Hendy, E. J., M. K. Gagan, C. A. Alibert, M. T. McCulloch, J. M. Lough, and P. J. Isdale (2002), Abrupt decrease in tropical Pacific sea surface salinity at end of Little Ice Age, *Science*, 295, 1511 – 1514, doi:10.1126/science.1067693.

Hendy, E. J., M. K. Gagan, J. M. Lough, M. McCulloch, and P. B. deMenocal (2007), Impact of skeletal dissolution and secondary aragonite on trace element and isotopic climate proxies in *Porites* corals, *Paleoceanography*, 22, doi:10.1029/2007PA001462.

Intergovernmental Panel on Climate Change (IPCC) (2007), Climate Change 2007: The Physical Science Basis. *Contribution of Working Group I to the Fourth Assessment Report of the Intergovernmental Panel on Climate Change*, edited by S. Solomon et al., Cambridge Univ. Press, Cambridge, U. K.

Knutson, T. R., and S. Manabe (1995), Time-mean response over the tropical Pacific to increased CO_2 in a coupled ocean-atmosphere model, *J. Clim.*, 8, 2181 – 2199, doi:10.1175/1520-0442(1995)008<2181: TMROTT>2.0.CO;2.

Levitus, S., R. Burgett, and T. P. Boyer (1994), World Ocean Atlas 1994, vol. 3, Salinity, NOAA Atlas NESDIS, vol. 3, 111 pp., NOAA, Silver Spring, Md.

McCulloch, M. T., M. K. Gagan, G. E. Mortimer, A. R. Chivas, and P. J. Isdale (1994), A high resolution Sr/Ca and $\delta^{18}O$ coral record from the Great Barrier Reef, Australia, and the 1982 – 1983 El Niño, *Geochim. Cosmochim. Acta*, 58, 2747–2754, doi:10.1016/0016-7037(94)90142-2.

McPhaden, M. J., and D. Zhang (2002), Slowdown of the meridional overturning circulation in the upper Pacific Ocean, *Nature*, 415, 603 – 608, doi:10.1038/415603a.

Meehl, G. A., and W. M. Washington (1996), El Niño-like climate change in a model with increased atmospheric CO_2 concentrations, *Nature*, 382, 56 – 60, doi:10.1038/382056a0.

Morrissey, M. L., and N. E. Graham (1996), Recent trends in rain gauge precipitation measurements from the tropical Pacific: Evidence for an enhanced hydrologic cycle, *Bull. Am. Met. Soc.*, 77, 1207 – 1219, doi:10.1175/1520-0477(1996)077<1207:RTIRGP>2.0.CO;2.

New, M., M. Todd, M. Hulme, and P. Jones (2001), Precipitation measurements and trends in the twentieth century, *Int. J. Clim.*, 21, 1889 – 1922, doi:10.1002/joc.680.

Rayner, N. A., P. Brohan, D. E. Parker, C. K. Folland, J. J. Kennedy, M. Vanicek, T. J. Ansell, and S. F. B. Tett (2005), Improved analyses of changes and uncertainties in sea surface temperature measured *in situ* since the mid-nineteenth century: The HadSST2 dataset. *J. Clim.*, 19, 446-469.

Ren, L., B. K. Linsley, G. M. Wellington, D. P. Schrag, and O. Hoegh-Guldberd (2003), Deconvolving the δ^{18}O-seawater component from subseasonal coral δ^{18}O and Sr/Ca at Rarotonga in the southwestern subtropical Pacific for the period 1726 to 1997, *Geochim. Cosmochim Acta*, 67, 1609 – 1621, doi:10.1016/S0016-7037(02)00917-1.

Reynolds, R. W., N. A. Rayner, T. M. Smith, D. C. Stokes, and W. Wang (2002), An improved in situ and satellite SST analysis for climate, *J. Clim.*, 15, 1609 – 1625, doi:10.1175/1520-0442(2002)015<1609:AIISAS>2.0.CO;2.

Reynolds, R.W., T. M. Smith, C. Liu, D. B. Chelton, K. S. Casey, and M. G. Schlax (2007), Daily high-resolution-blended analyses for sea surface temperature, *J. Clim.*, 20, 5473 – 5496, doi:10.1175/2007JCLI1824.1.

Schrag, D. P. (1999), Rapid analysis of high-precision Sr/Ca ratios in corals and other marine carbonates, *Paleoceanography*, 14, 97-102.

Solow, A. R., and A. Huppert (2004), A potential bias in coral reconstruction of sea-surface temperature, *Geophys. Res. Lett.*, 31, L06308, doi:10.1029/2003GL019349.

Urban, F. E., J. E. Cole, and J. T. Overpeck (2000), Influence of mean climate change on climate variability from a 155-year tropical Pacific coral record, *Nature*, 407, 989 – 993, doi:10.1038/35039597.

Vecchi, G. A., B. J. Soden, A. T. Wittenberg, I. M. Held, A. Leetmaa, and M. J. Harrison (2006), Weakening of tropical Pacific atmospheric circulation due to anthropogenic forcing, *Nature*, 441, 73– 76, doi:10.1038/nature04744.

Vecchi, G. A., A. Clement, and B. J. Soden (2008), Examining the tropical Pacific's response to global warming, *Eos Trans. AGU*, 89, 81 – 83, doi:10.1029/2008EO090002.

Xie, P., and P. A. Arkin (1997), Global precipitation: A 17-year monthly analysis based on gauge observations, satellite estimates, and numerical model outputs, *Bull. Am. Met. Soc.*, 78, 2539 – 2558, doi:10.1175/1520-0477(1997)078<2539:GPAYMA>2.0.CO;2.

CHAPTER 3

DECADAL-SCALE SST AND SALINITY VARIABILITY IN THE CENTRAL TROPICAL PACIFIC: SIGNATURES OF NATURAL AND ANTHROPOGENIC CLIMATE CHANGE

This chapter is submitted for publication as:

Nurhati, I. S., K .M. Cobb, and E. Di Lorenzo Decadal-scale SST and salinity variability in the central tropical Pacific: Signatures of natural and anthropogenic climate change (Submitted to *Journal of Climate*).

3.1. Abstract

Accurate forecasts of temperature and precipitation patterns in many regions of the world depend on quantifying anthropogenic signatures in tropical Pacific climate against a rich background of natural variability. However, the detection of anthropogenic signatures in the region is hampered by the lack of continuous century-long instrumental climate records. This study presents coral-based sea-surface temperature (SST) and salinity proxy records from Palmyra Island in the central tropical Pacific over the 20th century, based on Sr/Ca and the oxygen isotopic composition of seawater (δ^{18}Osw), respectively. On interannual timescales, the coral Sr/Ca-based SST proxy record captures El Niño-Southern Oscillation (ENSO) variability, reflected by significant correlations to eastern- and central-Pacific warming modes of ENSO (R=0.65 and 0.67, respectively). On decadal timescales, the SST proxy record is highly correlated to the North Pacific Gyre Oscillation (NPGO; R=-0.85), reflecting dynamical links between the central Pacific warming mode and extratropical decadal climate variability. Decadal-scale

salinity variations implied by the coral-based δ^{18}Osw record are significantly correlated with the Pacific Decadal Oscillation (PDO; R=0.54). The salinity proxy record is dominated by a statistically significant late 20th century trend towards lighter δ^{18}Osw values, implying that significant freshening has taken place at this site over the time period, most likely related to a strengthening of the hydrological cycle in a warmer climate. Taken together, the new coral proxy records suggest that low-frequency SST and salinity variations in the central tropical Pacific are controlled by different sets of dynamics, and anthropogenic climate change may dominate recent hydrological trends in the region.

3.2. Introduction

The detection of anthropogenic climate trends in the tropical Pacific is complicated by prominent interannual and decadal-scale natural climate variations in the region. Global temperature and precipitation patterns are heavily impacted by the interannual El Niño-Southern Oscillation (ENSO) phenomenon in the tropical Pacific, whose warm extremes are characterized by positive sea-surface temperature (SST) and precipitation anomalies in the eastern and central tropical Pacific, along with a weakening of the atmospheric Walker Circulation. On decadal timescales, the Pacific Decadal Oscillation (PDO), defined as the leading mode of SST variability in the North Pacific (Mantua et al. 1997), is associated with an "ENSO-like" (Zhang et al. 1997) pattern of SST anomalies. The PDO has been dynamically linked to ENSO, whereby ENSO-related variations in the Aleutian Low (Alexander et al. 2002) are integrated in the North Pacific Ocean to generate PDO variability (Newman et al. 2003).

Recent work has identified a tropical Pacific climate pattern characterized by central Pacific warming (CPW) with cooler SSTs in the eastern and western tropical Pacific (Latif et al. 1997; Trenberth and Stepahaniak 2001; Larkin and Harrison 2005; Ashok et al. 2007; Kug et al. 2007; Kao and Yu 2009). The interannual expression of the CPW pattern is often referred to as ENSO Modoki (Ashok et al. 2007). The atmospheric teleconnections associated with the ENSO Modoki and canonical ENSO differ significantly (Kumar et al. 2006; Wang and Hendon 2007; Weng et al. 2009), with important implications for tropical cyclone frequency in the Pacific and Atlantic basins (Kim et al. 2009; Chen and Tam 2010). On decadal timescales, the CPW pattern has been dynamically linked to the North Pacific Gyre Oscillation (NPGO; Di Lorenzo et al. 2008), which tracks the second leading mode of SST variability in the North Pacific. Much as canonical ENSO is linked to the PDO through variations in the Aleutian Low, CPW variations have been linked to the NPGO through variations in the atmospheric North Pacific Oscillation (Di Lorenzo et al., manuscript submitted to *Nature Geoscience*).

Significant natural climate variability in the tropical Pacific, when combined with large uncertainties in instrumental climate data from tropical Pacific in the early 20th century, complicate the detection of anthropogenic trends in this region. A majority of coupled global climate models (GCMs) in the Fourth Assessment of the Intergovernmental Panel on Climate Change (AR4 IPCC) project a trend towards "El Niño-like" conditions under continued anthropogenic forcing (Meehl et al. 2007), in line with analyses of select instrumental climate datasets (Vecchi et al. 2008). Recent analyses of GCM output suggest that anthropogenic warming may be concentrated in the central tropical Pacific (Xie et al. 2010) and along the equator (DiNezio et al. 2009), perhaps

related to a shift towards ENSO Modoki under anthropogenic forcing (Yeh et al. 2009). If these model projections of regional differences in anthropogenic SST warming are correct, they will have a profound effect on the pattern of global precipitation changes in the 21st century (Xie et al. 2010). Under uniform warming, the Clausius-Clapeyron relationship predicts a strengthening of the global hydrological cycle (Held and Soden 2006), but anthropogenic precipitation trends are difficult to extract from relatively short instrumental precipitation datasets. In the case of SST trends, Vecchi et al. (2008) illustrate that large discrepancies between the various gridded SST datasets yield SST trends of different signs for much of the tropical Pacific. Century-long, continuous proxy records from key locations in the tropical Pacific are required to identify potential anthropogenic trends in SST and hydrology against a rich background of interannual to decadal-scale natural climate variability in the tropical Pacific.

Monthly-resolved coral geochemical records that provide well-calibrated reconstructions of SST and/or hydrological variability have been used to investigate natural and anthropogenic climate variability over the last several centuries (see reviews by Gagan et al. 2000 and Corrège 2006). The oxygen isotopic composition ($\delta^{18}O$) of coral skeletal aragonite reflects changes in SST as well as changes in the $\delta^{18}O$ of seawater ($\delta^{18}Osw$), the latter is linearly related to seawater salinity (Fairbanks et al. 1997). In the tropical Pacific, coral $\delta^{18}O$ records have been used to reconstruct pre-instrumental ENSO variability (Cole et al. 1993; Tudhope et al. 2001; Evans et al., 2002; Cobb et al. 2003), decadal-scale tropical Pacific climate variability (Cobb et al. 2001; Ault et al. 2009), and tropical Pacific climate trends (Urban et al. 2000; Nurhati et al. 2009). When combined with measurements of coral Sr/Ca ratios as a proxy for SST

(Beck et al. 1992; Alibert and McCulloch 1997), coral $\delta^{18}O$ can be used to reconstruct changes in $\delta^{18}Osw$ as a proxy for salinity (McCulloch et al. 1994; Gagan et al. 1998; Hendy et al. 2002; Kilbourne et al. 2004; Linsley et al. 2006). To date, no long coral Sr/Ca records have been generated from the central tropical Pacific, despite the fact that models have identified this region as the locus for large anthropogenic trends in SST and hydrology.

This study presents monthly-resolved, century-long reconstructions of central tropical Pacific SST and salinity based on coral Sr/Ca and $\delta^{18}Osw$, respectively, from Palmyra Island. A previously published millennium-long compilation of living and fossil coral $\delta^{18}O$ records from Palmyra is characterized by a late 20^{th} century trend toward negative coral $\delta^{18}O$ values (Cobb et al. 2003). The fact that this negative coral $\delta^{18}O$ trend is unprecedented in the last millennium strongly suggests that anthropogenic climate forcing has caused appreciable warming and/or freshening in this region, in line with results from other coral $\delta^{18}O$ records (Evans et al. 1999; Urban et al. 2000). The new Palmyra Sr/Ca-derived SST and $\delta^{18}Osw$-based salinity proxy records presented in this study allows to distinguish between anthropogenic warming versus freshening in this key region, providing a much-needed test of GCM anthropogenic climate projections.

3.3. Methods

3.3.1. Study Site

Palmyra Island (6°N, 162ºW), located in the Line Islands chain in the central tropical Pacific, is heavily influenced by ENSO variability (Figure 3.1). During El Niño warm events, SST anomalies of roughly +0.2°C are accompanied by positive

precipitation anomalies of approximately +1 mmday^{-1} at the study site. During El Niño Modoki warm events, warming is concentrated in the central tropical Pacific, with positive precipitation anomalies displaced slightly westward towards the dateline (Figure 3.1-bottom). Note that the regressions of the ENSO Modoki Index of Ashok et al. (2007) on SST and precipitation at Palmyra show warming and positive precipitation anomalies

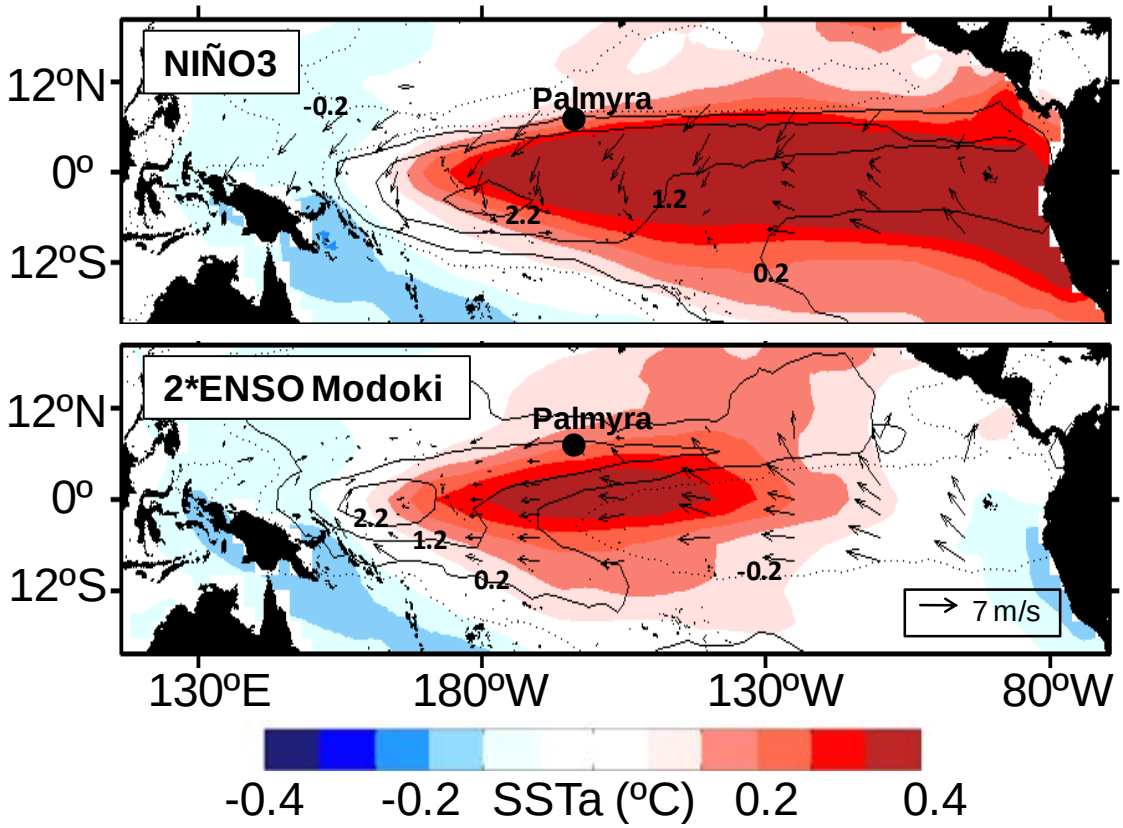

Figure 3.1. SST anomalies, precipitation anomalies and mean wind stress associated with eastern Pacific (top) and central Pacific (bottom) ENSO variability. (Top) SST anomaly (colors, in °C) and precipitation anomaly (contour lines, in mmday^{-1}) regressed on Niño-3 SST anomaly. Mean wind stress (arrows, in ms^{-1}) are shown during the peak months (December-January-February) of the 1982/83 and 1997/98 El Niño events (Niño-3 SST anomaly >2°C). (Bottom) SST and precipitation anomalies regressed on the ENSO Modoki Index, then multiplied by 2. Mean wind stress during the peak months (July-August-September) of the 1994 and 2004 El Niño events (ENSO Modoki Index SST anomaly >2°C). SST data are from Reynolds et al. (2002), precipitation data are from Xie and Arkin (1997), and wind stress data are from the Tropical Ocean Atmosphere buoys (http://www.pmel.noaa.gov/tao/; McPhaden et al. 1998).

that are roughly half as large as impacts associated with canonical El Niño events, therefore the ENSO Modoki Index is scaled by two throughout this paper. There is a profound difference in large-scale atmospheric circulation between canonical and Modoki ENSO, as previously documented by Weng et al. (2009). While canonical El Niño events result in weaker tropical Pacific trade winds, strong central tropical Pacific warming associated with Modoki El Niño events drives low-level convergence which maintains easterly winds across the eastern and central tropical Pacific.

3.3.2. Coral Sr/Ca Measurements

The *Porites* coral core analyzed for this study was collected in May 1998, and the associated 112-year-long $\delta^{18}O$ record and chronology were presented in Cobb et al. (2001). Sampling for coral Sr/Ca was conducted adjacent to the original $\delta^{18}O$ sampling transect at the same 1 mm increments used for $\delta^{18}O$ sampling, guaranteeing a point-by-point correspondence between the original coral $\delta^{18}O$ timeseries and the new coral Sr/Ca timeseries. Coral Sr/Ca ratios were measured using a JY Ultima 2C ICP-OES with analytical precision less than ±0.07% or 0.006 mmol mol^{-1}(1σ) using Schrag (1999)'s nearest-neighbor correction method. Details on intra- and inter-colony coral $\delta^{18}O$ and Sr/Ca reproducibility of Line Island corals are presented in the supplementary information of Nurhati et al. (2009).

3.3.3. Reconstructing SST and Salinity Records

The new Palmyra coral Sr/Ca record was transformed into SST by calibrating the coral Sr/Ca timeseries against 1°x1° IGOSS SST data over the period 1982-1998

(Reynolds et al. 2002). The Sr/Ca-SST calibration via the reduced major axis regression obtains the following equation:

$$SST = 130.43 - 11.39 \cdot Sr/Ca \ (R=-0.71, N_{eff}=28, CI>95\%) \quad (3.1)$$

The intercept and slope of the Sr/Ca-SST calibration at Palmyra fall within the range of existing Sr/Ca-SST relationships for *Porites* corals (Corrège 2006, and references therein). The reduced major axis regression technique used in this study minimizes residuals in two variables that have nonzero uncertainties, providing more robust and accurate SST estimates than the ordinary least-squared regression (Solow and Huppert 2004). Significance tests for correlation coefficients reported throughout this paper are based on a student's *t*-test after calculating effective degrees of freedom (N_{eff}) which accounts for serial autocorrelation in the timeseries (Bretherton et al. 1999).

The estimation of uncertainty in the coral Sr/Ca-based SST proxy reconstruction takes into account contributions of uncertainties from the analytical precision of Sr/Ca measurements and the Sr/Ca-SST calibration. Analytical uncertainty accounts for ±0.07ºC (1σ), while significant uncertainty associated with the intercept and slope of the SST-Sr/Ca relationship translates into a large error of ±7.85°C (1σ) for the SST proxy record. The compounded error bar for the reconstructed SST record is ±7.85°C (1σ), following a conservative error propagation approach (see the appendix). It is important to note that while the large errors in absolute SST space preclude from assigning a definitive SST value to any given coral Sr/Ca value in the timeseries, this study relies exclusively on the relative change in coral Sr/Ca through time to identify natural and anthropogenic SST signals at the site.

Changes in δ^{18}Osw as a proxy for salinity were reconstructed by subtracting the Sr/Ca-derived SST contribution from the coral δ^{18}O record following the method outlined in Ren et al. (2003), where the residual is the δ^{18}Osw. The compounded error bar for the δ^{18}Osw record is ±0.06 ‰ (1σ), which takes into account uncertainties in analytical measurements of coral δ^{18}O and Sr/Ca, Sr/Ca-SST calibration and coral δ^{18}O-SST regression (see the appendix).

3.3.4. Assessment of Diagenesis

Given that even minor diagenesis is associated with higher coral Sr/Ca values (cooler SSTs bias) in a suite of modern corals (Enmar et al. 2000; Quinn and Taylor 2006; Hendy et al. 2007), the skeletal surfaces of the Palmyra modern coral were examined by Scanning Electron Microscope (SEM). SEM images were obtained using a Hitachi S-800 Field Gun Emission SEM and a 126 LEO 1530 Thermally-assisted Field Emission SEM. Coral fragments were sampled in the 1886, 1905, 1917, 1922, 1927, 1939, 1949, and 1971 horizons of the core for diagenesis check (Figure 3.2). The SEM images reveal secondary aragonite needles at the base of the core (Figures 3.2a, b), but are not apparent in the more recent 1905 section of the core (Figure 3.2c). The ~2.5μm-long aragonite needle of are very small in comparison to the 20μm-long needles that are documented in compromised sections of other modern corals (Hendy et al. 2007; Nurhati et al. 2009). Smooth overgrowths are seen to coat the original skeleton in the 1917 horizon of the coral (Figure 3.2d). The unidentified coatings may contribute to relatively high Sr/Ca values (inferred cooling) measured in the 1917 time horizon of the core (Figure 3.3b), although ERSST data from the Palmyra gridpoint shows significant

cooling during that time interval, making it difficult to determine if this isolated diagenesis impacted coral Sr/Ca values. Therefore, with the possible exception of the 1917 horizon, the new 112-year-long Sr/Ca record presented here appears to be unaffected by diagenesis.

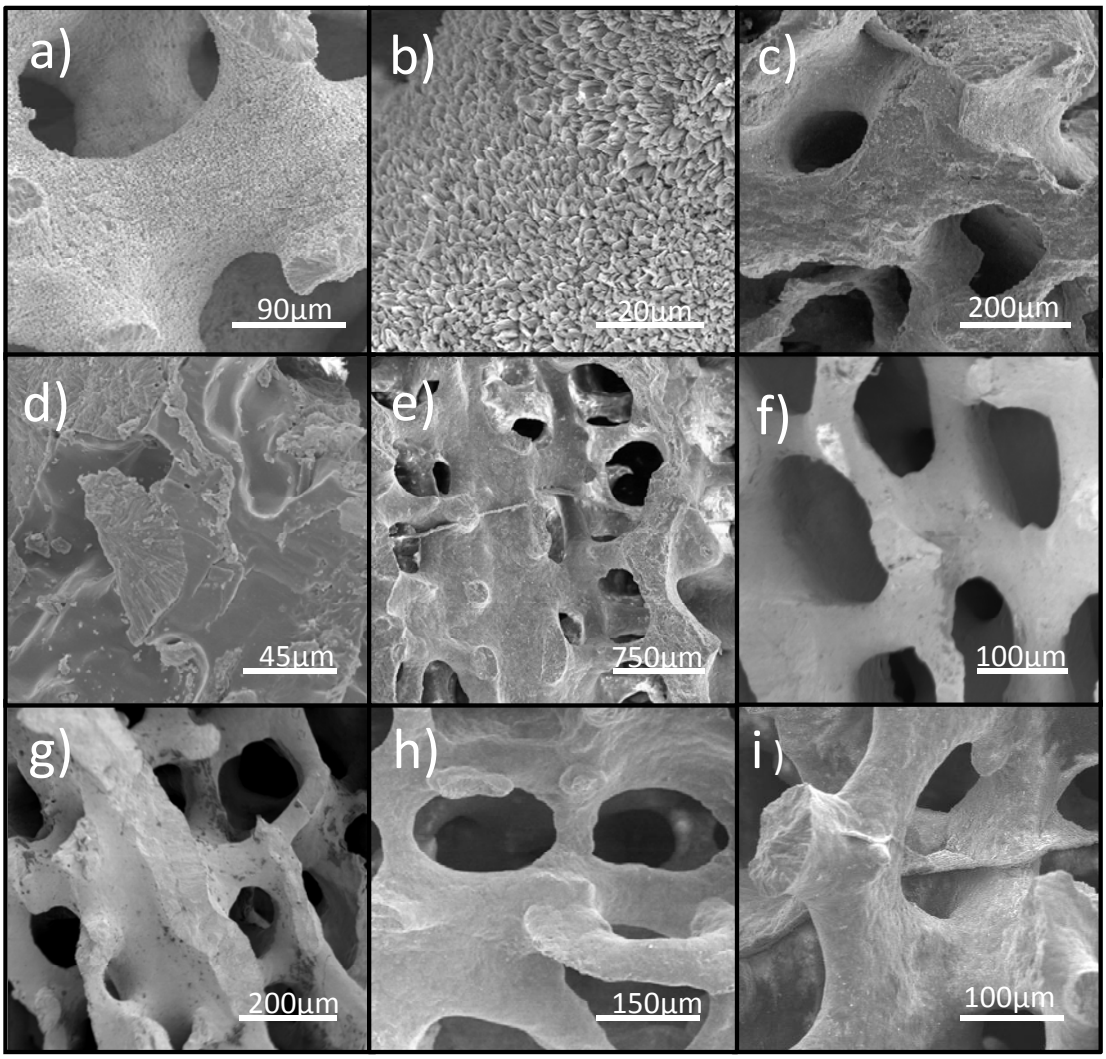

Figure 3.2. Scanning Electron Microscope (SEM) images of the Palmyra modern coral. From the (a, b) 1886, c) 1905, d) 1917, e) 1922, f) 1927, g) 1936, h) 1949, and i) 1971 horizons.

3.4. Results and Discussion

The previously published Palmyra coral $\delta^{18}O$ record reflects both SST and $\delta^{18}Osw$ variability, and is characterized by strong interannual and decadal-scale variability, as well as a prominent trend towards lower $\delta^{18}O$ values beginning in the mid-1970's (Figure 3.3a). The trend, which amounts to roughly -0.5‰ over the course of two decades, implies a trend towards warmer and/or wetter conditions in the central tropical Pacific, and is unprecedented in a millennium-long compilation of fossil coral $\delta^{18}O$ records from Palmyra (Cobb et al. 2003).

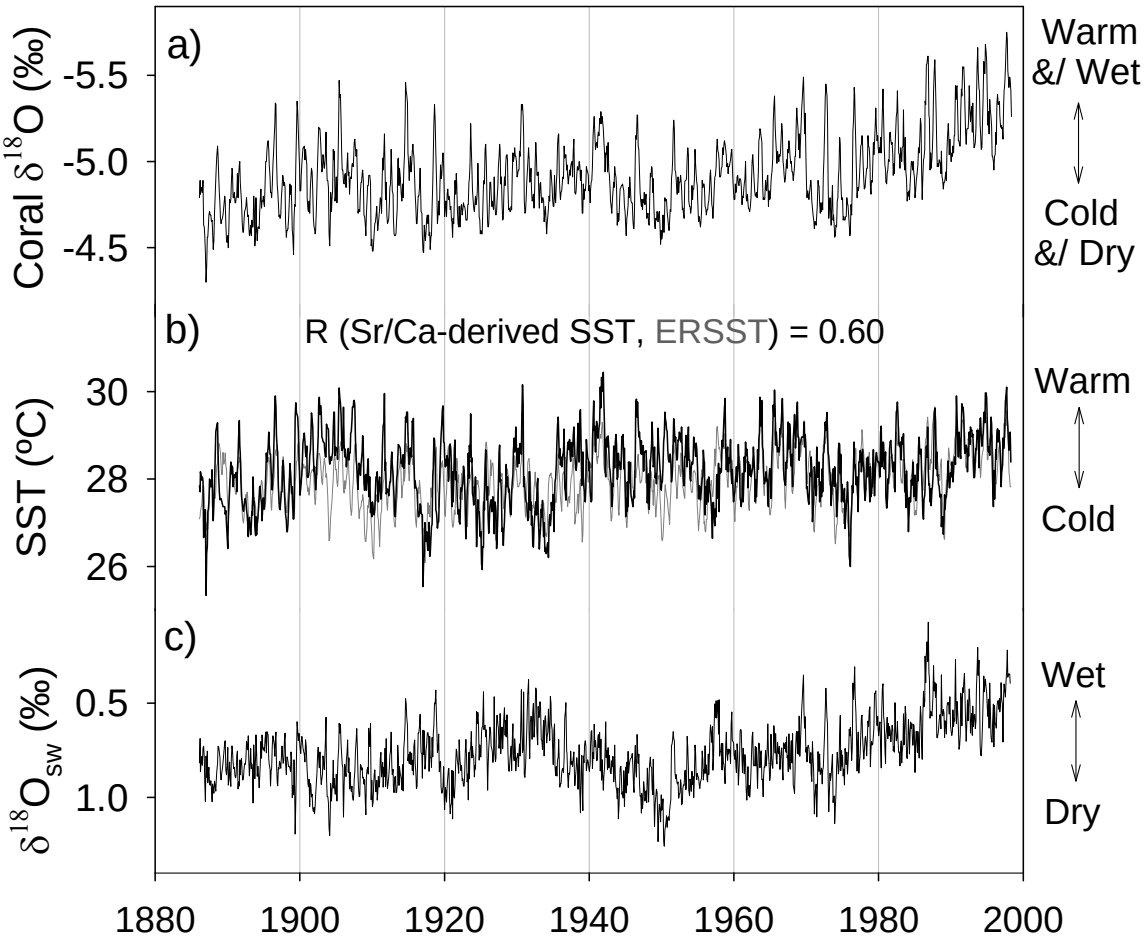

Figure 3.3. Palmyra coral monthly-resolved $\delta^{18}O$, Sr/Ca-derived SST, and $\delta^{18}Osw$ records from 1886-1998. (a) Palmyra coral $\delta^{18}O$ record (Cobb et al. 2001), (b) Sr/Ca-derived SST (black) plotted with ERSST (grey; Smith et al. 2008), and (c) $\delta^{18}Osw$ record.

The new coral Sr/Ca-derived SST proxy record exhibits interannual and decadal variability of roughly ±1°C (Figure 3.3b). There is a late 20th century warming trend, but it is difficult to discern a warming trend in the presence of strong interannual and decadal-scale variability contained in the SST proxy record. Overall, the coral-derived SST proxy record shows good agreement with reanalysis extended reconstruction SST (ERSST; Smith et al. 2008) from the Palmyra gridpoint (R=0.60 for raw monthly data), with similarly high correlations for interannual (R=0.72 for 2-7-year bandpassed) and decadal-scale (R=0.61 for 8-year low-passed) versions of the records.

The Palmyra coral δ^{18}Osw record is dominated by decadal-scale variability and a relatively large freshening trend over the late 20th century (Figure 3.3c). A visual comparison of the three coral records plotted in Figure 3.3 reveals that the δ^{18}Osw trend is responsible for the large trend in coral δ^{18}O, with warming playing a secondary role. The marked differences between the coral Sr/Ca-derived SST and the δ^{18}Osw-based salinity proxy records are striking, implying that SST and salinity variations are governed by different dynamics. The remainder of this paper investigates the large-scale climate controls on Palmyra SST and salinity on interannual, decadal, and secular timescales.

3.4.1. Interannual to Decadal-scale Tropical Pacific Climate Variability

3.4.1.1. Sr/Ca-derived SST Variability

On interannual (2-7 years) timescales, the SST proxy record captures ENSO variability in the central tropical Pacific, as reflected by significant correlations with the central tropical Pacific reanalysis instrumental Niño-3.4 SST index (SST anomalies averaged over 120-170ºW, 5ºN-5ºS; Kaplan et al. 1998) (R=0.71, N_{eff}=32, CI>95%).

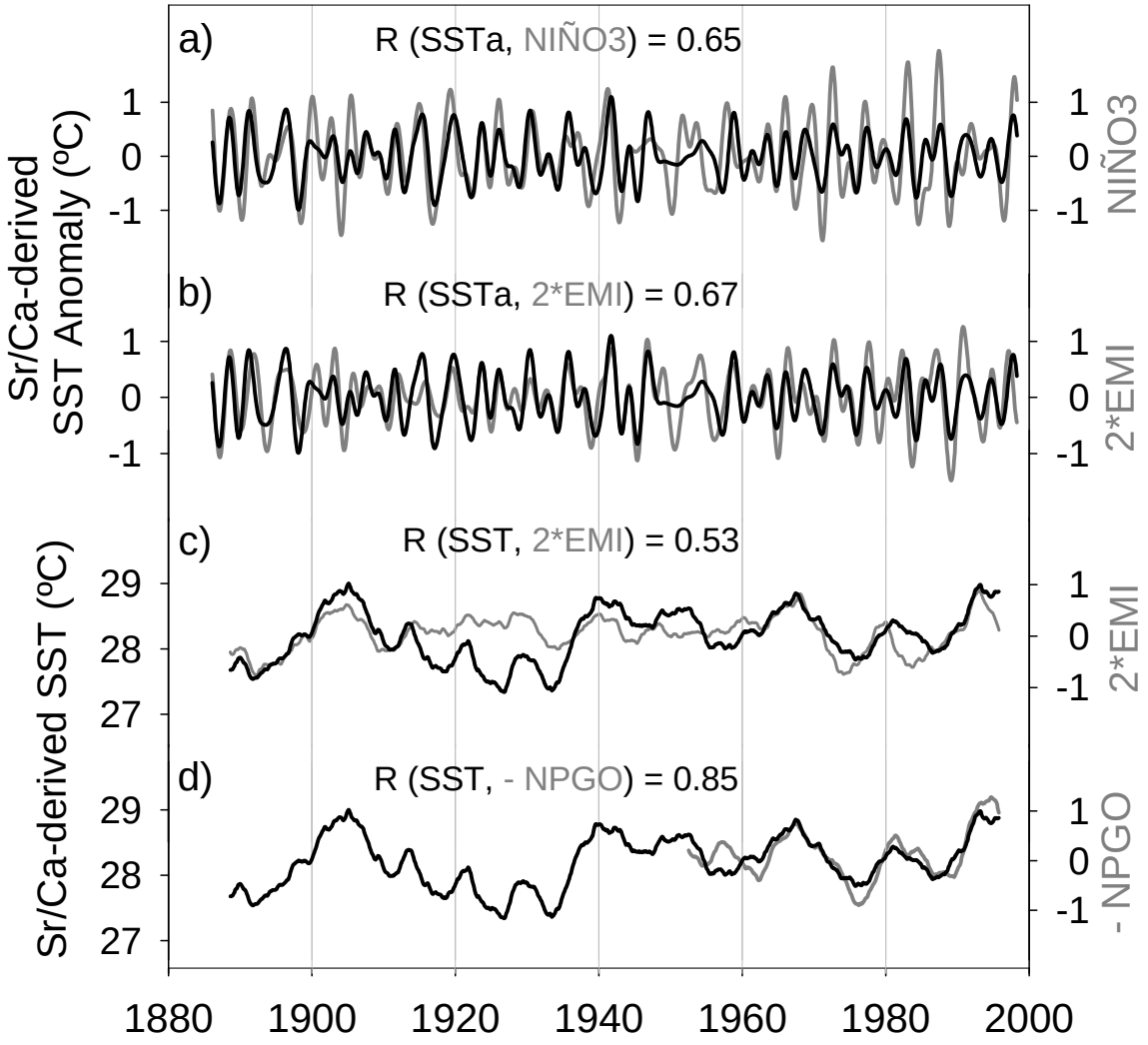

Figure 3.4. Interannual and decadal-scale coral Sr/Ca-derived SST variability at Palmyra plotted with tropical Pacific instrumental climate indices. (a) Interannual (2-7-year bandpassed) Sr/Ca-derived SST anomalies (black) and Niño-3 SST anomalies (grey). (b) Interannual (2-7-year bandpasssed) Sr/Ca-derived SST anomalies (black) and 2*ENSO Modoki Index (grey). (c) Decadal-scale Sr/Ca-derived SST (black) and 2*ENSO Modoki Index (grey), plotted as 5-year running averages. (b) Decadal-scale Sr/Ca-derived SST (black) and –NPGO Index (grey), plotted as 5-year running averages. All of the correlations are statistically significant at a 95% confidence level, using a student's *t*-test and adjusting for serial autocorrelation.

High correlations with SST anomalies in the Niño-3 region (90-150°W, 5°N-5°S; Kaplan et al. 1998) (R=0.65, N_{eff}=33, CI>95%; Figure 3.4a), as well as high correlations with the ENSO Modoki Index of Ashok et al. (2007) (R=0.67, N_{eff}=34, CI>95%; Figure 3.4b)

reflect the sensitivity of the Palmyra coral Sr/Ca record to eastern versus central Pacific "flavors" of ENSO variability, respectively. These high correlations reflect the fact that warm SST anomalies occur in the central tropical Pacific during both canonical El Niño events as well as ENSO Modoki warm events, and vice versa during their cold events.

On decadal timescales, the SST proxy record is highly correlated to low-frequency variability associated with the CPW, as evidenced by significant correlations between the 5-year running averaged versions of the SST proxy record and the ENSO Modoki Index ($R=0.53$, $N_{eff}=17$, CI>95%; Figure 3.4c). The correlation is much higher with the 5-year-averaged NPGO index (Di Lorenzo et al. 2008) ($R=-0.85$, $N_{eff}=10$, CI>95%; Figure 3.4d), reflecting strong dynamical linkages between central tropical Pacific SST and the decadal-scale NPGO, as investigated by Di Lorenzo et al. (manuscript submitted to *Nature Geoscience*). Statistically significant correlations between the coral Sr/Ca-derived SST proxy record, the ENSO Modoki Index, and the NPGO are also found when comparing 8-year low-passed versions of the records. The SST proxy record is not significantly correlated to the PDO index ($R=-0.03$), which is somewhat surprising given that the PDO is understood as the decadal expression of ENSO-related variability in the North Pacific (Alexander et al. 2002). This suggests that low-frequency central Pacific SST variations are more closely related to the NPGO than the PDO, and furthermore, likely play an important role in shaping the temporal evolution of the NPGO.

Regressions of the NPGO and the PDO with Pacific SST reveal that the amplitude of low-frequency central tropical Pacific SST anomalies associated with the NPGO are almost twice as large as those associated with the PDO (Figure 3.5). Both North Pacific

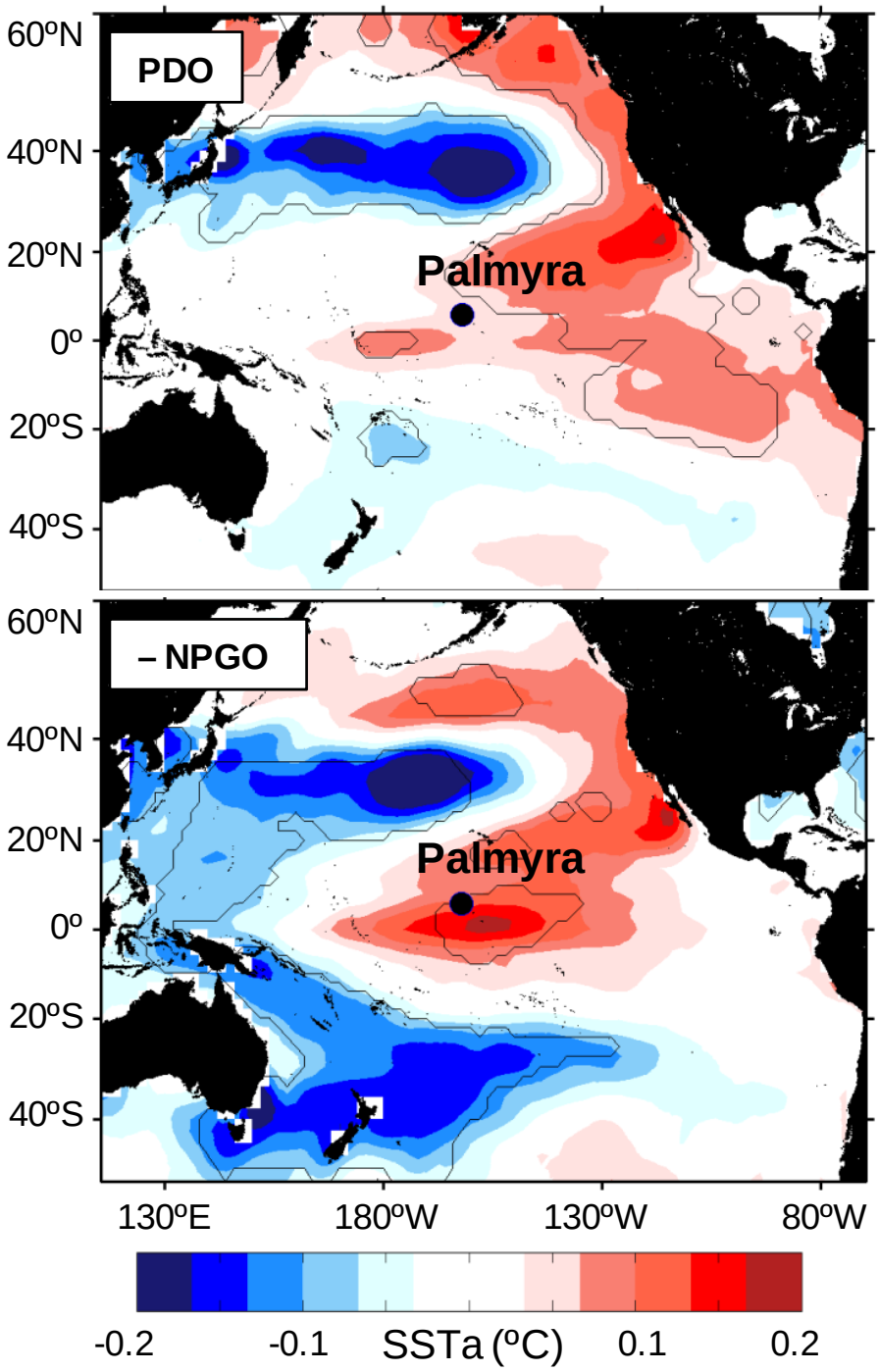

Figure 3.5. Regressions of Pacific SST anomalies with two indices of Pacific decadal-scale climate variability. (Top) SST regressed against an 8-year low-passed PDO index (Mantua et al. 1997) from 1900-2009. (Bottom) SST regressed against an 8-year low-passed -NPGO index (Di Lorenzo et al. 2008) from 1950-2009. Contour lines indicate areas where correlation coefficients (not plotted) exceed the 95% significance level, using a student's *t*-test and adjusting for serial autocorrelation. SST data from Reynolds et al. (2002).

decadal-scale climate modes are associated with a similar spatial pattern characterized by warming that extends from the central tropical Pacific to the northeast Pacific with maximum cool anomalies in the central North Pacific. However, at Palmyra, the SST anomalies associated with low-frequency variations in the NPGO are ±0.15°C, compared to ±0.05°C for low-frequency variations of the PDO. Therefore it is not surprising that the coral Sr/Ca-derived SST proxy record is more sensitive to the NPGO variations, given Palmyra's location in the central tropical Pacific.

The decadal-scale variability captured in the Palmyra Sr/Ca-derived SST proxy record is consistent with previous analyses of instrumental and proxy climate records from the tropical Pacific. First, wavelet analysis of instrumental SST data from the central tropical Pacific reveals decadal variability with a ~12-13 years periodicity (Kug et al. 2009), similar to that associated with the NPGO, but significantly shorter than the PDO's multi-decadal variability. Strong decadal variability with 12-13-year power was also uncovered in analyses of the original Palmyra coral $\delta^{18}O$ record (Cobb et al. 2001), and in analyses using multiple coral $\delta^{18}O$ records from across the tropical Pacific (Holland et al. 2007; Ault et al. 2009). Taken together, these results lend further support to the idea that decadal-scale SST variability in the central tropical Pacific is dynamically related to the CPW (Di Lorenzo et al., manuscript submitted to *Nature Geoscience*).

3.4.1.2. δ^{18}Osw-based Salinity Variability

On interannual timescales, the Palmyra coral-based δ^{18}Osw record is well-correlated to eastern Pacific ENSO variability, but is weakly correlated to central Pacific ENSO variability (Figure 3.6). Statistically significant correlation coefficients between 2-

7-year bandpassed version of the δ^{18}Osw record and the Niño-3 index (R=-0.49, N_{eff}=41, CI>95%) reflect the site's sensitivity to precipitation anomalies associated eastern Pacific ENSO extremes (Figure 3.1-top). Conversely, poor correlations between 2-7-year bandpassed versions of the δ^{18}Osw record and the ENSO Modoki Index (R=-0.19) reflect a muted influence of precipitation anomalies during central Pacific ENSO extremes.

In order to understand the coral-based δ^{18}Osw record's sensitivity to eastern Pacific ENSO variability, and its poor sensitivity to central Pacific ENSO variability, it is necessary to consider the various influences – both oceanographic and atmospheric – that determine seawater δ^{18}O at Palmyra. As previously documented in coral-based δ^{18}Osw records, precipitation exerts a primary control on surface seawater δ^{18}O (Gagan et al. 2000; Kilbourne et al. 2004; Linsley et al. 2006), because tropical Pacific rainwater is generally depleted in δ^{18}O relative to the surface ocean (Cole et al. 1990). Figure 3.1 illustrates that positive precipitation anomalies occur at Palmyra during both "flavors" of ENSO, but that during central Pacific warm events, the locus of maximum precipitation is shifted far west of Palmyra, with negative precipitation anomalies along the equator from 80-160ºW. Given prevailing easterly winds during central Pacific warm events (Figure 3.1b), horizontal advection will bring saltier waters from the cold tongue region, acting to diminish the effects of local precipitation at Palmyra. Furthermore, easterly winds across the cold tongue during central Pacific warm events will also maintain wind-driven upwelling, bringing relatively saline waters from the subsurface (Wyrtki 1981) to the surface in the central tropical Pacific. This analysis explains why eastern Pacific warm events are well-recorded in δ^{18}Osw at Palmyra, while central Pacific warm events are not.

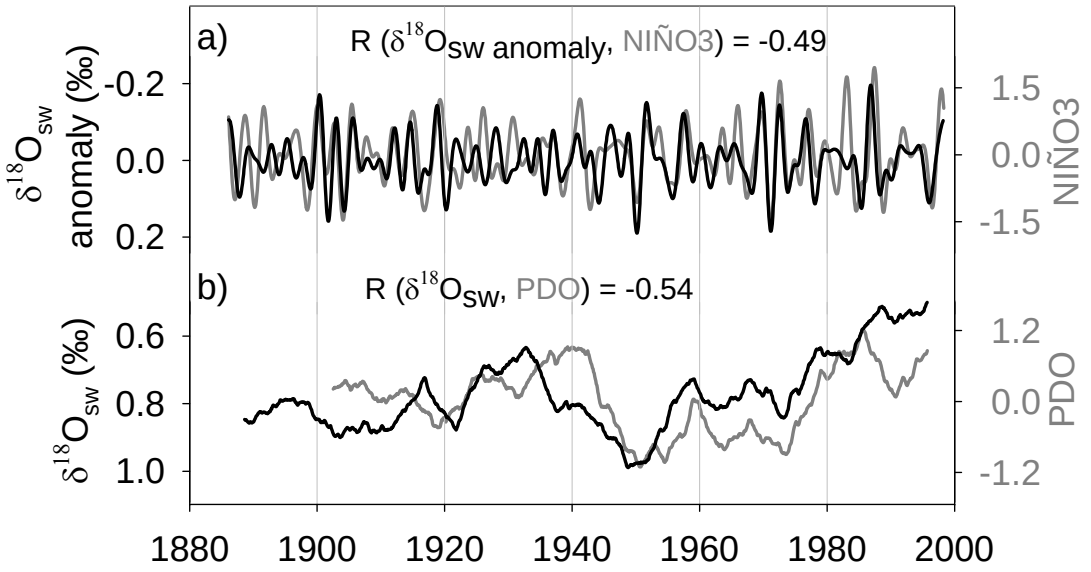

Figure 3.6. Interannual and decadal-scale variability of the Palmyra coral δ^{18}Osw record plotted with Pacific instrumental climate indices. (a) Interannual (2-7-year bandpassed) δ^{18}Osw anomalies (black) and Niño-3 SST anomalies (grey). (b) Decadal-scale δ^{18}Osw (black) and the PDO (grey) variability, plotted as 5-year running averages. All of the correlations are statistically significant at a 95% confidence level, using a student's *t*-test and adjusting for serial autocorrelation.

Echoing the interannual signals in δ^{18}Osw, large decadal-scale variations in δ^{18}Osw-based salinity proxy record are closely related to the PDO, but poorly correlated to both central Pacific warming and the NPGO. The correlation between 5-year running averaged versions of the δ^{18}Osw record and the PDO is -0.54 (N_{eff}=29, CI>95%; Figure 3.6b), versus -0.04 and 0.27 with ENSO Modoki and the NPGO, respectively. The δ^{18}Osw record implies that significant seawater freshening occurs during PDO warm regimes (1925-1946 and 1977-1998), with more saline conditions during the PDO cold regime of 1947-1975 (Mantua et al. 1997). Strong correlations between the δ^{18}Osw record and the PDO imply that the PDO impacts salinity in the tropical Pacific, as

hypothesized based on analysis of instrumental salinity data available in the late 20th century (Delcroix et al. 2007).

The fact that central tropical Pacific seawater $\delta^{18}O$ variations track canonical eastern Pacific ENSO and the PDO, with poor correlations to central Pacific warming and the NPGO, implies that the hydrological impacts of the eastern versus central Pacific modes are similar on interannual and decadal-scale timescales. Indeed, Delcroix et al. (2007) shows that PDO-related changes in salinity, precipitation, and wind-driven advection in the tropical Pacific are remarkably similar to those observed with eastern Pacific ENSO variability. No such analysis has been undertaken to investigate the similarities between central Pacific ENSO and NPGO impacts. However, the strong parallels between interannual and decadal-scale seawater $\delta^{18}O$ variability uncovered in this study fall far short of providing mechanistic insight on the causes of seawater $\delta^{18}O$ (or salinity) variability on decadal timescales. Whereas interannual seawater $\delta^{18}O$ variations can largely be explained by months-long changes in precipitation, with a lesser role for ocean circulation, decadal-scale seawater $\delta^{18}O$ variations must be maintained in the face of effective ocean mixing that occurs on decadal timescales. Ultimately, the atmospheric and the oceanographic contributions to decadal-scale changes in salinity across the tropical Pacific must be modeled in GCMs, even as the Palmyra $\delta^{18}Osw$ record suggests that such changes are relatively large.

3.4.2. Anthropogenic Signatures on Tropical Pacific Climate Variability

Having established that the Palmyra coral Sr/Ca-derived SST and $\delta^{18}Osw$-based salinity proxy records are robust indicators of basin-scale climate change on interannual

to multi-decadal timescales, these records can be used to analyze century-long records for trends that might be related to anthropogenic climate change.

3.4.2.1. Sr/Ca-derived SST Trend

The coral Sr/Ca-derived SST proxy record is characterized by a +0.53°C linear warming trend that is relatively uniform throughout the 20th century. However, strong decadal variability throughout the coral SST proxy record complicates the detection of a statistically linear SST trend over the last century, which is only significant at a 75% confidence level (as assessed with a Monte Carlo autoregressive significance test; N=3000). Nonetheless, the coral's inferred warming trend is roughly equivalent to the observed +0.6ºC increase in global SST over the 20th century (IPCC 2007), and falls well within the range of instrumental SST trends at Palmyra derived from various gridded SST datasets (+0.36°C for Hadley (Rayner et al. 2006), +0.48°C for Kaplan (Kaplan et al. 1998), and +0.74°C for ERSST (Smith and Reynolds et al. 2008)). The discrepancies among the instrumental SST datasets are likely associated with different strategies for bias correction and interpolation (Reynolds et al. 2007), and highlight the utility of generating an ensemble of coral Sr/Ca-based reconstructions of SST from across the tropical Pacific.

3.4.2.2. δ^{18}Osw-based Salinity Trend

The coral-based δ^{18}Osw salinity proxy record exhibits a strong freshening trend since the mid 20th century, consistent with an enhanced hydrological cycle under global warming (Held and Soden 2006). The century-long δ^{18}Osw trend of -0.25‰ is equivalent

to a roughly -0.9 psu salinity trend, applying an empirical relationship between seawater $\delta^{18}O$ and salinity observed in the central tropical Pacific (Fairbanks et al. 1997). Most importantly, the $\delta^{18}Osw$ trend is statistically significant at a 99% confidence level (as assessed with a Monte Carlo autoregressive significance test; N=3000). The magnitude of the late 20th century seawater $\delta^{18}O$ trend is large relative to the natural decadal-scale $\delta^{18}Osw$ variability implied by the coral record, implying that the trend is related to anthropogenic climate change.

Instrumental salinity data from the tropical Pacific resolve a freshening trend on the order of -0.15 psu from 1970 to 2003 near the central tropical Pacific (Delcroix et al. 2007) – six times smaller than the -0.9 psu salinity trend implied by the coral-based $\delta^{18}Osw$ record. The discrepancy between the instrumental and coral-based salinity trend estimates likely arises from large uncertainties associated with the relationship between seawater $\delta^{18}O$ and salinity, which is poorly constrained by a sparse dataset collected over a period of ~18 months (Fairbanks et al. 1997). However, uncertainties in the instrumental salinity data assembled from scant ships of opportunity, moored ocean buoys, and research cruises measurement may also contribute to the discrepancy.

The century-long $\delta^{18}Osw$-based salinity proxy record suggests that changes in the large-scale hydrological cycle may dominate anthropogenic climate changes in the tropical Pacific. Indeed, the unprecedented trend towards lower coral $\delta^{18}O$ values during the late 20th century observed in a millennium-long coral $\delta^{18}O$ reconstruction can be entirely explained by the observed seawater $\delta^{18}O$ trend. Similar late 20th century negative coral $\delta^{18}O$ trends have also been observed in other coral $\delta^{18}O$ records from the central and western tropical Pacific (Cole and Fairbanks 1990; Evans et al. 1999; Guilderson and

Schrag 1999; Urban et al. 2000; Tudhope et al. 2001; Kilbourne et al. 2004; Linsley et al. 2006; Quinn et al. 2006), consistent with pervasive changes in the tropical Pacific hydrological cycle. Analyses of rain gauge data (Morrissey and Graham 1996), instrumental salinity datasets (Delcroix et al. 2007), and coral-based δ^{18}Osw salinity proxy records (Linsley et al. 2006; Nurhati et al. 2009) indicate freshening trends likely associated with enhanced precipitation in regions characterized by convective activity, consistent with the strengthening of the hydrological cycle inferred from GCM simulations of 21st century climate.

3.5. Conclusion

This study presents monthly-resolved coral Sr/Ca-based SST and δ^{18}Osw-derived salinity proxy records from Palmyra Island, located in the central tropical Pacific, that span the 20th century. The century-long coral SST proxy record is dominated by interannual and decadal-scale variations that are linked to central Pacific warming variability. Conversely, the coral-based δ^{18}Osw salinity proxy record documents the influence of eastern Pacific ENSO and the PDO on tropical Pacific salinity variability, and is dominated by a prominent freshening trend in the late 20th century. The fact that the freshening trend is likely unprecedented in the last millennium means that it is most likely associated with anthropogenic climate change. Taken together, the proxy records reveal that SST and precipitation variations are largely decoupled on interannual, decadal, and secular timescales, and that anthropogenic hydrological trends may be more detectable than SST trends in the tropical Pacific. The records provide new insights into the mechanisms and basin-scale impacts of low-frequency Pacific climate variability, and

together with other such long, continuous coral climate reconstructions, may improve climate projections for regions that are heavily influenced by tropical Pacific climate variability.

3.6. Acknowledgements

The work was supported by the ACS-PRF grant to KMC. The authors thank Heather Crespo and Hussein Sayani for assistance with generating SEM images.

3.7. Appendix

3.7.1. Data Availability

Coral-based Sr/Ca-derived SST and δ^{18}Osw data presented in this study is available on NOAA Paleoclimatology website via:

ftp://ftp.ncdc.noaa.gov/pub/data/paleo/coral/east_pacific/palmyra2010.txt

3.7.2. Error Propagation Analysis for Sr/Ca-derived SST Record

The compounded error for SST estimates (σsst) includes uncertainties associated with (i) analytical precision of Sr/Ca measurements (σsrca), (ii) the intercept (σa), and (iii) the slope (σb) of the SST-Sr/Ca calibration. Starting with the equation for estimating SST from coral Sr/Ca:

$$\mathrm{SST} = a + b \cdot \mathrm{Sr/Ca} \qquad \text{(Eq.3.2)}$$

$$\mathrm{SST} \pm \sigma\mathrm{sst} = (a \pm \sigma a) + (b \pm \sigma b) \cdot (\overline{\mathrm{Sr/Ca}} \pm \sigma\mathrm{srca}) \qquad \text{(Eq.3.3)}$$

The multiplicative compounded error associated with the Sr/Ca-SST calibration slope and the analytical precision of Sr/Ca measurements, [(b ± σb) · (Sr/Ca ± σsrca)], is:

$$\sigma \text{ slope\_analytical} = |b \cdot \overline{SrCa}| \sqrt{(\frac{\sigma b}{b})^2 \cdot (\frac{\sigma srca}{\overline{SrCa}})^2} \quad \text{(Eq.3.4)}$$

Thus, the compounded error for SST estimates by adding the calibration intercept error (σa) is:

$$\sigma sst = \sqrt{\sigma a^2 + \sigma \text{ slope\_analytical}^2} \quad \text{(Eq.3.5)}$$

$$\sigma sst = \sqrt{\sigma a^2 + (b \cdot \overline{SrCa})^2 \cdot (\frac{\sigma b}{b})^2 \cdot (\frac{\sigma srca}{\overline{SrCa}})^2} \quad \text{(Eq.3.6)}$$

Plugging in known values for each term and their uncertainties,

$$SST \pm \sigma sst = (130.4 \pm 5.54) + (-11.39 \pm 0.62) \cdot (8.98 \pm 0.006) \quad \text{(Eq.3.7)}$$

The compounded error for SST estimates at Palmyra yields:

$$\sigma sst = \sqrt{5.54^2 + (-11.39 \cdot 8.98)^2 \cdot (\frac{0.62}{-11.39})^2 \cdot (\frac{0.006}{8.98})^2} = 7.85℃$$

3.7.3. Error Propagation Analysis for δ^{18}Osw-based Salinity Record

The compounded error for δ^{18}Osw estimates includes uncertainties associated with analytical precisions of (i) coral δ^{18}O and (ii) Sr/Ca, as well as the slopes of (iii) coral δ^{18}O-SST regression and (iv) Sr/Ca-SST calibration. Starting with the equation for calculating changes in δ^{18}Osw that is sensitive to coral δ^{18}O and SST variability, following the method of outlined in Ren et al. (2002):

$$\Delta\delta^{18}O_{CORAL} = \Delta\delta^{18}O_{SST} + \Delta\delta^{18}O_{SW} \quad \text{(Eq.3.8)}$$

$$\Delta\delta^{18}O_{CORAL} \pm \sigma_{\Delta\delta^{18}O_{CORAL}} = (\Delta\delta^{18}O_{SST} \pm \sigma_{\Delta\delta^{18}O_{SST}}) + (\Delta\delta^{18}O_{SW} \pm \sigma_{\Delta\delta^{18}O_{SW}}) \quad \text{(Eq.3.9)}$$

where the delta sign (Δ) refers to the difference between values from two adjacent months.

Taking the left-hand side of Equation 3.9 first, the equation for $\Delta\delta^{18}O_{CORAL}$ is:

$$\Delta\delta^{18}O_{CORAL} = \delta^{18}O_{CORAL\ t} - \delta^{18}O_{CORAL\ t-1} \quad \text{(Eq.3.10)}$$

$$\Delta\delta^{18}O_{CORAL} \pm \sigma_{\Delta\delta^{18}O_{CORAL}} = (\Delta\delta^{18}O_{SST} \pm \sigma_{\Delta\delta^{18}O_{SST}}) + (\Delta\delta^{18}O_{SW} \pm \sigma_{\Delta\delta^{18}O_{SW}}) \quad \text{(Eq.3.11)}$$

Thus, the calculation for the error associated with $\Delta\delta^{18}O_{CORAL}$ where the analytical precision for coral $\delta^{18}O$ measurements is ±0.06‰ (1σ) (Cobb et al. 2001), follows the equations:

$$\sigma_{\Delta\delta^{18}O_{CORAL}} = \sqrt{\sigma_{\delta^{18}O_{CORAL}}{}^2 + \sigma_{\delta^{18}O_{CORAL}}{}^2} = \sigma_{\delta^{18}O_{CORAL}}\sqrt{2} = 0.06\sqrt{2} = 0.09‰ \quad \text{(Eq.3.12)}$$

Taking the first term on the right-hand side of Equation 3.9, the equation for $\Delta\delta^{18}O_{SST}$ is:

$$\Delta\delta^{18}O_{SST} = \left[\overline{\Delta SrCa} \cdot \frac{\partial SST}{\partial SrCa} \cdot \frac{\partial\delta^{18}O_{CORAL}}{\partial SST}\right] \quad \text{(Eq.3.13)}$$

where $\overline{\Delta SrCa}$ is the mean of the absolute values of ΔSrCa (because the ΔSrCa timeseries contains both positive and negative signs). The calculated value for $\overline{\Delta SrCa}$ is 0.03 mmol mol^{-1}, with an error bar of ± 0.01 mmol mol^{-1} considering the ±0.006 mmol mol^{-1} analytical precision of Sr/Ca measurements and following these calculations

$$\Delta SrCa = SrCa_t - SrCa_{t-1} \quad \text{(Eq.3.14)}$$

$$\Delta SrCa \pm \sigma_{\Delta SrCa} = (SrCa_t \pm \sigma_{SrCa}) - (SrCa_{t-1} \pm \sigma_{SrCa}) \quad \text{(Eq.3.15)}$$

$$\sigma_{\Delta SrCa} = \sqrt{\sigma_{SrCa}{}^2 + \sigma_{SrCa}{}^2} = \sigma_{SrCa}\sqrt{2} = 0.006\sqrt{2} = 0.1 \text{ mmol mol}^{-1} \quad \text{(Eq.3.16)}$$

$\partial SST/\partial SrCa$ is the slope of the Sr/Ca-SST calibration, which is -11.39 ± 0.62 °C $(mmol/mol)^{-1}$. And $\partial\delta^{18}O_{CORAL}/\partial SST$ of -0.21 ± 0.03‰ $°C^{-1}$ is the mean empirical values of coral $\delta^{18}O$ sensitivity to SST compiled by Ren et al. (2002).

The calculation for the error associated with $\Delta\delta^{18}O_{SST}$ following Equation 3.9 is:

$$\sigma_{\Delta\delta^{18}O_{SST}} =$$

$$\left|\overline{\Delta SrCa} \cdot \frac{\partial SST}{\partial SrCa} \cdot \frac{\partial \delta^{18}O_{CORAL}}{\partial SST}\right| \cdot \sqrt{\left(\frac{\sigma_{\Delta SrCa}}{\Delta SrCa}\right)^2 + \left(\frac{\sigma_{SST-SrCa\ slope}}{SST-SrCa\ slope}\right)^2 + \left(\frac{\sigma_{coral\ \delta^{18}O-SST\_slope}}{coral\ \delta^{18}O-SST\_slope}\right)^2} \quad \text{(Eq.3.17)}$$

Plugging in the known values yields:

$$\sigma_{\Delta\delta^{18}O_{SST}} = |0.03 \cdot -11.39 \cdot -0.21| \cdot \sqrt{\left(\frac{0.01}{0.03}\right)^2 + \left(\frac{0.62}{-11.39}\right)^2 + \left(\frac{0.03}{-0.21}\right)^2} = 0.02\ ‰ \quad \text{(Eq.3.18)}$$

Having calculated $\Delta\delta^{18}O_{CORAL}$ and $\Delta\delta^{18}O_{SST}$, the compounded error for $\Delta\delta^{18}O_{SW}$ is calculated as the additive error propagation of the two terms:

$$\sigma_{\Delta\delta^{18}O_{SW}} = \sqrt{{\sigma_{\Delta\delta^{18}O_{CORAL}}}^2 + {\sigma_{\Delta\delta^{18}O_{SST}}}^2} = \sqrt{0.09^2 + 0.02^2} = 0.08\ ‰ \quad \text{(Eq.3.19)}$$

And since

$$\Delta\delta^{18}O_{SW} = \delta^{18}O_{SW_t} - \delta^{18}O_{SW_{t-1}} \quad \text{(Eq.3.20)}$$

$$\Delta\delta^{18}O_{SW} \pm \sigma_{\Delta\delta^{18}O_{SW}} = \left(\delta^{18}O_{SW_t} \pm \sigma_{\delta^{18}O_{SW}}\right) - \left(\delta^{18}O_{SW_{t-1}} \pm \sigma_{\delta^{18}O_{SW}}\right) \quad \text{(Eq.3.21)}$$

$$\sigma_{\Delta\delta^{18}O_{SW}} = \sqrt{{\sigma_{\delta^{18}O_{SW}}}^2 + {\sigma_{\delta^{18}O_{SW}}}^2} = \sigma_{\delta^{18}O_{SW}}\sqrt{2} \quad \text{(Eq.3.22)}$$

Thus, the compounded error for $\delta^{18}Osw$ is:

$$\sigma_{\delta^{18}O_{SW}} = \sigma_{\Delta\delta^{18}O_{SW}}/\sqrt{2} = 0.08/\sqrt{2} = 0.06\ ‰$$

3.8. References

Alexander, M. A., I. Bladé, M. Newman, J. R. Lanzante, N. C. Lau, and J. D. Scott, 2002: The atmospheric bridge: The influence of ENSO teleconnections on air-sea interaction over the global oceans. *J. Clim.*, **15,** 2205-2231, doi:10.1175/1520-0442(2002)015<2205:TABTIO>2.0.CO;2.

Alibert, C., and M. T. McCulloch, 1997: Strontium/calcium ratios in modern *Porites* corals from the Great Barrier Reef as a proxy for sea surface temperature: Calibration of the thermometer and monitoring of ENSO. *Paleoceanogr.*, **12,** 345-363. doi:10.1029/97PA00318.

Ashok, K., S. K. Behera, S. A. Rao, H. Weng, and T. Yamagata, 2007: El Niño Modoki and its possible teleconnection. *J. Geophys. Res.*, **112,** C11007, doi:10.1029/2006JC003798.

Ault, T. R., J. E. Cole, M. N. Evans, H. Barnett, N. J. Abram, A. W. Tudhope, and B. K. Linsley, 2009: Intensified decadal variability in tropical climate during the late 19th century. *Geophys. Res. Lett.*, **36**, L08602, doi:10.1029/2008GL036924.

Beck, J. W., R. L. Edwards, E. Ito, F. W. Taylor, J. Recy, F. Rougerie, P. Joannot, and C. Henin, 1992: Sea-surface temperature from coral skeletal strontium/calcium ratios. *Science*, **257,** 644-647, doi:10.1126/science.257.5070.644.

Bretherton, C. S., M. Widmann, V. P. Dymnikov, J. M. Wallace, and I. Bladé, 1999: Effective number of degrees of freedom of a spatial field. *J. Clim.*, **12,** 1990-2009, doi:10.1175/1520-0442(1999)012<1990:TENOSD>2.0.CO;2.

Chen, G., and C.-Y. Tam, 2010: Different impacts of two kinds of Pacific Ocean warming on tropical cyclone frequency over the western North Pacific. *Geophys. Res. Lett.*, **37**, L01803, doi:10.1029/2009GL041708.

Cobb, K. M., C. D. Charles, and D. E. A. Hunter, 2001: A central tropical Pacific coral demonstrates Pacific, Indian, and Atlantic decadal climate connections. *Geophys. Res. Lett.*, **28,** 2209-2212, doi:10.1029/2001GL012919.

Cobb, K. M., C. D. Charles, H. Cheng, and R. L. Edwards, 2003: El Niño/Southern Oscillation and tropical Pacific climate during the last millennium. *Nature*, **424,** 271-276, doi:10.1038/nature01779.

Cole, J. E., and R. G. Fairbanks, 1990: The Southern Oscillation recorded in the $\delta^{18}O$ of corals from Tarawa Atoll. *Paleoceanogr.*, **5,** 669-683, doi:10.1029/PA005i005p00669.

Cole, J. E., R. G. Fairbanks, and G. T. Shen, 1993: Recent variability in the Southern Oscillation: Isotopic results from a Tarawa Atoll coral. *Science*, **260,** 1790-1793, doi:10.1126/science.260.5115.1790.

Corrège, T., 2006: Sea surface temperature and salinity reconstruction from coral geochemical tracers. *Palaeogeogr., Palaeoclimatol., Palaeoecol.*, **232,** 408-428, doi:10.1016/j.palaeo.2005.10.014.

Delcroix, T., S. Cravatte, and M. J. McPhaden, 2007: Decadal variations and trends in tropical Pacific sea surface salinity since 1970. *J. Geophys. Res.*, **112,** C03012, doi:10.1029/2 006JC003801.

Di Lorenzo, E., and Coauthors, 2008: North Pacific Gyre Oscillation links ocean climate and ecosystem change. *Geophysical Research Letters*, **35,** L08607, doi:10.1029/2007GL032838.

Di Lorenzo, K. M. Cobb, J. C. Furtado, N. Schneider, B. Anderson, A. Bracco, M. A. Alexander, and D. Vimont. Central Pacific El Niño and decadal climate change in the North Pacific. Submitted to Nature Geoscience.

DiNezio, P. N., A. C. Clement, G. A. Vecchi, B. J. Soden, B. P. Kirtman, and S. K. Lee, 2009: Climate response of the equatorial Pacific to global warming, *J. Clim.*, **22**, 4873-4892, doi:10.1175/2009JCLI2982.1.

Enmar, R., M. Stein, M. Bar-Matthews, E. Sass, A. Katz, and B. Lazar, 2000: Diagenesis in live corals from the Gulf of Aqaba. I. The effect on paleo-oceanography tracers. *Geochim. Cosmochim. Acta*, **64,** 18, 3123-3132, doi:10.1016/S0016-7037(00)00417-8.

Evans, M. N., R. G. Fairbanks, and J. L. Rubenstone, 1999: The thermal oceanographic signal of El Niño reconstructed from a Kiritimati Island coral. *J. Geophys. Res.*, **104,** 13,409-13,421, doi:10.1029/1999JC900001.

Fairbanks, R. G., M. N. Evans, J. L. Rubenstone, R. A. Mortlock, K. Broad, M. D. Moore, and C. D. Charles, 1997: Evaluating climate indices and their geochemical proxies measured in corals. *Coral Reefs*, **16,** S93-S100, doi:10.1007/s003380050245.

Gagan, M. K., L. K. Ayliffe, D. Hopley, J. A. Cali, G. E. Mortimer, J. Chappell, M. T. McCulloch, and M. J. Head, 1998: Temperature and surface-ocean water balance of the mid-Holocene tropical western Pacific. *Science*, **279,** 1014-1018, doi:10.1126/science.279.5353.1014.

Gagan M. K., L. K. Ayliffe, J. W. Beck, J. E. Cole, E. M. Druffel, R. B. Dunbar, and D. P. Schrag D. P., 2000: New views of tropical paleoclimates from corals. *Quat. Sci. Rev.*, **19,** 45-64, doi:10.1016/S0277-3791(99)00054-2.

Guilderson, T. P., and D. P. Schrag, 1999: Reliability of coral isotope records from the western Pacific warm pool: A comparison using age-optimized records. *Paleoceanogr.*, **14,** 457-464, doi:10.1029/1999PA900024.

Held, I. M., and B. J. Soden, 2006: Robust responses of the hydrological cycle to global warming. *J. Clim.*, **19,** 5686-5699, doi:10.1175/JCLI3990.1.

Hendy, E. J., M. K. Gagan, C. A. Alibert, M. T. McCulloch, J. M. Lough, and P. J. Isdale, 2002: Abrupt decrease in tropical Pacific sea surface salinity at end of Little Ice Age. *Science*, **295,** 1511-1514, doi:10.1126/science.1067693.

Hendy, E. J., M. K. Gagan, J. M. Lough, M. McCulloch, and P. B. deMenocal, 2007: Impact of skeletal dissolution and secondary aragonite on trace element and isotopic climate proxies in Porites corals. *Paleoceanogr.*, **22,** doi:Pa410110.1029/2007pa001462.

Holland, C. L., R. B. Scott, S. I. An, and F. W. Taylor, 2007: Propagating decadal sea surface temperature signal identified in modern proxy records of the tropical Pacific. *Clim. Dyn.*, **28,** 163-179, doi:10.1007/s00382-006-0174-0.

Intergovernmental Panel on Climate Change (IPCC), 2007: *Climate Change 2007: The Physical Science Basis. Contribution of Working Group I to the Fourth Assessment Report of the Intergovernmental Panel on Climate Change*, edited by S. Solomon et al., Cambridge Univ. Press, Cambridge, U. K.

Kao, H.-Y. and J.-Y. Yu, 2009: Contrasting Eastern-Pacific and Central-Pacific types of ENSO. *J. Clim.*, **22,** 615-632, doi:10.1175/2008JCLI2309.1.

Kaplan, A., M. Cane, Y. Kushnir, A. Clement, M. Blumenthal, and B. Rajagopalan, 1998: Analyses of global sea surface temperature 1856-1991. *J. Geophys. Res.*, **103,** 18567-18589, doi:10.1029/97JC01736.

Kilbourne K. H., T. M. Quinn, F. W. Taylor, T. Delcroix, and Y. Gouriou Y, 2004: El Niño-Southern Oscillation-related salinity variations recorded in the skeletal geochemistry of a *Porites* coral from Espiritu Santo, Vanuatu. *Paleoceanogr.*, **19,** PA4002, doi:10.1029/2004PA001033.

Kim, H.-M., P. J. Webster, and J. A. Curry, 2009: Impact of shifting patterns of Pacific Ocean warming on North Atlantic tropical cyclones. *Science*, **325,** 77-80, doi:10.1126/science.1174062.

Kug, J. -S., F. –F. Jin, and S. -I. An, S.-I, 2009: Two types of El Niño events: cold tongue El Niño and warm pool El Niño. *J. Clim.*, **22,** 1499-1515, doi:10.1175/2008JCLI2624.1.

Kumar, K. K., B. Rajagopalan, M. Hoerling, G. Bates, and M. Cane, 2006: Unraveling the mystery of Indian monsoon failure during El Niño events. *Science*, **314,** 115-119, doi:10.1126/science.1131152.

Larkin, N. K. and D. E. Harrison, 2005: Global seasonal temperature and precipitation anomalies during El Niño autumn and winter. *Geophys. Res. Lett.*, **32,** L13705, doi:10.1029/2005GL022738.

Latif, M., R. Kleeman, and C. Eckert, 1997: Greenhouse warming, decadal variability, or El Niño? An attempt to understand the anomalous 1990s. *J. Clim*., **10,** 2221-2239.

Linsley, B. K., A. Kaplan, Y. Gouriou, J. Salinger, P. B. deMenocal, G. M. Wellington, and S. S. Howe, 2006: Tracking the extent of the South Pacific Convergence Zone since the early 1600s. *Geochem. Geophys. Geosyst.*, **7,** Q05003, doi:10.1029/2005GC001115.

Mantua, N. J., S. R. Hare, Y. Zhang, J. M. Wallace, and R. C. Francis, 1997: A Pacific interdecadal climate oscillation with impacts on salmon production. *Bull. Am. Met. Soc.*, **78,** 1069-1079, doi:10.1175/1520-0477(1997)078<1069:APICOW>2.0.CO;2.

McCulloch, M. T., M. K. Gagan, G. E. Mortimer, A. R. Chivas, and P. J. Isdale, 1994: A high resolution Sr/Ca and $\delta^{18}O$ coral record from the Great Barrier Reef, Australia, and the 1982-1983 El Niño. *Geochim. Cosmochim. Acta*, **58,** 2747-2754, doi:10.1016/0016-7037(94)90142-2.

McPhaden, M. J., and Coauthors, 1998: The Tropical Ocean-Global Atmosphere observing system: A decade of progress. *J. Geophys. Res.*, **103,** 14169-14240, doi:10.1029/97JC02906.

Meehl, G.A., and Coauthors, 2007: Global Climate Projections. In: *Climate Change 2007: The Physical Science Basis. Contribution of Working Group I to the Fourth Assessment Report of the Intergovernmental Panel on Climate Change* [eds. Solomon, S., D. Qin, M. Manning, Z. Chen, M. Marquis, K. B. Averyt, M. Tignor and H. L. Miller]. Cambridge University Press, Cambridge, UK and New York, NY, USA.

Morrissey, M. L., and N. E. Graham, 1996: Recent trends in rain gauge precipitation measurements from the tropical Pacific: Evidence for an enhanced hydrologic cycle. *Bull. Am. Meteorol. Soc*., **77,** 1207-1219, doi:10.1175/1520-0477(1996)077<1207:RTIRGP>2.0.CO;2.

Nurhati, I. S., K. M. Cobb, C. D. Charles, and R. B. Dunbar, 2009: Late 20th century warming and freshening in the central tropical Pacific. *Geophys. Res. Lett.,* **36,** L21606, doi:10.1029/2009GL040270.

Newman, M., G. P. Compo, and M. A. Alexander, 2003: ENSO-forced variability of the Pacific decadal oscillation. *J. Clim.*, **16**, 3853-3857.

Quinn, T. M., and F. W. Taylor, 2006: SST artifacts in coral proxy records produced by early marine diagenesis in a modern coral from Rabaul, Papua New Guinea. *Geophys. Res. Lett.*, **33,** 4, doi:L0460110.1029/2005gl024972.

Quinn, T. M., F. W. Taylor, and T. J. Crowley, 2006: Coral-based climate variability in the Western Pacific Warm Pool since 1867. *J. Geophys. Res.*, **111,** C11006, doi:10.1029/2005JC003243.

Rayner, N. A., and Coauthors, 2006: Improved analyses of changes and uncertainties in sea surface temperature measured in situ since the mid-nineteenth century: the HadSST2 data set. J. Clim., **19,** 446-469.

Ren L., Linsley B. K., Wellington G. M., Schrag D. P., and Hoegh- Guldberg O, 2003: Deconvolving the $\delta^{18}O$ seawater component from subseasonal coral $\delta^{18}O$ and Sr/Ca at Rarotonga in the southwestern subtropical Pacific for the period 1726 to 1997. *Geochim. Cosmochim. Acta*, **67,** 1609-1621, doi:10.1016/S0016-7037(02)00917-1.

Reynolds, R. W., N. A. Rayner, T. M. Smith, D. C. Stokes, and W. Wang, 2002: An improved in situ and satellite SST analysis for climate. *J. Clim.*, **15,** 1609-1625, doi:10.1175/1520-0442(2002)015<1609:AIISAS>2.0.CO;2.

Reynolds, R.W., T. M. Smith, C. Liu, D. B. Chelton, K. S. Casey, and M. G. Schlax, 2007: Daily high-resolution-blended analyses for sea surface temperature. *J. Clim.*, **20,** 5473-5496, doi:10.1175/2007JCLI1824.1.

Schrag, D. P., 1999: Rapid analysis of high-precision Sr/Ca ratios in corals and other marine carbonates. *Paleoceanogr.*, **14,** 97-102, doi:10.1029/1998PA900025.

Smith, T. M., R. W. Reynolds, T. C. Peterson, and J. Lawrimore, 2008: Improvements to NOAA's Historical Merged Land-Ocean Surface Temperature Analysis (1880-2006). *J. Clim.*, **21,** 2283-2296, doi:10.1175/2007JCLI2100.1.

Solow, A. R., and A. Huppert, 2004: A potential bias in coral reconstruction of sea-surface temperature. *Geophys. Res. Lett.*, **31,** L06308, doi:10.1029/2003GL019349.

Trenberth, K. E., and D. P. Stepaniak, 2001: Indices of El Niño evolution. *J. Clim.*, **14,** 1697-1701, doi:10.1175/1520-0442(2001)014<1697:LIOENO>2.0.CO;2.

Tudhope, A. W., and Coauthors, 2001: Variability in the El Niño- Southern Oscillation through a glacial-interglacial cycle. *Science*, **291,** 1511-1517, doi:10.1126/science.1057969.

Urban, F. E., J. E. Cole, and J. T. Overpeck, 2000: Influence of mean climate change on climate variability from a 155-year tropical Pacific coral record. *Nature*, **407,** 989-993, doi:10.1038/35039597.

Vecchi, G. A., A. Clement, and B. J. Soden, 2008: Examining the tropical Pacific's response to global warming, *Eos Trans. AGU*, **89,** 81-83, doi:10.1029/2008EO090002.

Wang, G., and H. H. Hendon, 2007: Sensitivity of Australian rainfall to inter–El Niño variations. *J. Clim.*, **20,** 4211-4226, doi:10.1175/JCLI4228.1.

Weng, H., S. K. Behera, and T. Yamagata, 2009: Anomalous winter climate conditions in the Pacific Rim during recent El Niño Modoki and El Niño events. *Clim. Dyn.*, **32,** 663-674, doi:10.1007/s00382-008-0394-6.

Wyrtki, K., 1981: An estimate of equatorial upwelling in the Pacific. *J. Phys. Oceanogr.*, **11,** 1205-1214, doi:10.1175/1520-0485(1981)011<1205:AEOEUI>2.0.CO;2.

Xie, P., and P. A. Arkin, 1997: Global precipitation: A 17-year monthly analysis based on gauge observations, satellite estimates, and numerical model outputs. *Bull. Am. Meteorol. Soc.*, **78,** 2539-2558, doi:10.1175/1520-0477(1997)078<2539:GPAYMA>2.0.CO;2.

Xie, S. P., C. Deser, G. A. Vecchi, J. Ma, H. Teng, and A. T. Wittenberg, 2010: Global Warming Pattern Formation: Sea Surface Temperature and Rainfall. *J. Climate., **233,** 966-986,* doi:10.1175/2009JCLI3329.1.

Yeh, S. W., J. S. Kug, B. Dewitte, M. H. Kwon, B. P. Kirtman, and F. F. Jin, 2009: El Niño in a changing climate. *Nature*, **461,** 511-514, doi:10.1038/nature08316.

Zhang, Y., J. M. Wallace, and D. S. Battisti, 1997: ENSO-like interdecadal variability: 1900-93. *J. Clim.*, **10,** 1004-1020, doi:10.1175/1520-0442(1997)010<1004:ELIV>2.0.CO;2.

VITA

Intan Suci Nurhati was born in Jakarta, Indonesia, on September 20, 1982. She received a B.A. in Earth and Environmental Sciences (with Honors), and Economics in 2005 from Wesleyan University, Middletown, Connecticut. She came to Georgia Tech in the same year to pursue a PhD in Earth and Atmospheric Sciences, with a certificate in Environmental Public Policy.

Publications:

Nurhati, I. S., Cobb, K. M., and E. Di Lorenzo. Decadal-scale SST and salinity variations in the central tropical Pacific: Signatures of natural and anthropogenic climate change (*in review*).

LaVigne, M., Nurhati, I. S., Cobb, K. M., and Sherrell, R. M. Reduction of nutrient availability in central equatorial Pacific surface waters in the 1980's (*in prep.*).

Sayani, H. R., Cobb, K. M., Cohen, A. L., Elliot, W. C., Nurhati, I. S., Rose, K. A. and Zaunbrecher, L. K. Effects of diagenesis on paleoclimate reconstructions from modern and young fossil corals (*in review*).

Nurhati, I. S., Cobb, K. M., Charles, C. D. and Dunbar, R. B. (2009). Late 20th century warming and freshening in the central tropical Pacific. *Geophysical Research Letters,* 36, L21606, doi:10.1029/2009GL040270.

Nurhati, I. S. (2005). *Spatial and temporal analyses of the Indonesian Throughflow sediments: Possible indicators of climate-induced hydrologic changes*. Undergraduate Honors Thesis. Wesleyan University.